FRM II
Forschungs-Neutronenquelle
Heinz Maier-Leibnitz

Technische Universität München

3rd FRM II User Meeting

October 15th, 2010

Garching

Technische Universität München
Forschungs-Neutronenquelle
Heinz Maier-Leibnitz (FRM II)
Lichtenbergstraße 1
85748 Garching, Germany

www.frm2.tum.de

Imprint

Eds.: Thomas Gutberlet, Peter Link, Ina Lommatzsch, Jürgen Neuhaus, Winfried Petry
FRM II User Meeting 2010 - Abstract Booklet
Technische Universität München
Forschungs-Neutronenquelle Heinz Maier-Leibnitz (FRM II)
D-85748 Garching
Oktober 2010

Welcome

Dear colleagues,

I am sure many of you will not have realized that the German Forschungs-Neutronenquelle Heinz Maier-Leibnitz (FRM II) has now been running for more than five years. Since the start of routine operation of this powerful new neutron source in May 2005, scientists from all over the world have been able to use the suite of modern neutron scattering instruments. There are currently 21 instruments available, with 9 more anticipated to be operational in the near future.

The deadline for the 12th proposal round was the 8th October 2010 and this 3rd FRM II User Meeting has been organized in close proximity. We were delighted to have more than 160 participants register for this event, however due to the limitation of a single day, only a small fraction of the submitted abstracts could be chosen for oral presentation. The topics presented will cover all areas of science performed at the FRM II; from biophysics to cultural heritage and from materials science to fundamental physics. We appreciate very much your engagement at the FRM II and the use of the still growing suite of instruments operated by our partners at the German universities and research institutes.

At the user meeting the latest developments at existing instruments will be presented along with new projects that are in the commissioning phase such as the new reflectometer MARIA operated by the JCNS, the BioDiffractometer being built by JCNS and TUM and the SANS-1 project of TUM and GKSS. In addition, information about the latest sample environment and complimentary sample characterization techniques available on site will be shown. Furthermore we hope for many interesting and stimulating discussions with our colleagues from abroad as well as those from the Garching campus.

Due to the exchange of the positron source at the FRM II, there will be a shutdown between the end of October 2010 and beginning of March 2011; beam time of the order of one cycle will be lost within the next few months. We hope this will not affect your requests for beam time at the FRM II and you will have more opportunities for science with neutrons and positrons in 2011.

With best regards and welcome to Garching,

Thomas Gutberlet
Head of the User Office

Contents

TALKS

POSTERS

Biology

Cultural Heritage

Excitations and Dynamics

Instrumentation

Material Science

Particle Physics

Soft Matter

Structure

General Information

Location

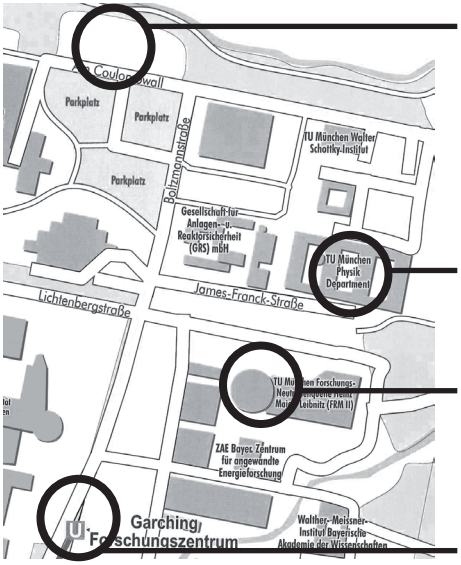

Parking

Venue:
Technische Universität München
Physik Department
James Franck Str.
85748 Garching

FRM II

Underground: U6,
“Garching, Forschungszentrum”

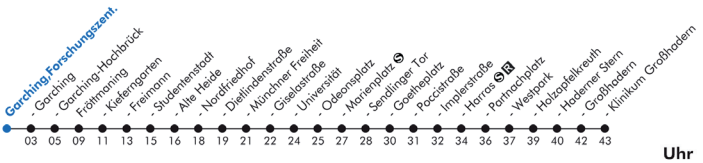

Public transportation

The **U6** takes you to the city centre. The timetable (right) tells you when a train leaves at „Garching, Forschungszentrum“. The timeline (above) informs you how long it will take to reach a station (in minutes).

User Office

In case you need other timetables, please contact the User Office. It is a mobile one today. In case you need help or have any questions, there will always be someone in front of the lecture hall to assist you.

Apart from that you can call **+49 (0)89.289.10794**

Uhr	Freitag					
5	10	30	50			
6	10	22	32	42	52	
7	02	12	22	32	42	52
8	02	12	22	32	42	52
9	02	12	22	32	52	
10	12	32	52			
11	12	32	52			
12	12	32	52			
13	12	22	32	42	52	
14	02	12	22	32	42	52
15	02	12	22	32	42	52
16	02	12	22	32	42	52
17	02	12	22	32	42	52
18	02	12	22	32	42	52
19	12	32	50			
20	10	30	50			
21	10	30	50			
22	10	30	50			
23	10	30	50			
0	10	30				
1	00	45x				

General Information

Venue:
Technische Universität München
Physik Department
James Franck Str.
85748 Garching

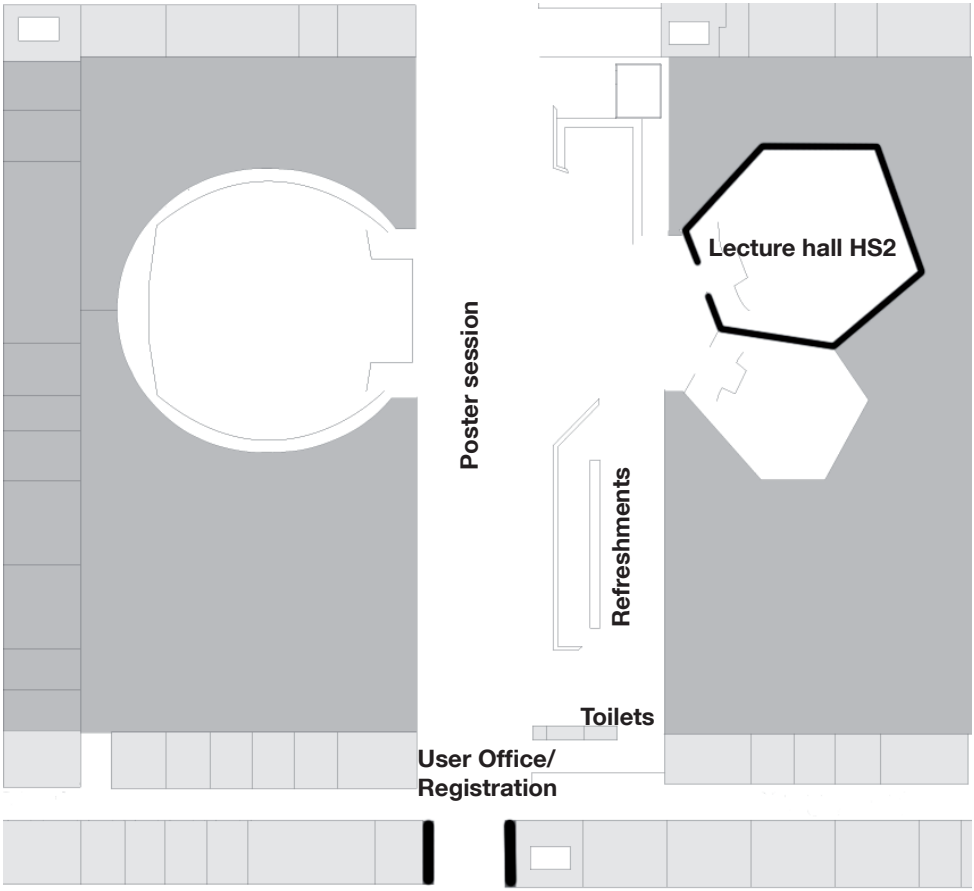

Main entrance from James Franck Str.

Programme

Friday, October 15th - morning

08:15	**Registration**	
09:00	**Welcome** by Winfried Petry, Scientific Director of the FRM II	
09:30	**T-01**: Small angle neutron scattering on light controled aggregation and disassembly of amyloid like structures	T. E. Schrader, JCNS
09:50	**T-02:** Asymmetric lipid distribution in supported bilayers and cell adhesive coatings	B. Nickel, LMU
10:10	**T-03:** A new class of potential antineoplastic agents based on ruthenium amphiphilic nanostructures	L. Paduano, Univ. of Naples
10:30	**Coffeebreak**	
11:00	**T-04:** Relaxation in protein surface water near the resolution limit of neutron spectroscopy	J. Wuttke, JCNS
11:20	**T-05:** Hydrogen rotational and translational diffusion in calcium borohydride from quasielastic neutron scattering and DFT calculations	D. Blanchard, DTU Risø
11:40	**T-06:** Hydration mechanisms of ultra high performance concrete	T. Gutberlet, TUM
12:00	**T-07:** Competing magnetic structures in Er_2PdSi_3	M. Loewenhaupt, TU Dresden
12:20	**Lunch**	

Programme

Friday, October 15th - afternoon

13:30	**T-08:** Bridging the gap between synchrotron and neutron diffraction for non destructive surface residual stress analysis	J. Gibmeier, KIT
13:50	**T-09:** Neutron diffraction on functional materials under electric fields	M. Hoelzel, TU Darmstadt
14:10	**T-10:** In-situ observation of hydrogen diffusion in iron using neutron radiography	A. Griesche, BAM
14:30	**T-11:** In-situ probing of fast defect annealing in Cu and Ni with a high-intensity positron beam	W. Sprengel, TU Graz
14:50	**Coffeebreak**	
15:20	**T-12:** Tailoring hybrid solar cell nanostructures with insights from advanced neutron scattering	P. Müller-Buschbaum, TUM
15:40	**T-13:** PERC - a clean, bright and versatile source of neutron decay products	B. Maerkisch, Univ. Heidelberg
16:00	**T-14:** Waveguide-enhanced polarized neutron reflectometry: a new approach in the study of magnetic proximity effects	Y. Khaydukov, FLNP JINR
16:20	**T-15:** Phonon properties of Ni-Mn-Ga shape memory alloys	S. Ener, TUM
16:50	Conference photo	
17:00 - 20:00	**Postersession**	

TALKS

Small angle neutron scattering on light controlled aggregation and disassembly of amyloid-like structures

A. A. Deeg[1], T. E. Schrader[2], A. Radulescu[2], S. Kempter[3], J. Pfizer[4], L. Moroder[4], W. Zinth[1]

[1] BioMolecular Optics and LMU, Center for Integrated Protein Science, München, Germany

[2] Jülich Centre for Neutron Science at FRM II, Garching, Germany

[3] LMU, Center for NanoScience, München, Germany

[4] MPI für Biochemie, Martinsried, Germany

The aggregation of peptides into amyloid structures is associated to a variety of diseases such as Creutzfeld Jacob and Alzheimer. On the other hand the unique material properties of amyloids make them interesting candidates for the production of nano-biomaterial. The model peptide used in this study contains two strands formed by 5 amino acids with an azobenzene switch in the centre. It has been confirmed by infrared spectroscopy and transmission electron microscopy (TEM) that the model peptide forms amyloid-like aggregates. To obtain additional information on the molecular structure small angle neutron scattering has been performed on solutions of the model peptide with and without light treatment. The resulting scattering curves of the aggregates in the dark revealed that the model peptide forms rod like structures. There are indications for a fractal nature which could originate from the branching of the rod like structures which was also observed in the TEM pictures. Illumination of the sample, switches the azobenzene to its cis isomer and causes structural changes of the aggregates. These structural changes are leading to a disaggregation, verified by a characteristic change in IR absorption. The measured small angle scattering curves after illumination showed a decrease of the overall size and the fractal nature. Switching the azobenzene chromophore back to the trans isomer leads to a change in the scattering curve indicative for the increase of the average size of the aggregates. The present preliminary neutron scattering experiments on the aggregated peptides have given interesting experimental information. In the future important new insight into aggregation dynamics and average structures is expected from extended neutron scattering experiments combined with other techniques.

Asymmetric lipid distribution in supported bilayers and cell adhesive coatings

S. Hertrich, J. Schmidt, M. Huth, J. Rädler, B. Nickel

LMU, Fakultät für Physik, Experimentalphysik, München, Germany

Lipid membranes of living cells are highly asymmetric. Negatively charged lipids such as POPS are a prominent example for this observation. Once a living cell presents PS to the outside leaflet, the cell is most likely undergoing apotosis, i.e. programmed cell death. Here we study the distribution of lipids in synthetic bilayers on SiO_2. We find that electrostatic interactions between the SiO_2 surface and the lipids suppresses the presence of PS in the substrate facing leaflet. The observed PS composition in the two leaflets can be understood from Debye shielding arguments. In a second example, we will show how neutron reflectometry identifies a dense on edge configuration of a RGD-containing polypeptide. The structural properties are complemented by cell growth experiments (submitted). Experiments have been performed at N-Rex$^+$ (A. Rühm) and REFSANS (J.F. Moulin and M. H. Seiller)

A new class of potential antineoplastic agents based on ruthenium amphiphilic nanostructures

A. Costantino[1], L. Simeone[2], G. Mangiapia[1], D. Montesarchio[2], A. Radulescu[3], H. Frielinghaus[3], L. Paduano[1]

[1] University of Naples, Department of Chemistry, Italy

[2] University of Naples, Department of Organic Chemistry, Italy

[3] Jülich Centre for Neutron Science at FRM II, Garching, Germany

Metastases rather than primary tumors are the leading cause for cancer death, and yet metastases are almost never the target of chemotherapy. At present, Ruthenium complexes have been found to offer new perspectives for chemotherapy [1,2]. Although a rather large number of studies on Ruthenium complexes have been published in the recent years, up to date in literature no examples of nanovectors carrying Ruhenium complexes for anti-cancer therapy are reported. At this aim, we have already synthesized a new amphiphilic unimer (DOPU) able to coordinate Ruthenium complexes (for a general schema see fig. 1) and to produce a rich variety of aggregates, namely unilamellar and oligolamellar vesicles, as well as the existence of more complex structures like cubosomes [3]. In order to obtain nanovectors with low or no immune response in the organism, such molecules has been led to co-aggregate with 1-palmitoyl-2-oleoyl-sn3-phosphocholine (POPC) (one of the main constituent of biological membrane) the and 1,2-dioleoyl-3-trimethylammonium-propane (chloride salt) (DOTAP) a negative lipid. Insertion of amphiphilic ruthenium complex in a lipid matrix has also the advantage to reduce the ruthenium complex degradation that usually take place by exchange of chloride ligand by hydroxyl ion present in solution that leads to the polyoxide complex formation.

In the present communcation the main result obtained by small-angle neutron scattering (SANS), dynamic light scattering (DLS) and Electron paramagnetic resonance (EPR) are discussed.

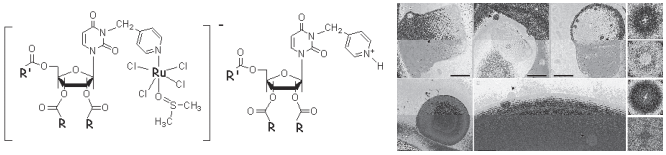

Fig. 1. Structure of the amphiphilic ruthenium complex, example of the aggregates they form.

[1] Dyson, P.J; Sava, G.; based antitumor drugs in the post genomic era, Dalton Transactions, 2006, (16), 1929-1933.

[2] Bergamo, A; Sava, G.; complexes can target determinants of tumor malignancy, Dalton Transactions, 2007, 13, 1267-1272.

[3] Vaccaro, M; Del Litto, R; Mangiapia, G; Carnerup, A.M.; D'Errico, G.; Ruffo, F.; Paduano, L.; based nanovectors containing ruthenium complexes: a potential route in cancer therapy, Chemical Communications, 2009, (11), 1404-1406.

Relaxation in protein surface water near the resolution limit of neutron spectroscopy

W. Doster[1], S. Busch[1], A. M. Gaspar[1], M.-S. Appavou[2], J. Wuttke[2], H. Scheer[3]

[1] TUM, Physik Department, Garching, Germany

[2] Jülich Centre for Neutron Science at FRM II, Garching, Germany

[3] LMU, Botanisches Institut II, München, Germany

Thin layers of water on biomolecular and other nanostructured surfaces can be supercooled to temperatures not accessible with bulk water. Chen et al. [1] suggested that anomalies near 220 K observed by quasielastic neutron scattering can be explained by a hidden critical point of bulk water. Based on more sensitive measurements of water on perdeuterated phycocyanin, using the new neutron backscattering spectrometer SPHERES, and an improved data analysis, we present results that show no sign of such a fragiletostrong transition. The inflection of the elastic intensity at 220 K has a dynamic origin that is compatible with a calorimetric glass transition at 170 K. The temperature dependence of the relaxation times is highly sensitive to data evaluation; it can be brought into perfect agreement with the results of other techniques, without any anomaly [2].
By the time of this conference, complementary results from a simpler model system, aquous LiCl solution, shall also be available [3,4].

[1] S.H. Chen et al., Proc. Natl. Acad. Sci. USA 103, 9012 (2006).
[2] W. Doster et al., Phys. Rev. Lett. 104, 098101 (2010).
[3] E. Mamontov, J. Phys. Chem. B 113, 14073 (2009).
[4] J. Wuttke (in preparation).

Rotational and translational diffusion in calcium borohydride from QENS and DFT calculations

D. Blanchard[1], M. D. Riktor[2], J. B. Maronsson[1,3], H. S. Jacobsen[1], J. Kehres[1], D. Sveinbjorsson[1], E. Gil Bardají[4], A. Léon[4], F. Juranyi[5], J. Wuttke[6], B. C. Hauback[2], M. Fichtner[4], T. Vegge[1]

[1] DTU, Risø National Laboratory for Sustainable Energy, Roskilde, Denmark

[2] IFE, Kjeller, Norway

[3] DTU, CAMD, Lyngby, Denmark

[4] KIT, Institut für Nanotechnologie, Karlsruhe, Germany

[5] ETH Zürich, Laboratory for Neutron Scattering @ PSI, Villigen, Switzerland

[6] Jülich Centre for Neutron Science at FRM II, Garching, Germany

Calcium borohydride is attracting as a hydrogen storage media. In $Ca(BH_4)_2$ hydrogen dynamics can originate from long-range diffusion or localized motions (rotations, librations and vibrations). In this study, the rotational and diffusional dynamics of hydrogen were investigated by quasielastic neutron scattering (QENS) combined with Density Functional Theory (DFT) calculations. QENS experiments were performed with the high resolution spectrometer SPHERES (FRM II, Garching, Germany), energy resolution: 0.65 μeV, and with MARS (SINQ, PSI, Villigen, Switzerland), energy resolution: 15 μeV. The DFT calculations were performed using the Atomic Simulation Environment package, the DACAPO plane wave basis set implementation to solve the electronic structure problem and the Nudged Elastic Band (NEB) method to calculate the energy paths of the re-orientational changes (Fig. 1).

Between 95 K and 280 K, two thermally activated rotational motions were observed around the 2-fold (C_2) and 3-fold (C_3) axis of the BH_4 units (Fig. 2). At the lower temperatures, only the C_3-rotation, the energetically easiest to activate, was detected while at higher temperatures a combination of the two rotations, with different characteristic times, was observed (Fig. 3). The DFT calculated energy barriers are similar to the experimental ones (Ea_{C2}= 0.15 eV and Ea_{C3}=0.11 eV). Long-range diffusion of hydrogen was also observed with SPHERES at 224 and 260 K (Fig. 3). The only process identified by DFT calculations that gives almost the same jump length for the same energy barriers (~0.12 eV, 2.1Å) corresponds to H_2 interstitial diffusion.

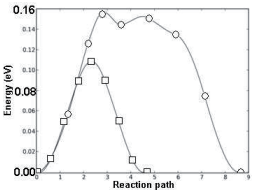

Fig. 1: NEB energy paths for C_2(O) and C_3( ) rotations.

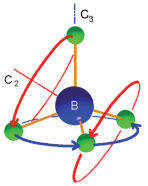

Fig. 2: C_2, C_3-axis of a BH_4 complex.

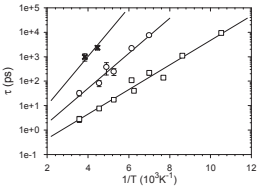

Fig. 3: Arrhenius plots of the characteristic times for the thermally activated C_2(O), C_3( ) rotations and long-range diffusion (x).

Hydration mechanisms of ultra high performance concrete

T. Gutberlet, H. Hilbig, R. E. Beddoe

TUM, Centrum Baustoffe und Materialprüfung, Germany

For the optimization of the mechanical and chemical properties of Ultra High Performance Concrete (UHPC), a scientific working knowledge of microstructure formation in dependence of temperature and composition is necessary. The strength-giving phase of UHPC is C-S-H (Calcium Silicate Hydrate) formed with $Ca(OH)_2$ by the hydration of Ca_3SiO_5 and SiO_2. At present, the evolution of C-S-H microstructure is not well understood and current models are inadequate. Therefore the quasi-elastic neutron scattering technique (QENS) is being used to study water-bonding and its kinetics in different Ca_3SiO_5-SiO_2-H_2O systems. Parallel investigations are being performed with ^{29}Si NMR to determine the structure (polymerisation) of C-S-H and XRD for the formation of $Ca(OH)_2$ and the consumption of Ca_3SiO_5 in the hydration process.
Surprisingly, the latest QENS results reveal a rapid increase in the amount of physically bound water (i.e. restricted) in the induction period before hydration begins even though only a small amount of water is chemically bound. This indicates that early C-S-H with a very large specific surface (800 m^2/g) forms on the surface of Ca_3SiO_5 particles following water contact. Further evidence for this effect was supplied by infrared spectroscopy, calorimetry and a model calculation. At the end of the induction period (>5 h) more C-S-H, but with a lower specific surface, forms on the surface of the Ca_3SiO_5 particles until the hydration process is controlled by diffusion of water through C-S-H to the unreacted Ca_3SiO_5.
The results further our understanding of the poorly-understood induction period during which fresh concrete may be poured and placed before it sets. Control of the induction period is of vital importance for construction with concrete.

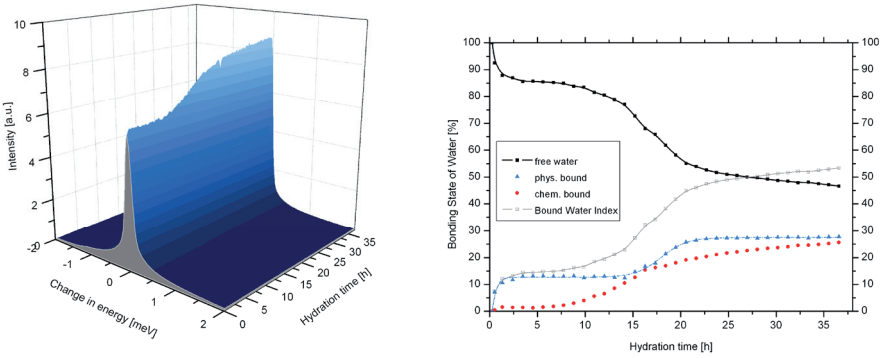

Fig. 1 left: Quasi-elastic neutron scattering of a Ca_3SiO_5-H_2O system at 20°C in the first 38 hours of hydration; right: resulting time dependent fractions of the different bonding states of water in the system. The Bound Water Index is the sum of chemically and physically bound water.

Competing magnetic structures in Er_2PdSi_3

M. Loewenhaupt[1,2], F. Tang[1], E. Faulhaber[2,3], U. Hoffmann[3], W. Löser[4]

[1] TU Dresden, Institut für Festkörperphysik, Germany

[2] Gemeinsame Forschergruppe HZB – TU Dresden, Berlin, Germany

[3] HZB für Materialien und Energie GmbH, Berlin, Germany

[4] Institut für Festkörper- und Werkstoffforschung Dresden, Germany

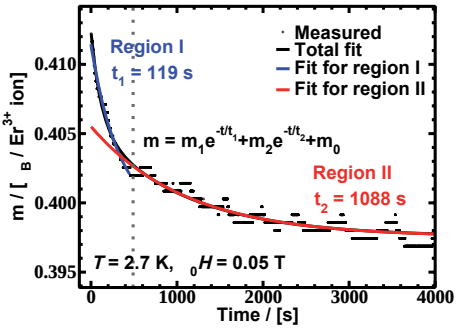

Fig. 1. Magnetization of Er_2PdSi_3 at 2.7 K and 0.05 T (after field sweep to 1 T) as function of time. The total curve is fitted with two exponential functions with relaxation times of 119 s and 1088 s as indicated by the blue and red lines, respectively.

R_2PdSi_3 compounds have been found to exhibit rich magnetic phenomena arising from the interplay between RKKY interaction, crystal electric field effect and geometric frustration due to the AlB_2 derived hexagonal structure. Er_2PdSi_3 orders antiferromagnetically at T_N = 7 K and undergoes a second (frequency dependent) phase transition at T_2 = 2 K [1]. Neutron diffraction measurements at 1.6 K in zero field revealed magnetic reflections from two unrelated propagation vectors (τ_1 = (1/9, 1/9, 0) and τ_2 = (0.133, 0, 0)) shortly after the sample was cooled from$T > T_N$. Although eventually the ground state (presumably τ_1) with slightly lower energy dominates, the whole process took longer times than usually expected. This indicates the coexistence and competition of at least two magnetic states which are energetically very close to each other at finite temperatures.

Correspondingly the macroscopic magnetic properties of Er_2PdSi_3 also demonstrated a time dependent behavior (Fig. 1; magnetization after field sweep to 1 T into FM phase and then down to 0.05 T). A clear exponential decay of the magnetization with two relaxation processes (119 s and 1088 s) can be observed. A possible explanation is to relate the faster process to the restoration of the AFM order either with propagation vector τ_1 or τ_2 from the induced FM state. Afterwards the system slowly settles to the real ground state corresponding to the slower relaxation process. In this contribution detailed time-, temperature- and field-dependent neutron scattering results will be compared to the macroscopic properties of Er_2PdSi_3.

[1] M. Frontzek et al., J. Phys.: Condens. Matter 19, 145276 (2007).

Bridging the gap between synchrotron and neutron diffraction for non destructive surface residual stress analysis

J. Rebelo Kornmeier[1], J. Gibmeier[2], M. Hofmann[1]

[1] Forschungs-Neutronenquelle Heinz Maier-Leibnitz (FRM II), Garching, Germany

[2] KIT, Institut für Werkstoffkunde I, Karlsruhe, Germany

Neutron strain measurements are critical at the surface. When scanning close to a sample surface, aberration peak shifts caused by so called spurious strains arise due geometrical and divergence effects. These aberration peak shifts can be of the same order as the peak shifts related to residual strains.
In this exemplary study it will be demonstrated that, by optimising the bending radius of a Si (400) monochromator, the spurious surface strains can be strongly reduced. The experiments were carried out at the STRESS-SPEC instrument at the research reactor FRM II, Munich, Germany, using a stress free steel sample of fine grained construction steel, S690QL. For optimised Si (400) monochromator settings it was possible to measure the residual stress depth gradient of a shot peened SAE 4140 steel sample through the surface dispensing of the laborious reference measurements to compensate for surface effects. The residual stress depth profile is in good agreement to results obtained by X-ray diffraction measurements obtained in an international round robin test (BRITE-EURAM-project ENSPED). These results open very promising possibilities to bridge the gap between X-ray diffraction and neutron diffraction for non destructive residual stress analysis close to surfaces.

Neutron diffraction on functional materials under electric fields and mechanical load

M. Hoelzel[1,2], M. Hinterstein[1], W. Schmahl[3], C. Merkel[3], N. Jünke[2], A. Senyshyn[1,2], H. Fuess[1]

[1] TU Darmstadt, FB für Material- und Geowissenschaften, Germany

[2] Forschungs-Neutronenquelle Heinz Maier-Leibnitz (FRM II), Garching, Germany

[3] LMU, Department für Geo- und Umweltwissenschaften, München, Germany

In this contribution recent results by neutron diffraction on technological important functional materials are reported: shape memory alloys and ferroelectrics were investigated under mechanical load or electrical fields, respectively. All experiments were carried out at the high-resolution neutron powder diffractometer SPODI. This instrument offers possibilities for the in-situ analysis of functional materials under special environmental conditions.
A rotatable load frame available at SPODI allows materials characterisation at different orientations of the load axis with respect to the scattering vector. Besides tensile stress, also pressure and torsion can be applied. Monoclinic nickel titanium shape memory alloys were measured at different strain levels to determine load-induced elastic strains, changes in twinning texture and resulting microstrains. In addition, diffraction studies under different sample orientations (i.e. different orientations of load axis) were carried out to analyse the anisotropy of the elastic response.
An apparatus for high electric fields was developed to analyse the poling mechanisms in ferroelectics at fields up to 7 kV/mm. The studies were carried out on samples of technological relevant systems like $PbZrxTi_{1-x}O_3$ and NBT-BT-KNN. In the composition 92-6-2 of that system, the electrical field induced strain at 6 kV/mm could be correlated with a field-induced phase transformation (tetragonal to rhombohedral phase). The phase transition is accompanied by a change in the tilt system of the oxygen octahedra identified by superlattice reflections in the neutron diffraction patterns.

In-situ observation of hydrogen diffusion in iron using neutron radiography

A. Griesche[1], K. Beyer[1], T. Kannengießer[1], B. Schillinger[2]

[1] BAM, Berlin, Germany

[2] Forschungs-Neutronenquelle Heinz Maier-Leibnitz (FRM II), Garching, Germany

Hydrogen assisted cracking of metals limits the durability of welds and constructions. Still the failure mechanisms are not fully understood, for instance the role of hydrogen mass transport during crack initiation. Measuring the hydrogen concentration as a function of time (and space) would allow to determine diffusion coefficients helping to enlighten this lack of understanding. Therefore, neutron radiography is a valuable tool for measuring in situ hydrogen transport in iron and steels [1].

The influence of grain boundaries on the hydrogen diffusion behaviour can be determined by comparing the diffusion behaviour of samples with e.g. different microstructure. In a first study we investigated in situ the simplest case, the hydrogen effusion out of pure iron (ARMCO) using neutron radiography at ANTARES [2]. Samples were charged electrochemically ex situ with a well defined amount of hydrogen, stored in liquid nitrogen and were then heat treated during a neutron radiography measurement whilst the change of neutron transmission was recorded. For analysis the gray values in the pictures were transformed into concentrations with help of an ex post calibration. Therefore, the experimental temperature-time profile of the heat treatment has been repeated with identical samples in the home lab and the amount of effusing hydrogen was measured by carrier gas hot extraction. In a first approximation the concentration of hydrogen in the sample can be calculated by subtracting the hydrogen concentration in the atmosphere from the initial one in the sample. We were able to measure hydrogen concentrations as low as 65 wt.ppm.

Simultaneously monitoring of hydrogenous sample and hydrogen-free reference allowed for in situ measurement of hydrogen effusion. Sample heating was done by infrared radiation. Diffusion coefficients for hydrogen effusion from iron have been calculated. They coincide fairly with literature data.

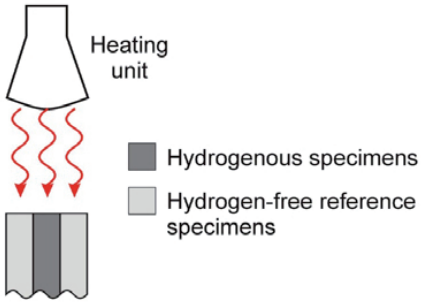

Fig. 1: Sketch of the sample arrangement. View in beam direction.

[1] E. H. Lehmann, P. Vontobel, N. Kardjilov, Hydrogen distribution measurements by neutrons, Applied Radiation and Isotopes 61, 2004, 503-509.

[2] K. Beyer, Th. Kannengiesser, A. Griesche, B. Schillinger, Talk on MSE 2010 conference, 25.08.2010, Darmstadt, Germany.

In-situ probing of fast defect annealing in Cu and Ni with a high-intensity positron beam (NEPOMUC at FRM II)

B. Oberdorfer[1], E.-M. Steyskal[1], W. Sprengel[1], W. Puff[1], P. Pikart[2], C. Hugenschmidt[2], M. Zehetbauer[3], R. Pippan[4], R. Würschum[1]

[1] TU Graz, Institut für Materialphysik, Austria

[2] Forschungs-Neutronenquelle Heinz Maier-Leibnitz (FRM II), Garching, Germany

[3] Universität Wien, Fakultät für Physik, Austria

[4] Österreichische Akademie der Wissenschaften, Erich Schmid Institut für Materialwissenschaft and Montanuniversität Leoben,Department Materialphysik, Austria

A complex atomic defect structure in solids as, e.g., present in Cu and Ni after severe plastic deformation (SPD), has been successfully analyzed by a combination of the atomistic technique of fast *in-situ* temperature dependent positron-electron annihilation and dilatometry. It was realized with the high-intensity positron beam at the NEPOMUC positron source of FRM II. This is a first study of its kind and was combined with macroscopic, high-precision length-change measurements. The combination of these two *in-situ* methods on short timescales as demonstrated in this case study gives a novel experimental approach for an unambiguous identification of structural defects in solids such as vacancies, dislocations and grain boundaries. It allows for basic studies of their physics comprising also fast defect annealing kinetics. The application of high-intensity monoenergetic positron beams to fast defect kinetics studies even at higher temperatures and also with variable energy opens new experimental fields for the application of positron beams.

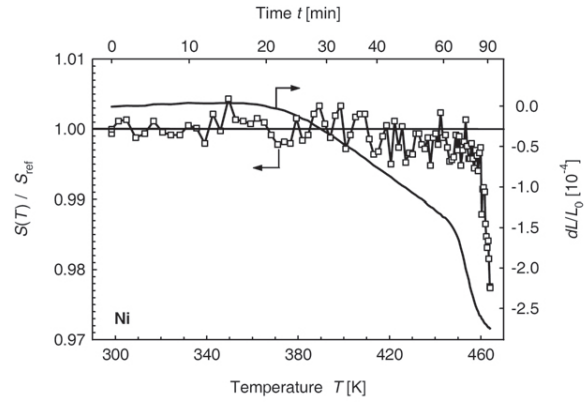

Fig. 1: Comparison of the temperature dependence of the valenceelectron parameter (S-parameter) as determined from positron-electron annihilation (open squares, left ordinate) and superimposed to the relative length change dL/L_0 (thick line, right ordinate) as determined by dilatometry of Ni after severe plastic deformation (SPD) by highpressure torsion (HPT). The data points for dilatometry were taken in time intervals of 1s. In both cases data were obtained by applying the identical temperature program in two independent measurements on identically prepared specimens. The corresponding time, *t*, valid for both curves is shown on the upper abscissa.

(accepted for publication in Physical Review Letters)

Tailoring hybrid solar cell nanostructures with insights from advanced neutron scattering

G. Kaune[1], M. Rawolle[1], M. Niedermeier[1], M. Memesa[2], J.S. Gutmann[2], R. Kampmann[3], J.-F. Moulin[3], M. Haese-Seiller[3], P. Müller-Buschbaum[1]

[1] TUM, Physik Department, Garching, Germany

[2] MPI für Polymerforschung, Mainz, Germany

[3] GKSS-Forschungszentrum Geesthacht, Germany

Photovoltaic energy conversion systems based on an inorganic semiconductor and an organic hole transporting material, so called hybrid solar cells, have emerged to a promising alternative technology for solar light harvesting [1]. In a common device, a nanosized structure with a large interface between the two components is necessary to separate efficiently excitons generated by incoming light. This can be achieved by application of a nanostructured inorganic semiconducting material, whose interspaces are filled with a polymeric hole transporting material. However, up to now the efficiencies of hybrid solar cells cannot compete with conventional semiconductor photovoltaics. One major challenge is the control of the interfacial area between donor-acceptor materials.

In our model system we use nanostructured titanium dioxide (TiO_2) films with a sponge-like morphology, which are prepared by application of a sol-gel process [2]. To further structure the films on micrometer scale colloidal particles are added to the sol-gel solution as a secondary template and subsequently removed from the spin coated films by calcinations [3]. Different polymer infiltration techniques are discussed with respect to the degree of pore filling.

The unique possibilities of neutron scattering with respect to the structural characterization of such hybrid structures with application for photovolatics is demonstrated [4]: Grazing incidence small angle neutron scattering (GISANS) enables to probe the nanoscale structure with high statistical relevance in a non-destructive manner. Moreover, the degree of pore filling can be obtained quantitatively.

[1] U. Bach, D. Lupo, P. Comte, J. E. Moser, F. Weissörtel, J. Salbeck, H. Spreitzer, M. Grätzel; Nature 395, 583 (1998).

[2] M. Memesa, S. Weber, S. Lenz, J. Perlich, R. Berger, P. Müller-Buschbaum, J. S. Gutmann, Energy Environ. Sci. 2, 783-790 (2009).

[3] J. Perlich, G. Kaune, M. Memesa, J.S. Gutmann, P. Müller-Buschbaum; Phil. Trans. R. Soc. A 367, 1783-1798 (2009).

[4] G. Kaune, M. Memesa, R. Meier, M. A. Ruderer, A. Diethert, J. S. Gutmann, P. Müller- Buschbaum; ACS Appl. Mater. Interfaces 1, 2862-2869 (2009).

[5] G. Kaune, M. Haese-Seiler, R. Kampmann, J.-F. Moulin, Q. Zhong, P. Müller- Buschbaum; J. Poly. Sci. Part B. 48, 1628-1635 (2010).

PERC - a clean, bright and versatile source of neutron decay products

B. Märkisch

Universität Heidelberg, Physikalisches Institut, Germany

Particle physics experiments at low energies, such as neutron decay experiments, contribute significantly to precision tests of the Standard Model and to searches for physics beyond. They are complementary to direct searches for new physics at the high energy frontier and competitive in sensitivity.
We present the new instrument PERC (Proton Electron Radiation Channel), which will be installed on the beam line Mephisto at the FRM II. With this instrument the precision on various observables in neutron decay will be increased significantly and new observables will become accessible for the first time.
PERC realizes a new concept: as a beam station it delivers not neutrons, but neutron decay products. The properties of the emerging beam of electrons and protons are defined precisely. Experiments at this source will have ten times better systematic accuracy and two orders of magnitude larger statistics than existing neutron decay experiments.
Central part of the new instrument is a neutron guide in a 10 m long superconducting magnet system. Electrons and protons from (polarised) neutron decay within the guide will be extracted magnetically and then separated from the remaining neutron beam. A strong magnetic filter will limit the angular distribution of the emerging particles.
Users will install specialized spectrometers to analyze the electron and proton beam and address different physics questions. This separates the experimental challenges related to the neutron beam (e.g. polarisation and background) from those of the detection of the decay products.

Waveguide-enhanced polarized neutron reflectometry: a new approach in the study of magnetic proximity effects

Y. N. Khaydukov[1,2], S. V. Kozhevnikov[1,4], Y. V. Nikitenko[1], V. L. Aksenov[1,2], B. Nagy[3], D. G. Merkel[3], L. Bottyán[3], A. Rühm[4]

[1] JINR, Frank Laboratory of Neutron Physics, Dubna, Russia

[2] Moscow State University, Skobeltsyn Institute of Nuclear Physics, Russia

[3] KFKI Research Institute for Particle and Nuclear Physics, Budapest, Hungary

[4] MPI für Metallforschung, Stuttgart, Germany

A number of intriguing physical phenomena are related with superconducting/ferromagnetic (S/F) heterostructures, where proximity effects can cause modification of superconducting and magnetic parameters [1,2]. Study of such systems is the challenge for PNR as pronounced effects are small and/or number of proximity interfaces is restricted.
In this paper we propose a new sensitive approach on the base of the use of waveguide enhancement of the intensity of magnetic scattering [3] (fig). The S/F bilayer V(60 nm)/ Fe(1-4.5 nm) placed in waveguide structure have been investigated by PNR. The measure of the temperature dependence of the magnetic scattering intensities (spin-flip and diffuse) at the waveguide mode allowed to detect new magnetic phases at temperatures $T < T_C$, where T_C is the superconducting temperature of the S layer [4].

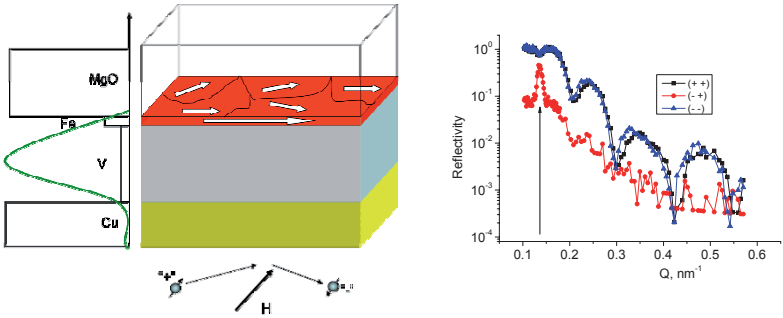

Fig. 1. a) Scheme of the PNR experiment with waveguide S/F structure. Left side - SLD profile. Red and blue layers are F and S layers corr. b) Reflectivity curves for the S/F sample Cu(30nm)/V(60nm)/Fe(1.5nm) measured at reflectometer NREX+. Position of the waveguide mode is shown by arrow

[1]. F. S. Bergeret, A. F. Volkov and K. B. Efetov, Rev. Mod. Phys. 77 1321 (2005).
[2]. A.I. Buzdin, Rev. Mod. Phys. 77, 935 (2005).
[3]. Yu.N. Khaydukov, Yu.V. Nikitenko, L. Bottyan, A. Rühm and V.L. Aksenov, Cryst. rep. 2010 (accepted); arXiv:1001.2895.
[4]. Yu.N. Khaydukov, V.L. Aksenov, Yu.V. Nikitenko et al., J. of Superconductivity and Novel Magnetism (submitted at 2010); arXiv:1005.0685.

Phonon properties of Ni-Mn-Ga shape memory alloys

S. Ener[1], J. Neuhaus[2], R. Mole[2], K. Hradil[2], W. Petry[2]

[1] TUM, Physik Department, Garching, Germany

[2] Forschungs-Neutronenquelle Heinz Maier-Leibnitz (FRM II), Garching, Germany

Ni-Mn-Ga ferromagnetic shape memory alloys (FSMAs) are potential materials for technical applications due to their magnetic field induced phase transition (FIT) and their magnetic field induced reorientation (FIR) in the low temperature (martensite) phase. In these FSMAs it is known that the instability in the lattice causes this structural transition by changing either temperature, by applying stress or a magnetic field in a particular direction. To understand the physics behind the shape memory effect we investigated the vibrational properties of two NiMnGa samples with different compositions in the high temperature $L2_1$ (austenite) phase. The full phonon dispersions of the austenite phases (fig.1) are measured for stoichiometric (Ni_2MnGa) and offstoichiometric ($Ni_{49}Mn_{32}Ga_{19}$) samples to see the effect of the compositional change on the vibrational properties. First principle calculations were performed by the group of P. Entel at the University of Duisburg-Essen for the stoichiometric composition at 0 K.

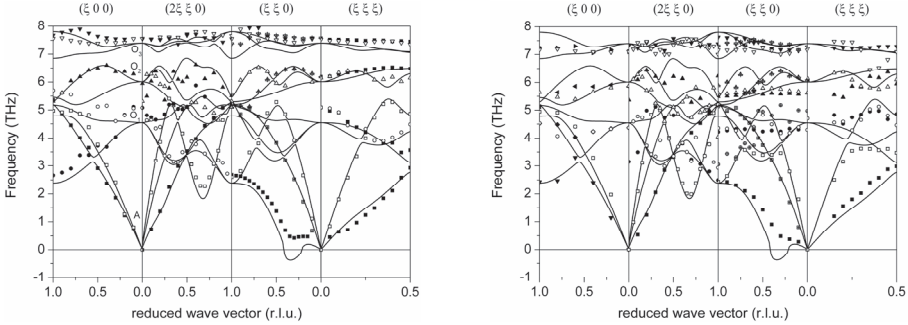

Fig. 1: Phonon dispersions of the stoichiometric (left) and off-stoichiometric (right) NiMnGa alloys in the $L2_1$ phase.

The results show that for the stoichiometric sample the calculated phonons and the experimental phonons are in good agreement. The first principle calculations at 0 K (solid lines in fig. 1) showed the instability of the lattice resulting in imaginary phonons in the $TA_2[\xi\xi 0]$ branch. For the offstoichiometric sample the experimental results fits well to the theoretical calculations but the optical branches differ significantly.

To investigate the instability of the lattice, we measured the $TA_2[\xi\xi 0]$ phonon branch as a function of temperature. The measurements show similar overall behavior for the stoichiometric and offstoichiometric samples. The phonons get soft while reaching the structural transition temperature from either side of the phase transition. As reported in literature, the slope of the temperature dependent phonons changes near the Curie temperature. However this holds true only for the stoichiometric sample. DSC and magnetization measurements approved that this is not the case for the off-stoichiometric sample which leaves doubt about the interpretation of this change in general.

A figure had been left out by editors for reasons of space.

POSTERS

Biology

B-01

SANS Studies on human recombinant a-crystallins

Y. Georgalis[1], J. Peschek[2], M.-S. Appavou[3], J. Buchner[2], S. Weinkauf[1]

[1] TUM, Department Chemie - Elektronenmikroskopie, Garching, Germany

[2] LMU, Center for Integrated Protein Science, München, Germany

[3] Jülich Centre for Neutron Science at FRM II, Garching, Germany

Crystallins are complex multifunctional proteins. Most of them are directly involved in vision and they are responsible for the development of cataract. Crystallins are also involved in a variety of neurodegenerative diseases like Alzheimer's, Parkinson's, Alexander's and concomitant diseases. Overviews on these aspects have been given recently by Horwitz (2009). In recent works we have examined the properties of recombinant human α-crystallin isoforms and their mixtures using dynamic light scattering (DLS) and transmission electron microscopy (TEM) (Peschek et al. 2009, Georgalis et al., 2010a, b). In the present work we have extended these studies using SANS covering the dilute to semi-concentrated regimes.
The data collected so far in KWS-1 and KWS-2 are of high quality and allowed for determination of radii of gyration and distance functions for the two major isoforms αA- and αB-crystallin and their (3:1) mixture αAB-crystallin. The latter resembles the native lens protein. All three proteins exhibit quite similar dimensions and neither polydispersity nor subunit exchange posed any sub-stantial difficulties during data collection and evaluation.
The research is directed towards modeling the structure factors using schemes like the Hypernetted Chain Approximation (HNC) and applying additional neutron-based techniques like Spin-echo, Time-of-Flight and Back-scattering techniques in order to draw conclusions on the degree of hydration and the flexibility of the surrounding water molecules.

[1] Horwitz, J. (2009) α-crystallin: The quest for a homogeneous quaternary structure. Exp. Eye Res. 88, 190-194.

[2] Peschek, J., Braun, N., Franzmann, T.M., Georgalis, Y., Haslbeck, M., Weinkauf, S. and Buch-ner, J. (2009) The eye lens chaperone α-crystallin forms defined globular assemblies Proc. Natl. Acad. Sci. U.S.A 106, 13272-13277.

[3] Georgalis, Y. Peschek, J, Buchner, J. and Weinkauf, S. (2010) Interparticle Interactions in Hu-man Recombinant α-Crystallins: A Dynamic Light Scattering Study, Biophys. J. (submitted).

B-02

Neutron reflectometry studies on supported lipid bilayers at REFSANS

S. Hertrich, J. Schmidt, K. Fritz, S. Stanglmeier, B. Nickel

LMU, Fakultät für Physik, Experimentalphysik, München, Germany

Solid supported lipid bilayers (SLBs) act as a model system of biological cell membranes, and can be deployed to study protein or cell adhesion by a variety of experimental methods such as surface sensitive neutron and xray techniques and fluorescence microscopy. The neutron reflectometer REFSANS at FRM II offers the possibility to resolve the structure of SLBs by determining layer thicknesses and scattering length densities of the sample. Using contrast variation in the buffer and partially deuterated lipids, the SLB sample's components can be differentiated and their hydration can be determined. Additional information of lateral structure in the sample can be gained by use of the GISANS mode of the REFSANS machine. In a recent experiment, negatively charged lipids in SLBs were asymmetrically distributed in the two leaflets because of electrostatic repulsion from the silicon oxide surface. Further experiments include measurements on lipid bilayers grafted to the surface an elevated through a PEG cushion, and the binding of proteins to the SLBs. Also a GISANS study of small vesicles is planned. In addition, the SLB samples' fluidity is studied by fluorescence techniques, continuous bleaching and FCS.

B-03

Influence of macromolecular crowding on protein stability

S. Longeville[1], C. Le Coeur[1], J. Teixeira[1], P. Busch[2], B. Demé[3]

[1] Laboratoire Léon Brillouin, CEA Saclay, Gif-sur-Yvette, France

[2] Jülich Centre for Neutron Science at FRM II, Garching, Germany

[3] Institut Laue–Langevin, Grenoble, France

Cell interior is a complex environment filled with a variety of different objects with respect to shape and size. Macromolecules are present at a total concentration up to several hundred grams per litre and the overall occupied volume fraction can reach $\varphi \approx 0.3\text{-}0.4$. Under crowding environment protein-protein interaction play a fundamental role because the distances between molecules are of the order of few nanometres. The crowding environment can affect some physical, chemical, and biological properties of biological macromolecules. For example, structure and activity of proteins can be strongly modified by the environment. Traditionally, protein folding is studied *in vitro* at very low concentration (less than about 1 $mg.ml^{-1}$) of proteins. Under such conditions, small globular single chain proteins can unfold and refold quite rapidly depending mainly to the nature of the solvent. Such processes have been very intensively studied, since folding of proteins into their native structure is the mechanism, which transforms polypeptide into its biologically active structure. Protein misfolding is involved in a very high number of diseases (.g. Alzheimer, Parkinson, and Kreuzfeld-Jacob diseases, type II diabetes, ...). Theoretically, the problem was studied by the introduction of the concept of excluded volume [5]. In recent papers, Minton uses statistical thermodynamic models to address the question. He predicted that inert cosolutes *stabilize* the native state of proteins against unfolding state mainly by *destabilizing* the unfolded state (which occupies a higher volume than the more compact states including the native state: their chemical potential is thus more affected by the presence of other molecules) and that the dimension of the unfolded state decreases with increasing the concentration of cosolute in a measurable way. In this theory, the unfolded state is considered as having a Gaussian like chain conformation. Experimentally, the effect of macromolecular crowding is studied by adding macromolecules to the solution, which mimic those in cells. Small Angle Neutron Scattering (SANS) is a technique of choice for such study because, by using appropriate mixtures of light and heavy water, it is possible to match the scattering length density of the solvent to the one of the cosolute and thus to measure the conformation of a molecule at low concentration in a presence of a high concentration of another one. We undertook to verify experimentally the theoretical mechanism responsible for the protein stabilization by macromolecular crowding. In a first series of experiments we have studied the effect of introducing high concentration of inert cosolutes on the conformation of a Gaussian chain [7]. We observed two important effects: the different molecules in the mixture have a strong tendency to segregate and the conformation of the chain must be studied by extrapolation at zero chain concentration ("Zimm plot"). The radius of gyration of the chain is decreased by a factor of 2 when increasing crowder mass fraction from 0 to 0.35 corresponding approximately to the one observed in cells. Such a compression of the chain correspond to what was predicted theoretically. In a second series of experiment [8], we changed the size of the Gaussian chain to test the scaling laws of the excluded chain theory and also verified that the behaviour of the radius of gyration when increasing the size of the chain corresponds to theoretical predictions. In the last step, still under progress we study the effect of macromolecular crowding on the unfolding of a real protein: the first results show that protein stabilization and compression of the unfolded state are correlated.

References had been left out by editors due to lack of space.

B-04

Characterization of vesicles formed by lipopolysaccharides: from the molecular structure to the aggregate architecture

E. Vaselli[1], G. D'Errico[1], A. Silipo[2], A. Molinaro[2], R. Lanzetta[2], A. Radulescu[3], L. Paduano[1], G. Mangiapia[1]

[1] University of Naples, Department of Chemistry, Italy

[2] University of Naples, Department of Organic Chemistry, Italy

[3] Jülich Centre for Neutron Science at FRM II, Garching, Germany

Lipopolysaccharides (LPSs) are amphiphilic macromolecules indispensable for the growth and the survival of Gram-negative bacteria, one of the most diffuse classes of pathogenic bacteria. [1] are composed of a hydrophilic heteropolysaccharide unit, covalently linked to a lipophilic moiety called lipid A, which is embedded in the outer leaflet and anchors these macromolecules to the lipid membrane. Recent studies have revealed that presumably the physical characteristics of these molecules are correlated to their biological activity. Here we present a structural study on the architecture and the conformation assumed by LPSs in the lipid membrane. Particularly, we try to connect their self-aggregation behavior to the molecular structure. The investigation has been performed using an experimental strategy which has been proved to be extremely informative on vesicle aqueous suspension and combines dynamic light scattering (DLS) to estimate vesicle dimension, small angle neutron scattering (SANS) to analyze the aggregate morphology and to estimate the thickness of the lipid bilayer and electron paramagnetic resonance (EPR) to investigate the dynamics of the lipid hydrophobic tail in the bilayer.

[1] A. Silipo et al. Prokaryotic Cell Wall Compounds; Structure and Biochemistry, ed. H. König, H. Claus and A. Varma, Springer, Heidelberg, 2010.

[2] G. D'Errico et al. Chemistry Chemical Physics, 2009, 11 (13), 2314–2322.

B-05

The calcium phosphate binding properties of the serum protein fetuin-A explored with SANS contrast variation technique

A. Hiess[1], V. Pipich[2], W. Jahnen-Dechent[1], D. Schwahn[3]

[1] RWTH Aachen, Biomedical Engineering, Germany

[2] Jülich Centre for Neutron Science at FRM II, Garching, Germany

[3] FZ Jülich GmbH, Institut für Festkörperforschung, Germany

The patho-physiologic relevance of the serum protein fetuin-A/alpha$_2$ HS-glycoprotein as a systemic inhibitor of uncontrolled mineral deposition in the soft tissue has been demonstrated in fetuin-A knockout mice [1]. Moreover, clinical studies showed that patients with a low fetuin-A serum level are exposed to an increased calcification risk [2]. To elucidate the inhibition mechanism of calcification by the protein fetuin-A, we explored several *in vitro* model systems with SANS contrast variation technique [3]. The principle outcome was a two stage formation process of transiently stable nanometer sized colloidal composites of fetuin-A and calcium phosphate, which we denoted as calciprotein particles (CPPs); the initial form is spherical with a diameter in the 500 Å range which, after several hours at room temperature, transform to elongated particles of about twice the initial size. The CPPs consist of fetuin of about 25 % volume fraction and of the octacalcium phosphate (OCP) polymorph representing the mineral phase [3]. The secondary CPPs are stable for at least 24 hours, which can be explained by a dense fetuin monolayer covering the mineral as determined from SANS contrast variation experiments [3].
However, a detailed analysis suggested that the buffering of calcium and phosphate ion super saturation by the CPPs is not the whole story of the inhibition mechanism. The analysis of the SANS scattering patterns revealed that 3-5 % of the total fetuin-A and about half of the total mineral can only be attributed to the CPPs. As SANS reflects the presence of fetuin monomers at large momentum transfer, we speculated that the other half of the mineral is attached to the monomers. Recent contrast variation experiments indeed identified these particles as calciprotein monomers (CPM) with varying amount of the mineral when changing the fetuin concentration [4]. So, the inhibition mechanism of mineralization in the presence of the protein fetuin-A proceeds on two pathways, namely by CPP and CPM formation.

[1] C. Schäfer et al. (2003) J. Clin. Invest. 112, 357.
[2] M. Ketteler et al. (2003) Lancet 361, 827.
[3] A. Heiss, W. Jahnen-Dechent, H. Endo, D. Schwahn, (2007) Biointerphases 2, 16.
[4] A. Heiss, V. Pipich, W. Jahnen-Dechent, D. Schwahn, (2010) Biophys. J. (submitted).

B-06

Protein-protein interactions in concentrated electrolyte solutions studied by SANS

F. Zhang[1], M. W. A. Skoda[2], R. M. J. Jacobs[3], P. Callow[4], H. Frielinghaus[5], V. Pipich[5], S. Prévost[6], F. Schreiber[1]

[1] Universität Tübingen, Institut für Angewandte Physik, Germany

[2] ISIS, Rutherford Appleton Laboratory, Chilton, Didcot, United Kingdom

[3] University of Oxford, Department of Chemistry, United Kingdom

[4] Institut Laue–Langevin, Grenoble, France

[5] Jülich Centre for Neutron Science at FRM II, Garching, Germany

[6] HZB für Materialien und Energie GmbH, Berlin, Germany

Proteins are commonly found in relatively concentrated salt solutions during protein crystallization and purification. The protein-protein interactions under these conditions are far from understood on a fundamental level, despite the obvious practical relevance. We have studied a model globular protein (bovine serum albumin, BSA) in concentrated salt solutions (up to 4 M) as a function of ionic strength and the type of salt by small-angle neutron scattering (SANS). The data are also compared with previous study using SAXS [1,2]. SANS results for dilute protein solutions (below 20 mg/mL) give an averaged dimension of BSA of 13×42×42 Å^3, corresponding to a volume of 95,800 Å^3 which is in good agreement with the volume of serum albumin determined from the crystal structure (92,000 Å^3). This dimension is smaller than that determined by SAXS as 17×42×42 Å^3 with a volume of 125,300 Å^3 [1]. The difference in volume (30 %) fits nicely to the contribution of hydration shell with a hydration level of 0.3 g/g protein. It is therefore concluded that SANS on protein solutions in D_2O probe mainly the “dry” volume of the protein without significant contribution from hydration shell, whereas SAXS probes the “wet” volume by including the hydration shell. In concentrated electrolyte solutions, the electrostatic repulsion due to the surface charge is significantly screened and the forward intensity I(0) determined from Guinier analysis can be used to determine the second virial coefficient, A_2 which describes the overall protein interactions in solution. It is found that the A_2 follows the reverse of the Hofmeister series, i.e. $(NH_4)_2SO_4$<NaOAc<Na_2SO_4<NaCl<$NaNO_3$<NaSCN. The contribution from the hard core A_2^{HS} and the salts are also discussed. SANS data are further analyzed on the full q-range based on liquid theory, which provide the details of the origin of the interactions.

[1] Zhang, F.; Skoda, M. W. A.; Jacobs, R. M. J.; Martin, R. A.; Martin, C. M.; Schreiber, F. J. Phys. Chem. B 2007, 111, 251.

[2] Zhang, F.; Skoda, M. W. A.; Jacobs, R. M. J.; Zorn, S.; Martin, R. A.; Martin, C. M.; Clark, G. F.; Weggler, S.; Hildebrandt, A.; Kohlbacher, O.; Schreiber, F. Phys. Rev. Lett. 2008, 101, 148101.

Cultural Heritage

CH-01

Neutron Imaging of archaeological waterlogged wood

T. Demoulin[1], R. Gebhard[1], B. Schillinger[2]

[1] Archäologische Staatssammlung München, Germany

[2] Forschungs-Neutronenquelle Heinz Maier-Leibnitz (FRM II), Garching, Germany

As an organic material, wood is prone to decay. However, under specific conditions, even very old wooden artifacts can be found in a good state. That is the case for wood found in humid places, where the water inside the wood helps to preserve the original shape of the object.

The main challenge for the curator is to dry the wood without deteriorating the object. This is often done by replacing some of the water by polyethylene glycol (PEG), and then removing the remaining water by freeze-drying, with the PEG serving as a consolidant. The present study is an attempt to locate the PEG by means of neutron imaging, which largely relies on the strong interaction of neutrons with hydrogen. Hydrogen being the main component of PEG, the cross section of the PEG is much higher than the one of wood.

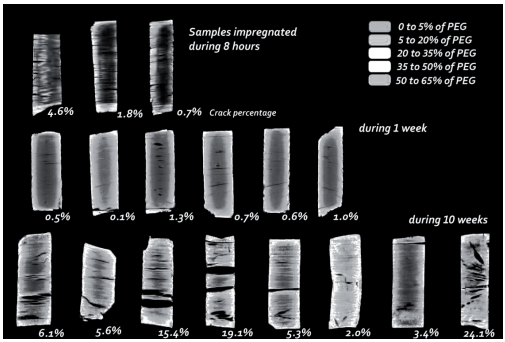

Fig.1: Distribution of PEG in wood derived from neutron attenuation.

Eighteen samples with a size of 2 x 1 x 6 cm treated in different ways have been studied. In particular, the impact of the duration of the impregnation and of the use of PEG of different molecular weight has been investigated. Results for the neutron attenuation in wood treated in different ways are shown in Fig. 1.

While impregnation during eight hours does not allow the PEG to penetrate fully into the wood, impregnation for one or ten weeks leads to good PEG penetration, though the homogeneity of the PEG distribution is better after ten weeks of impregnation.

The efficiency of the PEG treatment is essential for avoiding the formation of cracks and voids during freeze-drying, but often this cannot be completely avoided. Fig. 2 shows that, owing to the large difference in neutron attenuation in the wood and cracks and voids, neutron tomography can be used very effectively to monitor the distribution of such defects in dried wood.

Fig. 2: Imaging of cracks.

CH-02

Elemental determination of archaic ceramics using PGGA

I. M. Siouris[1], P. Lazaropoulou[1], S. Katsavounis[1], S. Söllradl[2]

[1] Democritus University of Thrace, Production and Management Engineering Department, Xanthi, Greece

[2] Forschungs-Neutronenquelle Heinz Maier-Leibnitz (FRM II), Garching, Germany

During the present work we have perform non-destructive elemental analysis on three archaic Grecian ceramic vases which are currently under reconstruction and restoration at the Kavala Museum. The goals set during this analytical study intended to : a) evaluate the method in obtaining the elemental compositions of the various ceramic samples and b) compare the results obtained by PGAA to those collected using non- destructive as well as destructive SEM –EDX analysis. Additionally we discover traces of secondary elements dissolved in the primary matrix as initially anticipated, which enable us to correlate the staring materials to certain pertinence.

Evaluation measurements on twenty one (21) ceramic shards were performed. The selected items are shown on picture 1. The samples were collected from the the excavation at Via Egnatia from the interchange of Chrisoupolis to Nestos in North East Greece (see attached map). They were of different style or usage and found to be at various stages of damage, with many pieces scattered around, so a complete reconstruction of the items based only on visual means would be tedious as well as inadequate.

Recently, we used both destructive and non-destructive SEM, on the same samples, to measure the elemental compositions. Although we could identify a plethora of main and additional elements even in trace amounts (see table 1), the results obtained on the elemental compositions, between the two techniques, in most of the cases differed by a factor of 10- 20. On the other hand, evaluating the non-destructive capabilities of PGAA on the same pottery pieces, it was proved that quantitative elemental distributions can be derived from the bulk of the material, which is far better and more detailed than either of the SEM methods (see table 2).

From this work we concluded that in order to obtain more precise data, when dealing with high cross section elements, particularly in the lower energy spectrum, it is necessary to use a less intense beam, to reduce Compton scattering and apply longer exposure times for improved statistics. The cooling down parameters was also found to be no more than 24 hours.

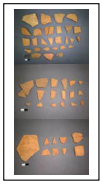

Reconstruction of the ceramic ornaments from shards

Furthermore the analysis of the PGAA data has provided complementary information on the elemental constitution of the ceramic shards which helped to the reconstruction of the pottery (see fig.2). Additionally the trace element study resulted in obtaining comparative information on provenance showing that the pottery pieces 12 and 14 were of local origin, whereas No 13 was a product of a different kiln.

CH-03

Non destructive stoichiometric determination of archaic metallic artefacts using PGGA

I. M. Siouris[1], L. Canella[2]

[1] Democritus University of Thrace, Production and Management Engineering Department, Xanthi, Greece

[2] Forschungs-Neutronenquelle Heinz Maier-Leibnitz (FRM II), Garching, Germany

Non-destructive evaluation measurements were conducted on eight bronze coins of Greco Roman dated around the 1st century AC, in the Lithochori, North East Greece and currently preserved in Kavalla Museum. The aim of this work was two fold: a)to determine the metallurgical distributions of the various Cu-Sn/Zn/Sb – main phases and identify traces of secondary elements dissolved in the primary matrix. Additionally this work has served as a guide in establishing the cooling down parameters and check the feasibility of method on such samples for future investigation of massive bronze samples items.

The over all experimental aims were achieved. Spectral analyses of the PGGA patterns (Fig.1) showed that the bulk metallurgical distributions with the corresponding weight fractions of the primary elements Cu/Sn - Cu/Sb - Cu/Zn and the Fe may be determined rather accurately. Furthermore traces of secondary elements dissolved in the primary matrix, that have not been discovered in the SEM investigation, can also been identified within the experimental limitations. The results are listed in Table 1. Additionally, it was established beyond any doubt that no silver or silver traces are contained in the any metallic object, contrary to the initial assumptions which were based on archeological (mainly visual) deductions.

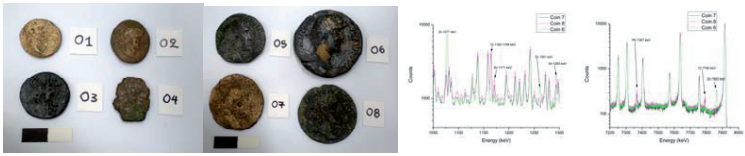

Samples and selected high and low energy PGAA spectra associated with the coin samples.

	Coin	Cu %	Zn %	Sn%	Pb%	Fe %	H %	Ni %	Co ppm	Cl% ppm
SEM	No 6	86.9	13.1							
PGAA		84. 6	13.5	1.9						
SEM	No 8	78	-	4.7	17.3					
PGAA		68.9	1.9	9.3	19.8					0.09
PGAA	No17b	3.6				94.0	1.79	0.26	410	330

List of the elemental compositions on three coins are presented. Results of SEM analysis are shown for comparison

This study showed that in order to obtain more precise data, longer exposure times should be applied for improved statistic. Moreover, to reduce Compton scattering it is necessary to use a less intense beam.

Furthermore the secondary goals set were also accomplished.

- The feasibility of method on measuring such type samples was found to be excellent.
- Exposure times to obtain good statistics were established.
- The cooling down parameters for future investigation of massive bronze samples items were also determined.

CH-04

Inside Mesopotamian “heamatite” objects

D. Visser[1,2], M. Schulz[3], B. Schillinger[3], M. Hofmann[3], C. Randau[4]

[1] TU Delft, RID, The Netherlands

[2] Loughborough University, Department of Physics, United Kingdom

[3] Forschungs-Neutronenquelle Heinz Maier-Leibnitz (FRM II), Garching, Germany

[4] GKSS-Forschungszentrum Geesthacht @ FRM II, Garching, Germany

Iron stone Mesopotamian seals are common objects in the Old Babylonian Period (2500 -1600 BC) and the much later Sassanide Period (226 -651 BC). The material is commonly referred to in museum collections as ‘heamatite’. However, recently we have demonstrated that these objects consists not only of the mineral hematite (Fe_2O_3), but also magnetite (Fe_3O_4), goethite (FeO(OH)) and iron oxide - loaded calcite (FeOx – $CaCO_3$) as well as a black glassy material (Fe-silicate glass?).

Time of flight powder neutron diffraction patterns can be used to obtain the phase content of the objects as well as determine changes to the crystal structure.

We proved using STRESS-SPEC, via texture measurements, that the ‘powder‘ approach is valid.

Neutron tomography shows that the objects are far from homogeneous. The grayscale distribution can also be used to identify the type of iron oxide material one is dealing with.

Indications of weathering on the surface of the objects is observed. Restoration attempts, crack lines: weak spots in the objects can be identified as well as the bore holes can be examined in detail.

Both neutron diffraction and the tomography data indicate that the origin of the ‘hematite ’objects is sedimentary.

The ‘heamatite’ collections of the RMO Leiden (NL), the Liagre–Böhl collection of the NINO Leiden (NL) and half fabricates and raw material from the LMU excavation of Tell-Bazi (Syria) were studied.

CH-05

Lost letters found

D. Visser[1,2], S. Badham[3], M. Mühlbauer[4], B. Schillinger[4], Z. Kazstovszky[5], A. Scherillo[6]

[1] TU Delft, RID, The Netherlands

[2] Loughborough University, Department of Physics, United Kingdom

[3] Monumental Brass Society, Burlington House, London, United Kingdom

[4] Forschungs-Neutronenquelle Heinz Maier-Leibnitz (FRM II), Garching, Germany

[5] KFKI Research Institute for Particle and Nuclear Physics, Budapest, Hungary

[6] ISIS, Rutherford Appleton Laboratory, Didcot, United Kingdom

Monumental tomb slabs in English country churches were, after the middle of the 13th Century, for the first time decorated with individual inlay lettering made of layton (brass). Towards the end of the 14th Century the individual lettering was replaced by lettering on brass strips. We investigated with neutron tomography a letter L which was found by means of metal detection in the bedding of a brook near North Stoke (OXON, UK) and a letter strip which was bought by the president of the Monumental Brass Society in an antique shop. We have been able to trace the letter L back to an incised tomb slab on the floor in the Norman church of North Stoke (OXON, UK). This monument is dated to ~1270 AD and therefore the letter L is also the earliest dated brass letter. The letter strip could be traced back to a monument in the Buckinghamshire church of Shootesbrooke.

We performed neutron tomography on both objects to determine the state of conservation of both objects. The letter L shows a deep uneven corrosion layer. The letter slab is in a much better state. There is an indication of possible coloring of the incised letters.

The brass composition has been further studied by means of PGAA and neutron time of flight diffraction.

This study forms part of a research program into the production, and workshop attribution of English monumental brass letters.

CH-06

Neutron tomography as a tool for art history and conservation

D. Visser[1,2], M. Mühlbauer[3], B. Schillinger[3]

[1] TU Delft, RID, The Netherlands

[2] Loughborough University, Department of Physics, United Kingdom

[3] Forschungs-Neutronenquelle Heinz Maier-Leibnitz (FRM II), Garching, Germany

In the Renaissance Bronze Cast Statuettes where a much appreciated art form. Attribution of statuettes to individual artist is often extremely difficult due to the lack of signature and/or art historical evidence. Attributions are made by visual inspection and comparison.
The casting techniques and reproduction processes for a number of objects have been based on often low-resolution X-ray radiography.
One of the authors pioneered the use of neutron tomography on Renaissance Bronze from the collection of the Rijksmuseum Amsterdam. The results were presented in the exhibition "From Vulcan Forge" shown at several around in Europe.
With neutron tomography we can dissect the 3-D reconstruction and study in detail the casting process, the core build up and the material us.
At FRM II we have studied 7 Renaissance bronzes varying in height between 10 – 35 cm. Different casting techniques are observed. In several cases we can establish that we are dealing with an original cast. Finally based on art historical information we may attribute the sculptures to a particular artist.
This research is part of a program to establish a protocol for non-destructive investigation of Renaissance bronzes with aim to shed more light on the functioning of different artist's workshops and providing sound scientific information for assisting curators in attribution and conservators in repair and conservation of these objects.

Excitations and Dynamics

ED-01

Effect of magnetic field on phonons in martensitic $Ni_{49}Mn_{32}Ga_{19}$

S. Chillal[1], S. Ener[1], J. Neuhaus[1,2], R. Mole[2], W. Petry[1,2]

[1] TUM, Physik Department, Garching, Germany

[2] Forschungs-Neutronenquelle Heinz Maier-Leibnitz (FRM II), Garching, Germany

Ferromagnetic shape memory materials exhibit a change of their shape on applying an external magnetic field. The magnetic field can induce two effects: the field induced structural transition (FIT) or a field induced variant reorientation (FIR) in the low temperature martensitic phase. For off-stoichiometric Ni-Mn-Ga alloys, the maximum recoverable strain attained by FIR is found to be ~10 % around room temperature [1].

Our previous studies showed that a softening anomaly occurs on approaching the structural phase transition in a $Ni_{49}Mn_{32}Ga_{19}$ at a particular region of the $TA_2[\xi\ \xi\ 0]$ phonon branch. Additionally, low energy excitations of the modulated martensitic structure are observed as shown in fig 1.a.

In the present work, we investigate the effect of the magnetic field (parallel to the magnetic easy axis of the alloy) on FIR property of a martensitic $Ni_{49}Mn_{32}Ga_{19}$. The $TA_2[\xi\ \xi\ 0]$ phonon branch and the low energy excitations were measured as a function of a magnetic field along the caxis. Later, the field is inverted in order to possibly induce a reorientation of variants. The $TA_2[\xi\ \xi\ 0]$ and low energy excitations were measured at 0T, 4T, 5T, -1T and -2T for specific phonon modes of ξ = 0.35, 0.375, 0.45 which are the reduced wave vector points close to the phonon softening observed by varying the temperature. We show that the frequencies of $TA_2[\xi\ \xi\ 0]$ and low energy excitations lie within the error bars and do not show significant change in the phonon frequencies values as a function of magnetic field as shown in fig 1.b. As crystallographic axis is the direction of easy axis of magnetization for $Ni_{49}Mn_{32}Ga_{19}$, the applied field does not induce directly a reorientation. Therefore a horizontal field would be required. To distinguish between the reorientation and a magnetic field dependence of the phonons this experiment approved the zero value for further studies. We conclude that the application of a magnetic field along the easy axis of magnetization does not affect the vibrational properties of the alloy significantly.

a) b)

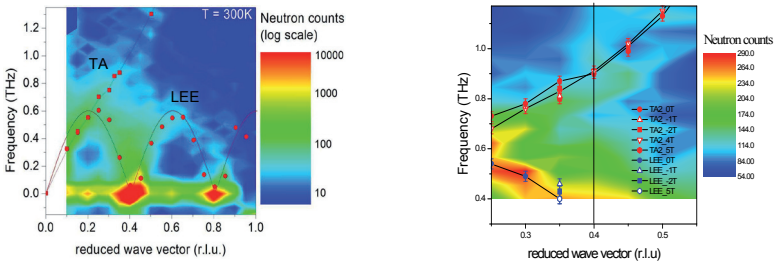

Fig 1: Low frequency region of phonon dispersion in high symmetry direction [110] of Ni superstructure bragg peaks at commensurate positions in zero magnetic field, b) Part of the phonon frequency region under magnetic fields of 0T, 4T, -1T, -2T and LEE at 0T. (LEE: low energy excitations)

[1] A. Sozinov al, App. Phys.Lett 80, 10, 1747 (2002).

ED-02

Time-resolved phonons in demixing systems

F. Güthoff, J. Davaasambuu, K. Hradil, G. Eckold

Universität Göttingen, Institut für Physikalische Chemie, Germany

Phonons reflect most directly the chemical interactions in solids. Hence, time-resolved lattice-dynamical experiments yield detailed information about the trajectories and mechanisms of solid state reactions.
Using the example of demixing-processes in the model-systems of silver-alkali halides we were able to demonstrate that the phase separation is a two stage process. While stroboscopic inelastic neutron scattering from phonons unambiguously prove that chemical demixing in the spinodal regime takes place on a time-scale of seconds, the relaxation of the lattice as reflected by the structural Bragg reflections is a subsequent step on much longer temperature dependent time scale of hours, days or even months [1].
While previous real-time investigations were focussed on acoustic phonons, we have now extended our experiments to optical phonons that are particularly sensitive to the local structure. Lattice dynamical model calculations allow us to provide a microscopic interpretation of the experimental results. Additional phonon modes observed in the homogeneous phase can be interpreted on the basis of locally ordered structure. This seems to be different from the findings in metallic alloys, where usually broad phonon spectra are observed, rather than well defined local modes. The possible reason for the different behaviour of binary salts is the almost rigid frame of the anion sublattice that remains invariant during demixing and homogenization.
Of particular interest is the time-evolution of phonon life times. It will be demonstrated that these depend strongly on the overall composition of the sample. Minority phases that are formed during the initial stage of decomposition exhibit large phonon line widths due to the small special extend. Thus surface effects disturb the prolongation of lattice vibrations. Only if the precipitates grow beyond some critical size by coarsening effects, the width of phonon spectra is drastically reduced. Using the information of time resolved small angle scattering experiments, it is possible to estimate the precipitation size depending on the concentration of the silver alkali halide systems. This coarsening effect correlates with the evolution of the Bragg reflections.

[1] P. Elter, G. Eckold, H. Gibhardt, W. Schmidt, A. Hoser, J. Phys.: Condens.Matter 17, 6559 (2005). G. Eckold, D. Caspary, H. Gibhardt, W. Sschmidt, A. Hoser, J. Phys.: Condens.Matter 16 (2004) 5945. D. Caspary, G. Eckold, F. Güthoff, W. Pyckhout-Hintzen, J.Phys. Cond. Matter 13, 11521 (2001). G. Eckold, J. Phys. Cond. Matter 13, 217 (2001).

ED-03

Symmetry of spin excitation spectra in 122-ferropnictides

J. T. Park[1], D. S. Inosov[1], A. Yaresko[1], S. Graser[2], D. L. Sun[1], P. Bourges[3], Y. Sidis[3], Y. Li[1], J. Kim[1], D. Haug[1], A. Ivanov[4], K. Hradil[5,6], A. Schneidewind[5,7], P. Link[5], E. Faulhaber[5,7], I. Glavatskyy[8], C. T. Lin[1], B. Keimer[1], V. Hinkov[1]

[1] MPI für Festkörperforschung, Stuttgart, Germany
[2] Universität Augsburg, Institut für Physik, Germany
[3] Laboratoire Léon Brillouin, Gif-sur-Yvette, France
[4] Institut Laue-Langevin, Grenoble, France
[5] Forschungs-Neutronenquelle Heinz Maier-Leibnitz (FRM II), Garching, Germany
[6] Universität Göttingen, Institut für Physikalische Chemie, Germany
[7] Gemeinsame Forschergruppe HZB – TU Dresden, Berlin, Germany
[8] HZB für Materialien und Energie GmbH, Berlin, Germany

We have studied the symmetry of spin excitation spectra in 122-ferropnictide superconductors by comparing the results of first-principles calculations with inelastic neutron scattering (INS) measurements on $BaFe_{1.85}Co_{0.15}$ and $BaFe_{1.91}Ni_{0.09}As_2$ that exhibit neither static magnetic phases nor structural phase transitions. In both the normal and superconducting (SC) states, the spectrum lacks the three-dimensional (3D) $4_2/m$ symmetry around the (1/2 1/2 *L*) that is implied by the *I*4/*mmm* group. This is manifest both in the in-plane anisotropy of the normal- and SC-state spin dynamics and in the out-of-plane dispersion of the spin-resonance mode. We show that this effect originates from the higher symmetry of the magnetic Fe-sublattice with respect to the crystal itself, hence the INS signal inherits the symmetry of the unfolded Brillouin zone (BZ) of the Fe-sublattice. The in-plane anisotropy is temperature-independent and can be qualitatively reproduced in normal-state density-functionaltheory calculations without invoking a symmetry-broken ("nematic") ground state that was previously proposed as an explanation for this effect. Below the SC transition, the energy of the magnetic resonant mode ω_{res}, as well as its intensity and the SC spin gap inherit the normal-state intensity modulation along the out-of-plane direction *L* a period twice larger than expected from the body-centered-tetragonal BZ symmetry. The amplitude of this modulation decreases at higher doping, providing an analogy to the splitting between even and odd resonant modes in bilayer cuprates. Combining our and previous data, we show that at odd L universal linear relationship $\hbar\omega_{res} \approx 4.3 k_B T_c$ for all Fe-based superconductors, independent of their carrier type. Its validity down to the lowest doping levels is consistent with weaker electron correlations in ferropnictides as compared to the underdoped cuprates.

Preprint: arXiv:1007.3722

ED-04

Anisotropy gapped incommensurate magnetic excitations in $La_{(2-x)}Sr_xCuO_4$ (x=0.12)

K. Lefmann[1,2], A. T. Rømer[1], J. Chang[3], N. B. Christensen[1,3,4], B. M. Andersen[1], L. Mähler[3], J. Gavilano[3], C. Niedermayer[3], H. M. Rønnow[5], A. Schneidewind[6], P. Link[6], M. Oda[7], M. Ido[7], N. Momono[7], J. Mesot[3]

[1] University of Copenhagen, Niels Bohr Institute, Nanoscience Center, Denmark

[2] European Spallation Source, Lund, Sweden

[3] ETH Zürich, Laboratory for Neutron Scattering @ PSI, Villigen, Switzerland

[4] Technical University of Denmark, Materials Research Division, Risø, Denmark

[5] EPFL Lausanne, Switzerland

[6] Forschungs-Neutronenquelle Heinz Maier-Leibnitz (FRM II), Garching, Germany

[7] Hokkaido University, Department of Physics, Japan

We present high-resolution neutron spectroscopy of magnetic fluctuations in the high-temperature superconductor $La_{(2-x)}Sr_xCuO_4$. The Sr-doping is close to 1/8, which denotes the regime of suppressed superconductivity and enhanced magnetic order. The incommensurate magnetic fluctuations are observed for temperatures below and above the superconducting transition, T_c, and the scattering peaks above T_c, but then decreases rapidly above a threshold temperature. This threshold increases with fluctuation energy. At low temperatures, we observe an energy gap below which the intensity is partially suppressed. We attribute this gap to residual anisotropies of the magnetism in the mother compound $LaCuO_4$.

ED-05

Phonon anomalies and the BCS gap

N. Munnikes[1], T. Keller[1,2], B. Keimer[1]

[1] MPI für Festkörperforschung, Stuttgart, Germany

[2] Forschungs-Neutronenquelle Heinz Maier-Leibnitz (FRM II), Garching, Germany

The neutron resonance spin-echo (NRSE) spectrometer TRISP can be used to measure the natural linewidths of acoustic phonons throughout the Brillouin zone. We studied the contribution of electron-phonon (*e-ph*) interaction to the phonon linewidths in BCS superconductors. Phonons with energies smaller than the gap $2\Delta(T)$ cannot excite electrons, while the *e-ph* interaction for phonons with energies just above the gap is increased. This translates into a dip-peak structure in the linewidth as a function of phonon energy or, equivalent, wavevector with respect to the normal state linewidth just above the superconducting transition temperature. An unprecedented effect was observed in Nb and Pb in the lowest transverse acoustic branches in both [100] and [110] directions in reciprocal space: remarkably, at the same wavevector as the peak of the saturated gap $2\Delta(T \rightarrow 0)$, a linewidth broadening is present also in the normal state, at temperatures exceeding the transition temperature by far [1,2,3]. The linewidth broadening could in all cases be identified as being due to Fermi surface nesting, which is reflected in the phonon dispersion by a kink named Kohn anomaly. The fact that Nb and Pb have different structures and Fermi surface topologies suggests that the overlap is not a coincidence. If the superconducting energy gap indeed adjusts itself to the energy of phonons broadened by nesting whenever the two are close enough in energy, this could explain gap anisotropy in BCS superconductors.
To study the general validity of the lock-in effect, we continued research on the Tl-Pb-Bi alloy system. Bi, Pb and Tl are neighbors in the Periodic System of Elements, so that their alloys offer a gradually increasing Fermi surface and electron-phonon coupling strength. Detailed dispersion and linewidth data of three alloyed single crystals will be presented here. Also, results of measurements on tantalum and $NbSe_2$ will be shown. The consistency of dispersion and linewidth phenomena will be briefly discussed.

[1] T. Keller, P. Aynajian, K. Habicht, L. Boeri, S.K. Bose, B. Keimer, Phys. Rev. Lett. 96, 225501 (2006).
[2] P. Aynajian, T. Keller, L. Boeri, S.M. Shapiro, K. Habicht, B. Keimer, Science 319, 1509-1512 (2008).
[3] P. Aynajian, T. Keller, L. Boeri, B. Keimer, to be published.

ED-06

Kondo-Cluster-Glass formation in $CePd_{1-x}Rh_x$. A neutron depolarization study at milli-Kelvin temperatures

P. Schmakat[1], M. Schulz[2], C. Pfleiderer[1], P. Böni[1]

[1] TUM, Physik Department, Garching, Germany

[2] Forschungs-Neutronenquelle Heinz Maier-Leibnitz (FRM II), Garching, Germany

We have investigated the magnetic phase diagram of $CePd_{1-x}Rh_x$, a material which shows strong electronic correlation effects. At very low Rh-content x this Heavy-Fermion system shows quiet normal ferromagnetic behavior with Curie-temperatures in the Kelvin-range. With increasing Rh-content this ferromagnetic phase seems to split into a ferromagnetic phase and a strange spin-glass phase at even lower temperatures. The spin-glass formation might be driven by a quantum phase transition, a transition where quantum fluctuations can overcome thermal fluctuations. So far available magnetic phase diagrams do not reveal this second phase border, although some spin-glass features have already been discovered in previous bulk measurements. The phase border curvature for $x>0.6$ is considered to be an effect of disorder in the sample and could be the onset of the so called Quantum-Griffith-Phase. A distribution of lattice constants resulting in a distribution of Kondo-Temperatures is considered to induce this kind of phase border. Bulk measurements of the magnetization, AC-susceptibility, specific heat and thermal expansion have revealed the possible formation of a new phase in the region $0.6<x<0.9$ that was named Kondo- Cluster-Glass. The Kondo-Cluster-Glass is comparable to a spin-glass with magnetic clusters due to disorder in the system. The origin of this cluster-formation is assumed to be an interplay of metallurgical inhomogeneities and the effect of two competing interactions namely the Kondoscreening and the long-range RKKY-interaction. Our aim was to investigate the magnetic properties of this new state by means of Neutron Depolarization Imaging, a technique introduced at ANTARES, FRM II by M. Schulz during his doctoral thesis. This technique allows one to map inhomogeneities of the transition temperature and the low temperature spontaneous magnetization over the sample. With the current setup we were able to achieve a real-space resolution of about 300µm. An example of our measurements is shown in the figure below. The transition temperature of the shown sample is near 3K, the sample has a thickness of 1mm and a diameter of roughly 10mm. Of particular interest was the possible signature in depolarization data due to the Kondo-Cluster-Glass formation. Using a $^3He^4He$ dilution CCI in a ^4He CCR a low-temperature study was performed down to 75mK. With an additional coil-pair we were indeed able to trace the spin-freezing effect in four samples in the critical concentration range. Polarization-Curves, the resulting phase diagram and maps of the transition temperature and magnetization shall be presented on a poster.

A figure had been left out by editors for reasons of space.

ED-07

Neutron study of crystal field excitations in single crystal $CeCu_2Ge_2$

A. Schneidewind[1], M. Loewenhaupt[2], E. Faulhaber[1],M. Deppe[3], K. Hradil[4]

[1] Gemeinsame Forschergruppe HZB – TU Dresden, Berlin, Germany

[2] TU Dresden, Institut f˙ur Festkörperphysik, Germany

[3] MPI für Chemische Physik fester Stoffe, Dresden, Germany

[4] Forschungs-Neutronenquelle Heinz Maier-Leibnitz (FRM II), Garching, Germany

$CeCu_2Ge_2$ is the counterpart of the heavy-fermion superconductor $CeCu_2Si_2$. $CeCu_2Ge_2$ is a magnetically ordering (T_N= 4.1 K) Kondo lattice with a moderate Sommerfeld coefficient of 140 mJ/molK^2 [1]. Inelastic neutron measurements on a polycrystalline sample revealed a doublet ground state and a quasi-quartet at 16.5 meV [1] though a splitting of the 4f^1 (J=5/2) ground state multiplet into 3 doublets is expected from the point symmetry of the Ce^{3+} ions. We performed detailed inelastic neutron scattering experiments on the thermal triple-axis spectrometer PUMA at FRM II at temperatures between 3 K and 300 K along the (00L) and the (HH0) crystallographic directions from low to high momentum transfers. In this way we obtained a reliable separation of magnetic and phonon contributions. From our results we infer that the quasi-quartet consists in fact of two doublets at 17 and 18 meV which exhibit a strong directional dependence of their transition matrix elements to the ground state doublet. Finally we will present a new set of crystal field parameters and their implications on other magnetic properties.

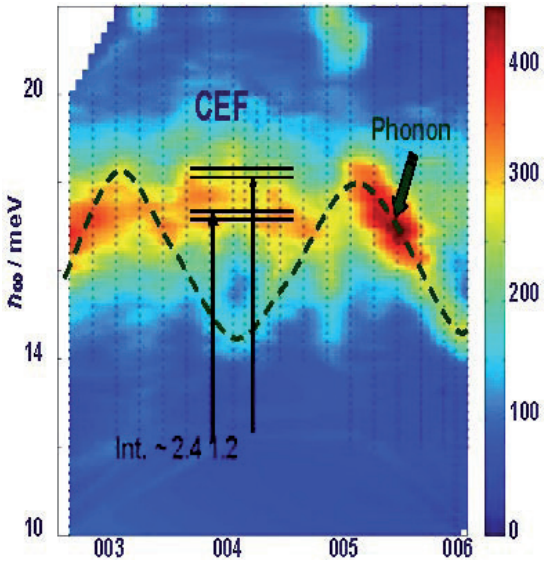

Fig. 1: Energy transfer map along the (00L)-direction in $GeCu_2Ge_2$ at T = 10K. Phonons hamper data acquisition, but on selected *q*-points (e.g. 004) the CEF and phonon contributions are well separated. With the line shapes and line widths determined there, a careful balancing of fix and variable parameters allows to fit the overlapping contributions in the whole *q*-range. The intensity ratios of CEF transitions observed along (00L) / (HH0) directions agree well with the calculated ratio.

[1] G. Knopp et al., Z. Physik B 77 (1989) 95.

ED-08

Low-frequency excitations in niobium-phosphate glasses for Raman gain applications probed by inelastic neutron and Raman scattering

A. Schulte[1], W. Schirmacher[2,3], T. Cardinal[4], S. Seal[5], T. Unruh[2,6]

[1] University of Central Florida, Physics Department and College of Optics & Photonics, Orlando, USA

[2] TUM, Physik Department, Garching, Germany

[3] Universität Mainz, Institut für Physik, Mainz, Germany

[4] University of Bordeaux, ICMCB, CNRS, Pessac, France

[5] University of Central Florida, Nanoscience Technology Center and Department of Mechanical Materials and Aerospace Engineering, Orlando, USA

[6] Forschungs-Neutronenquelle Heinz Maier-Leibnitz (FRM II), Garching, Germany

In disordered solids the breakdown of the wave-vector selection rule of crystalline Raman scattering leads to first-order continuous spectra of glasses instead of the discrete Raman spectrum of crystals [1,2]. The Raman and neutron spectra of glasses show a low-frequency enhancement of the vibrational density of states ('Boson peak') suggesting a significant gain profile for applications in Raman amplifiers [3]. We present measurements of the low frequency vibrational spectrum of niobium phosphate glasses using inelastic neutron and Raman scattering. The results of both spectroscopic probes can be reconciled within a recent theoretical model [4] that involves a spatially fluctuating shear modulus and spatially fluctuating Pockels coefficients. Inelastic neutron scattering experiments were carried out with the time-of-flight spectrometer (TOFTOF) at the FRM II neutron source. We compare the reduced Raman intensity at 295 K with the reduced q-averaged neutron intensity [5]. By averaging the neutron intensity $S(q,\nu)$ the full accessible scattering angle (wavevector q) we obtain a $g(\nu)$ which gives an approximate spectral distribution of the vibrational modes. The DOS was obtained by an iterative procedure after correcting for the Debye-Waller factor and multiphonon contributions. It can be seen that the positions of the maxima of the spectra do not coincide. Experimental data have in the past been interpreted in terms of a frequency dependent light-vibration coupling coefficient $C(\nu)$. However, it follows from a recently published rigorous theoretical treatment [4], based on the concept that light couples to the elastic strains via spatially fluctuating elasto-optic (Pockels) constants, that the Raman intensity is not to the DOS but to a convolution of $S(q,\nu)$ the Pockels-constant correlation function. Using this theory Raman and neutron intensities can be treated on the same footing without resorting to an empirical function $C(\nu)$.

We also present results of a recent experiment is to measure the low-frequency density of vibrational modes in powders of cerium oxide nanoparticles. Through comparison with the Raman data we discuss the state of coherence of the vibrational excitations and contributions from acoustical vibrations in nanoparticles.

A figure had been left out by editors for reasons of space.

[1] R. Shuker and R. W. Gammon, Phys. Rev. Lett. 25, -225 (1970).

[2] J. Jäckle, in: (Ed.), Amorphous Solids, . By W. A. Phillips, Springer, New York, p. 135 (1981).

[3] Y. Guo, S. Nonnenmann, A. Schulte, C. Rivero, K. Richardson, R. Stegeman, G. Stegeman, T. Cardinal, Conference on Lasers and Electro-Optics Technical Digest (OSA) CThP2 (2004).

[4] B. Schmid and W. Schirmacher, Phys. Rev. Lett 100, (2008); . 103, (2009).

[5] T. Unruh, A. Schulte, Y. Guo, W. Schirmacher, B. Schmid, J. Non-Cryst. So, in press (2010).

Instrumentation

I-01

Elliptical guide setup at MIRA

T. Adams[1], J. Repper[1,2], M. Rahn[1], R. Georgii[1,2], G. Brandl[1], R. Schwikowski[1,2], P. Böni[1], C. Pfleiderer[1]

[1] TUM, Physik Department, Garching, Germany

[2] Forschungs-Neutronenquelle Heinz Maier-Leibnitz (FRM II), Garching, Germany

Cold neutron diffraction is a powerful method to investigate magnetic properties of materials. In these experiments the signal intensity is directly proportional to the irradiated sample volume. Therefore, especially for small sample volumes high-intensity neutron beams are requested. The intensity of cold neutron beams, however, are limited. Elliptic neutron guides focus the beam intensity to a small focal point on the sample position. Here we present first experimental results with a portable elliptical guide setup, which is easy to mount on the sample table of the neutron instrument MIRA (figure 1). The gain in signal intensity as well as the improved signal to background ratio is shown.

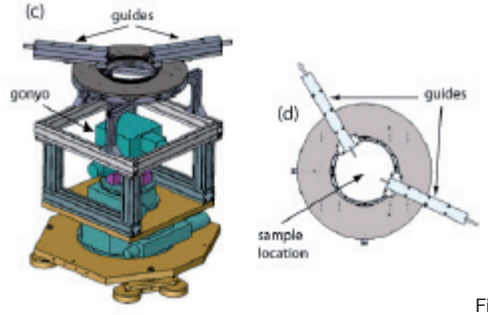

Fig. 1: The portable elliptical guide setup used at MIRA.

I-02

High pressure for small angle neutron scattering investigation

M.-S. Appavou

Jülich Centre for Neutron Science at FRM II, Garching, Germany

High Pressure is a physical parameter which allows to investigate volume change in system like polymer and protein. For biomolecules studies, this is also important because of the use of high pressure for new sterilization and bio-conservation processes. In a fundamental point of view, pressure leads to new protein folding pathways [1]. Structural investigations on protein can be performed using small angle neutron scattering (SANS) techniques [2]. We will present the new high pressure developed for SANS studies at the Forschungszentrum Jülich GmbH and available for neutron scattering users. This pressure cell is based on sapphire windows and can sustain pressure up to 5000 bar. The sample is prepared in a pill which will be set between two sapphire blocks. The body is made in a non-magnetic material in order to perform measurement with polarization analysis and, later, using neutron spin echo scattering technique for dynamical investigation. We will present also the Jülich small angle neutron scattering instruments KWS-1 and KWS-2 which are installed in the neutron guide hall of FRMII facility in Garching near Munich [4]. Preliminary results on myoglobin in solution under pressure using this new sample environment will be presented.

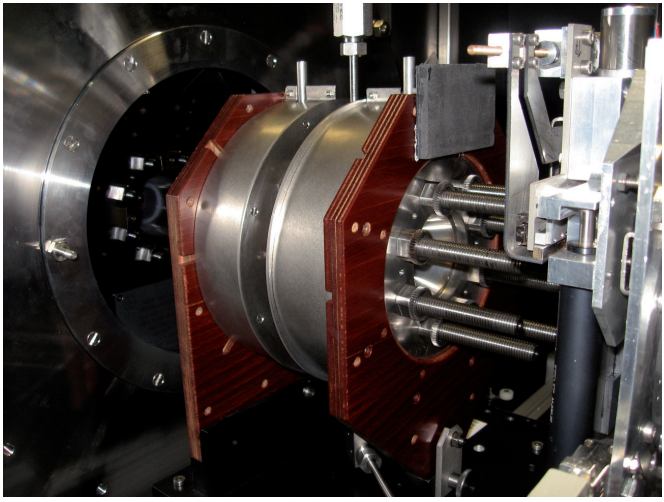

[1] Balny C, Masson P, Heremans K (2002), Biochim. Biophys. Acta 1595, pp 1–402.
[2] Loupiac C, Bonetti M, Pin S, Calmettes P (2002), Eur. J. Biochem., 269, 2002, pp 4731-4737.
[3] Kohlbrecher J., Bollhalder A., Vavrin R., Meier G, Rev. Sci. Instr., 78, 2007, pp1251011-1251016.
[4] A. Radulescu and A. Loffe, Nucl. Instrum. Methods A 586, 2008, p 55.

I-03

NECTAR – A fission neutron radiography and tomography facility

T. Bücherl[1], C. Lierse von Gostomski[1], H. Breitkreuz[2], M. Jungwirth[2], F. M. Wagner[2]

[1] TUM, Institut für Radiochemie, Garching, Germany

[2] Forschungs-Neutronenquelle Heinz Maier-Leibnitz (FRM II), Garching, Germany

NECTAR (**Ne**utron **C**omputerized **T**omography **A**nd **R**adiography) is a versatile facility for radiographic and tomographic investigations as well as for neutron activation experiments using fission neutrons.

The radiation sources for this facility are two plates of highly enriched uranium situated in the moderator vessel in the FRM II. Thermal neutrons origin from the main fuel element of the reactor, generate in these plates fast neutrons. These can escape through a horizontal beam tube without moderation. The beam can be filtered and manipulated in order to reduce the accompanying gamma-radiation and to match the specific experimental tasks, both.

A summary of the main parameters required for experimental set up and for (quantitative) data evaluation is presented. The (measured) spectra of the neutron and gamma-radiation are shown as well as the effect of different filters on their behaviour. The neutron and gamma flux, dose-rates, L/D-ratios etc. and the main parameters of the actually used detection systems for neutron imaging are given, too.

I-04

The new PGAA facility implementation process at ITN, Portugal: environmental applications

N. Canha[1], H. M. Dung[1], M. do Carmo Freitas[1], S. M. Almeida[1], L. Canella[2], S. Söllradl[2], P. Kudějová[2], Z. Révay[3]

[1] Instituto Tecnológico e Nuclear, Unit of Reactors and Nuclear Safety, Sacavém, Portugal

[2] Forschungs-Neutronenquelle Heinz Maier-Leibnitz (FRM II), Garching, Germany

[3] Hungarian Academy of Sciences, Institute of Isotopes, Budapest, Hungary

Prompt γ neutron activation analysis (PGAA or PGNAA) is a radioanalytical technique which has several advantages towards others NAA methods, such as the quick acquisition of results, the non-destructive analysis of samples with neutrons and the easy determination of some light elements (for example H, B, C, N and S). To complement our available NAA techniques, mainly for environment samples, a new PGAA facility has been implemented at the RPI (Portuguese Research Reactor) at ITN, Portugal. Implementation process is described and our facility design is discussed attending the reactor characteristics. The main properties and characteristics of the facility are presented. Several experiments were conducted at the new facility with reference materials to confirm its reliability.

A set of environmental samples (soils and air filters) was also analyzed at the new PGAA facility and it was analyzed as well in the Budapest reactor (Institute of Isotopes, KFKI, Hungary) and in the Munich reactor (FRM II at the TUM, Germany). Results obtained between PGAA facilities were compared and the performance of our facility was assessed towards this type of samples. The main goals of this work is 1) to describe the implementation process of the PGNAA facility at ITN, its main characteristics and analysis potential through the comparison of the results obtained in this new facility with the results obtained in two others european facilities; 2) to apply PGAA to air particulate matetr collected at a traffic tunnel downtown Lisbon. Analysis sofar were performed at FRM II. Comparison will bw done with INAA results whenever possible.

In the past 30 years, outdoor levels of some pollutants are decreasing in many cities of Europe and US, due to emission controls on vehicles, heating, power generation and industry. However in developing countries the outdoor air pollution is worsening due to the increasing number of vehicles and industry. The major outdoor air pollutants are particulates, O3, CO, SO_x, H_2S, acid gases (HF, HCl), NO_x, Pb and other metals, volatile organics, solvents, pesticides, methane, bioaerosols, and gamma radiation. Many of them are under regulation by European Union. 100 % of new cars sold in USA and 85 % of new cars sold worldwide are being equipped with catalytic converters in order to keep them meeting the vehicle emission standards of gaseous pollutants.

In this work, we measured several particles with different aerodynamic diameter, from the very fine (0.025 μm to 10 μm) in a city tunnel where 200,000 vehicles from commuters circulate at traffic hours. The total number of samples rounds 25. This is the ideal situation where traffic is the only possible emission source. PGAA are being applied to assess the pollutant concentrations. Results show a concentration of pollutants at rush hours, with substantial decrease during the weekends. Data are discussed taking into account the EU legislation. Quality control is done by analyzing NIST 2783 standard reference material.

I-05

Positronenlebensdauerspektroskopie mit dem gepulsten Positronenstrahlsystem PLEPS

W. Egger, L. Ravelli, B. Löwe, P. Sperr, G. Kögel, G. Dollinger

Universität der Bundeswehr München, Institut für Angewandte Physik und Messtechnik, Germany

Positronen sind ideale Sonden zur zerstörungsfreien Untersuchung von leerstellenartigen Defekten im Festkörper. Aus Positronenlebensdauermessungen erhält man Information über Art und Konzentration von Leerstellen, Leerstellenclustern und Versetzungen. Konventionelle Positronenannihilationsmethoden erlauben jedoch keine tiefenselektive Zuordnung der Defekte, da über makroskopische Volumina gemittelt wird. Zudem beschränkt Sättigungseinfang der Positronen in einem Defekt die Möglichkeit zur Bestimmung der Defektkonzentration.

Diese Nachteile werden durch den Einsatz gepulster, niederenergetischer Positronenstrahlen zur Lebensdauermessung weitgehend beseitigt. Mit gepulsten Positronenstrahlen variabler Energie können Tiefenauflösungen im Nanometerbereich erzielt werden. Aus Tiefenprofilmessungen kann zudem selbst bei Sättigungseinfang die Defektkonzentration ermittelt werden.

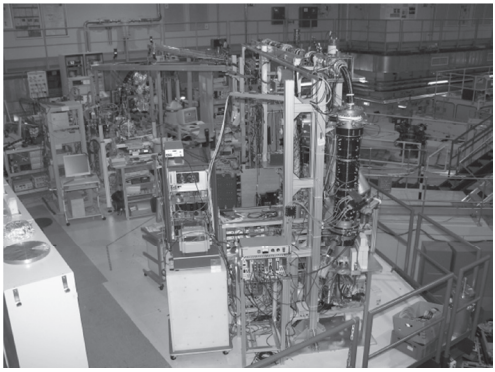

Seit April 2008 betreibt die Universität der Bundeswehr das europaweit einzigartige gepulste Positronenstrahlsystem PLEPS (Pulsed Low Energy Positron System) [1] (Abb.1) an der hochintensiven Positronenquelle NEPOMUC am FRM II [2]. In Zusammenarbeit mit externen Usern wurden mit PLEPS zahlreiche Untersuchungen an Metallen, Legierungen, Halbleitern, Isolatoren und Polymeren erfolgreich durchgeführt (Beispiele siehe [3-9]). In diesem Poster stellen wir PLEPS vor, präsentieren ausgewählte Beispiele für tiefenaufgelöste Defektuntersuchungen mit PLEPS und gehen auf zukünftige Weiterentwicklungen und geplante Messungen ein.

[1] P. Sperr et al., Appl. Surf. Sci. 255 (2008) 35.
[2] C. Hugenschmidt et. al., Nucl. Instr. Meth. A 593 (2008) 616.
[3] J. Čížek et al., phys. stat. sol. (c) 6 (2009) 2364.
[4] V. Kršjak et al., phys. stat. sol. (c) 6, (2009), 2339.
[5] P. Mazzoldi et al., J. Phys. D: Appl. Phys. 42 (2009) 115418.
[6] D. Keeble et al., Phys. Rev. B 81 (2010) 064108.
[7] A. Cano-Odena et al., J. Phys. Chem. B 113 (2009) 10170.
[8] R. Ferragut et al., J. Phys.: Conf. Ser. 225 (2010) 012007.
[9] K. Rätzke et al., Acta Biomater. 6 (2010) 2690.

I-06

Polarized neutron scattering on the triple-axis spectrometer PANDA: first results

E. Faulhaber[1], A. Schneidewind[1], F. Tang[2], P. Link[3], D. Etzdorf[3], M. Loewenhaupt[1,2]

[1] Gemeinsame Forschergruppe HZB – TU Dresden, Berlin, Germany

[2] TU Dresden, Institut für Festkörperphysik, Germany

[3] Forschungs-Neutronenquelle Heinz Maier-Leibnitz (FRM II), Garching, Germany

Typical applications of cold neutron triple-axis spectrometers comprise studies of spin dynamics and lattice dynamics, magnetic excitations and magnetic structures. In the past years, the PANDA spectrometer, located at the German research reactor FRM II, has shown excellent performance in these fields operating in conventional, unpolarized mode. To complement this normal mode of operation, a full polarization analysis of the scattered neutrons was highly desired and, therefore, was recently implemented at PANDA. First tests to characterize the different components for the polarization mode were performed with neutron spin directions perpendicular to the scattering plane, utilizing static vertical guide fields between sample, Heusler monochromator and Heusler analyzer and spin flipper. The very promising results obtained this way are shown in Figs. 1 and 2. At optimum compensation current, the direct beam intensity varies with the flip-field current of the spin flippers as shown in Fig. 1. Both spin flip (sf) and non spin flip (nsf) scans for the (2 0 0) Bragg reflection of lead are shown in Fig. 2a and for the spin incoherent scattering of vanadium in Fig. 2b. From this data a flipping ratio in the order of 40 is obtained, resulting in a beam polarization of about 0.95. Finally, a fully automated setup of split coils around the sample space was implemented to allow for longitudinal polarization analysis for arbitrary configurations. We will present first results obtained by the completed set-up in various polarization modes and discuss the status of the polarization analysis on PANDA in detail.

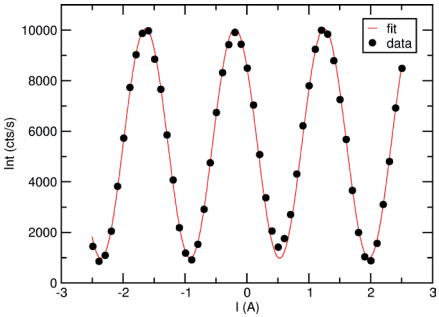

Fig. 1: Direct beam intensity, varying with the spin flippers flip field current at optimized compensation current, showing a minor depolarization.

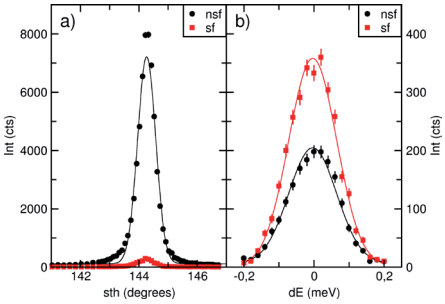

Fig. 2: Scans with polarized neutrons (P⊥Q) on the (2 0 0) Bragg reflection of Pb (a) and on the elastic line of vanadium (b). (Red: spin flip (sf), black: non spin flip.)

I-07

The improved state of STRESS-SPEC for texture characterization

W. Gan[1], C. Randau[2], M. Hofmann[3], H.-G. Brokmeier[1,2], M. Müller[1], A. Schreyer[1]

[1] GKSS-Forschungszentrum Geesthacht, Germany

[2] TU-Clausthal, Institut für Werkstoffkunde und Werksofftechnik, Germany

[3] Forschungs-Neutronenquelle Heinz Maier-Leibnitz (FRM II), Garching, Germany

Thermal neutron diffraction is the leading method for non-destructive global texture measurement in metals, alloys, composites, ceramics and rocks up to sample volumes in the cm^3 range. Moreover, local or gradient texture analysis along samples' main axis by neutron diffraction takes more advantages over those by normal X-ray and EBSD in desirable detected volume fraction, sample preparation and data processing, etc.
STRESS-SPEC is a high flux neutron diffractometer and offers a flexible instrument setup suitable for fast global and local texture analysis. With a great efficiency increase of the newly installed 2D area detector the pole figure measurement has been speeded up. In-situ strain and FWHM pole figure can also be investigated using the upgraded tensile machine nowadays. In addition, the newly developed robot system will allow the automatic and precise sample changing and positioning which will greatly improve the efficiency of beam time.
In this contribution, recent examples will be shown to indicate the improved state of STRESS-SPEC for texture characterization. Local texture analysis in a Cu ring using the robot system firstly will also demonstrate more flexibilities of STRESS-SPEC for texture analysis.

I-08

The new SANS-1 instrument at FRM II

R. Gilles[1], T. Heller[1], S. Semecky[1], H. Türck[1], K. Zeitelhack[1], A. Ostermann[1], I. Defendi[1], J. Krüger[1], U. Reinecke[1], C. Breunig[1], T. Keller[1], W. Petry[1], A. Heinemann[2], A. Beldowski[2], O. Frank[2], D. Heims[2], J. Buhrz[2], G. Musielak[2], H. Eckerlebe[2], J. Burmester[2], A. Vogel[2], M. Müller[2], A. Schreyer[2]

[1] Forschungs-Neutronenquelle Heinz Maier-Leibnitz (FRM II), Garching, Germany

[2] GKSS-Forschungszentrum Geesthacht, Germany

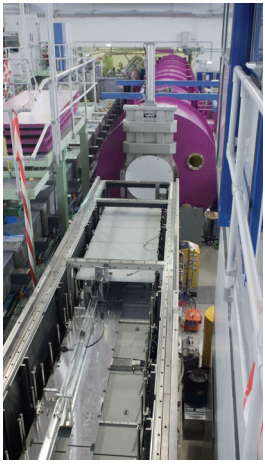

Fig. 1: Open collimation and detector vessel.

The new small-angle scattering instrument SANS-1, a project of the Technische Universität München and the GKSS in Geesthacht is currently build at the new Foschungsneutronenquelle Heinz Maier-Leibnitz, FRM II. This contribution describes the concept, the technical features, and the currently status of the instrument. To optimise the SANS-1 instrument with the claim to be at the "state of the art" many calculations and variations of instrument parameters were performed by Monte Carlo simulations in advance. Results of these simulations are a vertical S-shaped neutron guide with extreme suppression of fast background neutrons optimized for complementary wavelength packages, a tower with two eligible selectors, one for medium resolution at high intensity and one for high resolution (optional) and two optimised Fe/Si transmission polarizers. After passing the selector tower a collimation system with four parallel horizontal tracks is installed, one track is occupied with a neutron guide, another one with apertures for improving resolution, one position is for a laser system to support alignment and the last one is equipped with background apertures and could be used for lenses. The sample position is equipped with a tower allowing lateral movements and different rotations of the samples and the sample environ-ment in a flexible way. The detector tube of around 2.4 m inner diameter allows to use an area detector of 1 x 1 m^2 with lateral movement of more than 0.5 m. The detector is equipped with 128 position sensitive detectors to provide 8 mm x 8 mm pixel resolution. A second detector will be installed behind this large area detector for measurements simultaneously at low q-values.

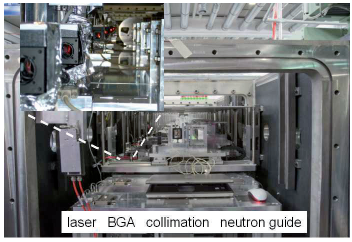

Fig. 2: The four tracks of the collimation system.Inset: A zoom of the laser alignment equipment.

[1] R. Gilles, A. Ostermann, C. Schanzer, B. Krimmer, W. Petry, 2006, Physica B, 385-386, 1174.
[2] R. Gilles, A. Ostermann, W. Petry, 2007, J. Appl. Cryst., 40, s428.

http://www.frm2.tum.de/sans1

I-09

Completion of the comprehensive KWS-3 upgrade: High resolution small-angle neutron scattering at FRM II available since December 2009

G. Goerigk

Jülich Centre for Neutron Science at FRM II, Garching, Germany

Small-Angle Scattering (SAS) is used for the analysis of structures with sizes just above the atomic scale between 1 and about 100 nanometers (nm), which cannot be assessed or sufficiently characterized by microscopic techniques. KWS-3 is an important supplementary instrument, which extends the accessible range of scattering angles to very small scattering angles with a superior neutron flux when comparing to a conventional instrumental setup with pinhole geometry. Thus the length scale, which can be analyzed, is extended beyond 1 micrometer for numerous materials from physics, chemistry, materials science and life science, like alloys, diluted chemical solutions and membrane systems.
After moving from Jülich to Munich the instrument underwent a fundamental evaluation with the final result, that a major upgrade for the whole instrument became necessary. The main topic of the upgrade project was a general mirror refurbishment i.e. a new polishing and subsequently a new coating of the mirror surface with the isotop ^{65}Cu with the aim to improve the resolution properties of the whole instrument. The mirror refurbishment was successfully performed by Carl Zeiss Laser Optics GmbH. Due to the minimization of the mirror's micro roughness the parasitic scattering contributions have been reduced by about a factor of 3, when comparing to the old mirror coating. In parallel to the mirror refurbishment comprehensive upgrade activities in the vacuum system, electronics and programming have been performed with the aims of protecting the new mirror coating from aging (degradation of the mirror's surface properties), transforming the instrument into a user-friendly state and introducing conceptual improvements like an additional sample position at 1 m distance bridging into the Q-range of the other SANS machines.

I-10

Slow motions observed with the neutron spin-echo spectrometer J-NSE

O. Holderer[1], M. Zamponi[1], M. Monkenbusch[2], D. Richter[2]

[1] Jülich Centre for Neutron Science at FRM II, Garching, Germany

[2] FZ Jülich GmbH, Institut für Festkörperforschung, Germany

Neutron spin-echo (NSE) spectroscopy is the highest resolution technique in inelastic neutron scattering and therefore allows observing slow processes on mesoscopic length scales. Spin manipulations of the neutrons are used to convert tiny velocity changes of the neutron during the scattering process into changes of the polarization of the neutron beam. The final polarization is proportional to the intermediate scattering function S(Q,t) of the sample. The maximum achievable Fourier time, t, determines the slowest observable movements. The wave vector Q determines the spatial length scale of observation. The time- and length scales investigated are of the order of ~0.1...10 nanometer and 0.01...100 nanoseconds. The diffusion or internal motions of polymers or thermally activated membrane fluctuations in microemulsions take place in that region of time and space.
Examples from experiments from different fields, as e.g. the dynamics of microemulsions, microgels or polymers in confinement will be presented. Beyond that NSE offers the opportunity to measure slow diffusion on the molecular to mesoscopic scale down to 10-14 to 10-15 m2/s, e.g. of protons in solid electrolytes or other ions, in hydrogen storage materials or molecules in catalysts.

[1] O. Holderer et al., Nucl. Instr. Meth. A, 586 (2008) 90.
[2] O. Holderer et al., Meas. Sci. Technol. 19 (2008) 034022.

I-11

The triple axis neutron spectrometer PUMA (FRM II) and its application for the investigation of solid state materials

K. Hradil[1], N. Jünke[1], V. Meyer[2], G. Eckold[2]

[1] Forschungs-Neutronenquelle Heinz Maier-Leibnitz (FRM II), Garching, Germany

[2] Universität Göttingen, Institut für Physikalische Chemie, Germany

The triple axis spectrometer PUMA is situated at beam tube SR7 at the Heinz Maier-Leibnitz neutron source (FRM II). It was set into operation during 2006 for the basic single detector version and is now available to the user community within the proposal system of the FRM II. The main characteristics of the instrument can be summarized as follows: high neutron flux on sample position concomitant with a low background; flexible and straightforward change of components as collimation, monochromators/analyzers; Eulerian cradle for flexible scattering plane adjustment; diverse and powerful sample environment. The wide range of applications of the instrument covers beside the study of phonon and magnon dispersion curves also the study of diffuse scattering, critical phenomena, soft-mode phase transitions, anharmonical effects or direction dependent quasi-elastic scattering. A salient feature of PUMA is the stroboscopic measurement technique implemented within the instrument control opening the possibility to perform kinetic real time investigations of reversible processes in dependence of an external field also on weak excitation signals. A highly flexible multianalyzer/-detector option was recently commissioned, which allows survey measurements in (**Q**, ω) - space and provides in combination with a time-resolved counter electronics new opportunities for single shot real time investigations.
Within the presentation we will introduce the characteristics and the applications of the instrument exemplified by selected measurements.

I-12

The positron beam facility and positron instruments at NEPOMUC

C. Hugenschmidt

Forschungs-Neutronenquelle Heinz Maier-Leibnitz (FRM II), Garching, Germany

The **NE**utron induced **PO**sitron source **MU**ni**C**h NEPOMUC provides a high intensity positron beam with $9x10^8$ moderated positrons per second with a primary beam energy of 1 keV. After remoderation, the positron beam is magnetically guided to five experimental setups: a coincident Doppler-broadening spectrometer (CDBS), a positron annihilation induced Auger-electron spectrometer (PAES), a pulsed low-energy positron system (PLEPS), an apparatus for the production of the negatively charged positronium ion Ps-, as well as an interface in order to provide a pulsed beam with further improved brilliance.
Within this presentation, an overview of the positron beam facility NEPOMUC with its instrumentation at the research reactor FRM II is given. In addition, recent developments as well as possible experiments, which might profit from the high intensity of low-energy positrons, are presented.

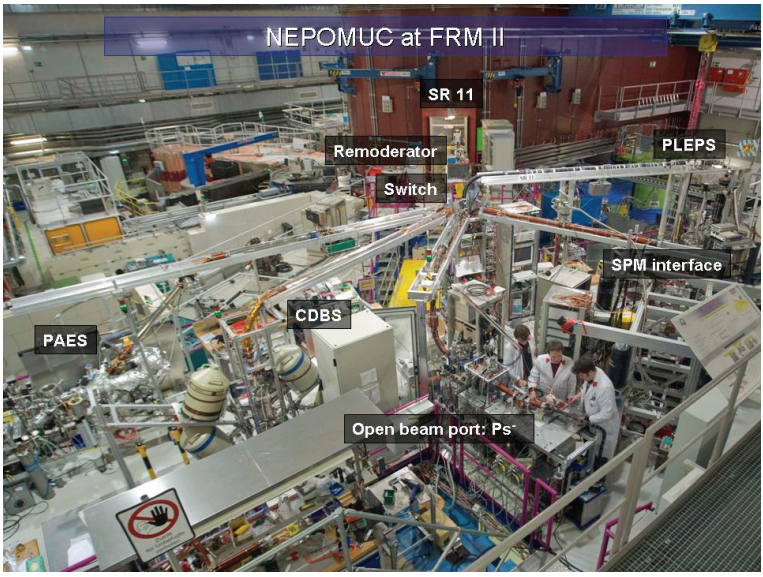

Fig. 1: NEPOMUC at FRM II: The in-pile positron source is located inside the beam tube SR11 which delivers the primary 1 keV positron beam. The remoderated positron beam is magnetically guided via a beam switch to five different instruments.

I-13

Spherical neutron polarimetry (SNP) on new POLI-HEiDi diffractometer at FRM II

V. Hutanu[1,2], M. Meven[2], G. Roth[1], G. Heger[1]

[1] RWTH Aachen, Institut für Kristallographie, Germany

[2] Forschungs-Neutronenquelle Heinz Maier-Leibnitz (FRM II), Garching, Germany

POLI-HEIDI is a new single crystal polarized neutron diffractometer [1] at the hot source of the Forschungs-Neutronenquelle Heinz Maier-Leibnitz (FRM II) in Garching. It is designed to perform spherical neutron polarimetry (SNP) in zero field as well as classical polarized neutron diffraction (PND) measurements (flipping ratio) under applied magnetic fields. Among the intended applications of this instrument are: complex magnetic structures and magneto-electric coupling in multiferroics, magnetic structure and spatially resolved spin densities in molecular magnets, magnetically ordered superconductors, strongly correlated transition metal oxides and spin chain compounds.

The instrument is unique in the sense that it combines a variable wavelength focussing monochromator with the use of ^{3}He spin-filter cells (SFC) to create polarized, short wavelength neutrons. This combination on the one side increase the flux of the polarised neutrons on the other side assures higher resolution in comparison to the classical Heussler monochromator. A new zero-field polarimeter Cryopad [2] has been recently built in cooperation between RWTH and ILL and successfully implemented on POLI-HEiDi. On the detector side, the polarisation-analysis and detection unit DECPOL (again with ^{3}He-spin filter cells) is used. This setup is - as of July 2010 - operational and open for user proposals at FRM II. The magnetic and magneto-electric domain structure of the sample has been changed by application of external magnetic and electric fields and studied by polarimetry during the first experiments on samples like $HoNi_2B_2C$ or Cr_2O_3.

[1] V. Huțanu, M. Meven, E. Lelièvre-Berna, G. Heger, Physica B 404, 2633 (2009).
[2] E. Lelièvre-Berna, I. Anderson & B. Guérard, Edit., Proc. of SPIE 4785, 112-125 (2002).

I-14

Spin-echo spectroscopy and diffraction at TRISP

T. Keller[1,2], N. Munnikes[1], B. Keimer[1]

[1] MPI für Festkörperforschung, Stuttgart, Germany

[2] Forschungs-Neutronenquelle Heinz Maier-Leibnitz (FRM II), Garching, Germany

The TRISP spectrometer at the FRM II is based on the resonance spin-echo technique (NRSE) invented by Golub and Gähler and applies the spin echo phonon focusing proposed by Mezei. Linewidths of dispersive excitations with energies up to 50meV can be measured with a resolution in the μeV-range [1-3]. The instrument also incorporates Rekveldt's *Larmor diffraction* technique. In the present configuration, d-spacings can be measured with a relative resolution of 10^{-6}, i.e. more than one order of magnitude more sensitive than conventional diffraction techniques. Applications of the Larmor Diffraction (LD) technique include the determination of mechanical stress and the measurement of thermal expansion under extreme conditions [4, 5]. Limitations of LD technique as well as the outline of a dedicated Larmor-diffractometer will be discussed.

[1] T. Keller, P. Aynajian, K. Habicht, L. Boeri, S:K: Bose, B. Keimer, Phys. Rev. Lett. 96, 225501 (2006).
[2] S. Bayrakci, T. Keller, K. Habicht, B. Keimer, Science 312, 1928 (2006).
[3] P. Aynajian, T. Keller, L.Boeri, S.M. Shapiro, K. Habicht, B. Keimer, Science 319, 1509 (2008).
[4] C. Pfleiderer, P. Böni, T. Keller, U.K. Rößler, A. Rosch, Science 316, 1871 (2007).
[5] J. Repper, T. Keller, M. Hofmann, C. Krempaszky, W. Petry, E. Werner, Acta Materialia 58, 3459 (2010).

I-15

The instrument area MEPHISTO in the west and east hall

J. Klenke[1], C. Klauser[2], T. Soldner[2,3]

[1] Forschungs-Neutronenquelle Heinz Maier-Leibnitz (FRM II), Garching, Germany

[2] TUM, Physik Department, Garching, Germany

[3] Institut Laue–Langevin, Grenoble, France

The instrument MEPHISTO (**ME**asurement facility for particle **PH**ys**I**c**S** with cold neu**T**r**O**ns) offers a white neutron beam with a mean wavelength of 5 Å and a capture flux of 1.5 10^{+10} n/s cm^2. It is dedicated to experiments in the field of nuclear and particle physics. Such high precision experiments allow to determine coupling constants with increased accuracy and thus to test current theoretical models. Nevertheless all experiments which need a white beam can be conducted at the experimental area. The experiments are planned and built up by external groups and installed in close cooperation with the scientific staff at FRM I. The old experimental area in the west neutron hall is limited in space for experiments. The demand for more space makes it essential to move the experimental area to the new east neutron hall. Also the radiation background and the disturbance of the neutron beam will be significantly decreased in the new place. The new beam is solely for the experiment MEPHISTO. The authors will present the actual simulations of the new neutron guide in comparison with the old experimental area. Of special interest is the interdependency between the planned MEPHISTO guide and the new PERC experiment which will be hosted at this guide in the east hall.

I-16

Emission channeling measurements at the PGAA station of FRM II

U. Köster[1], C. Granja[2], J. Jakůbek[2], V. Kraus[2], O. Valach[2], L. Canella[3], P. Kudějová[3], S. Söllradl[4], R. Schulze[5]

[1] Institut Laue–Langevin, Grenoble, France

[2] Czech Technical University in Prague, Institute of Experimental and Applied Physics, Czech Republic

[3] Forschungs-Neutronenquelle Heinz Maier-Leibnitz (FRM II), Garching, Germany

[4] PSI, Villigen, Switzerland

[5] Universität zu Köln, Institut für Kernphysik, Germany

The elliptical neutron guide of the PGAA station at FRM II was (ab-)used to deliver an intense and focused cold neutron beam for studies of particle channeling by neutron induced reactions in crystals doped with ^{10}B and ^{7}Be. The emitted charged particles were detected with the energy- and position-sensitive TimePix silicon pixel detector. We report on the use of the elliptical neutron guide of the PGAA station at FRM II in comparison to a collimated straight neutron beam at ILL Grenoble.

The lattice location of He, Li, Be or B host or impurity atoms in single crystals can be studied by slow-neutron-induced charged particle emission channeling measurements. The TimePix silicon pixel detector can cover an entire emission channeling pattern in a single measurement and allowed reviving this technique for practical applications. However, the counting statistics is still limited by the usually small concentration of the dopant atoms. Hence a very high neutron flux at the sample position is essential for such applications. At present no dedicated instrument for neutron-induced emission channeling exists anywhere. We constructed a setup that was previously used at the neutron beamlines of Neutrograph, ILL (thermal neutrons) and PF1B, ILL (cold neutrons). Now we transferred the setup to the PGAA station at FRM II (cold neutrons) to study the additional gain that can be achieved by employing a focused neutron beam provided by an elliptic neutron guide.

The focusing neutron guide provides a higher neutron flux at the sample position, but also far more background. Enhanced capture in the focusing section of the guide leads to massive gamma ray background. Also neutrons emitted under larger angles from the guide cause additional gamma ray background when captured at various locations. We used the single-event-counting semiconductor detector Timepix which has 65536 pixels with individual energy-measurement per pixel. Gamma rays cause undesirable Compton electron tracks in the detector which can be distinguished from the wanted proton or alpha events by a pattern recognition algorithm. To cope with the enhanced gamma ray background, the frame rate had to be increased. For the first time we operated this device with the new fast interface FITPix which allows for up to 80 frames per second. With the faster readout and the pattern recognition algorithm background events could be suppressed by a factor 7000. First results on ^{7}Be doped GaN crystals will be presented.

Acknowledgments: This work is carried out within the Medipix Collaboration.

I-17

Magnetic waveguides for the production of polarized neutron microbeams

S. V. Kozhevnikov[1,2], A. Rühm[1], F. Ott[3], N. K. Pleshanov[4], J. Major[1]

[1] MPI für Metallforschung, Stuttgart, Germany

[2] JINR, Frank Laboratory of Neutron Physics, Dubna, Russia

[3] Laboratoire Léon Brillouin, Gif-sur-Yvette, France

[4] Petersburg Nuclear Physics Institute, Gatchina, Russia

A neutron waveguide is a three-layer structure in which a guiding layer with low optical potential is placed between two cladding layers with high optical potential. Under proper operation conditions, the neutron density is resonantly enhanced inside the guiding layer. In our experimental scheme, the neutron beam enters through the surface of the top layer at glancing angle and goes out from the edge of the guiding layer, with an angular distribution corresponding to Fraunhofer diffraction from a narrow slit. The incident neutron beam is relatively wide (0.1 mm) and highly collimated (0.01°). The outgoing submicron beam is extremely narrow at the outlet (0.1 μm) and more divergent (0.1°). The gain factor at the exit of the waveguide can be of the order of 100. So far only the production of unpolarized submicron neutron beams has been reported. Here we present first experiments on polarized submicron neutron beams. For these studies a polarized incident beam was used and two types of magnetic waveguides were investigated: a polarizing magnetic waveguide Fe(20nm)/Cu(140nm)/Fe(50nm)//glass and a non-polarizing magnetic waveguide Py(10nm)/Al(140nm)/Py(50nm)//glass (where Py is permalloy). The waveguide samples were characterized by polarized neutron reflectometry.

I-18

^{3}He neutron spin filters for neutron polarization analysis at the FRM II

S. Masalovich

Forschungs-Neutronenquelle Heinz Maier-Leibnitz (FRM II), Garching, Germany

HELIOS, the optical pumping facility, provides polarized ^{3}He gas for neutron polarization analysis at the FRM II. The straight-line passage of a neutron beam through a ^{3}He gas with no change of a neutron trajectory enables one to measure a neutron polarization for nearly any divergent scattered beam. Furthermore, ^{3}He Neutron Spin Filters (NSF) offer homogeneous analyzing efficiency with a predictable value, predictable transmission, a negligible small angle scattering from a ^{3}He cell and a low gamma-ray background produced. All of these properties make ^{3}He spin filters extremely useful in such applications as neutron imaging with polarization analysis, small-angle neutron scattering, off-specular reflectometry and large solid angle polarization analysis. In addition, ^{3}He spin filters allows for a very precise measurement of a neutron beam polarization either with an opaque spin filter or with a recently proposed 2x1 NSF. So, the use of ^{3}He cells may be of advantage for fast calibration of any other polarizing devices with nearly any neutron energy.
We present some results of an application of ^{3}He NSFs at FRM II.

I-19

MARIA – The new high-intensity polarized neutron reflectometer of JCNS

S. Mattauch[1] , U. Rücker[2], D. Korolkov[1], E. Babcock[1], A. Ioffe[1], T. Brückel[2]

[1] Jülich Centre for Neutron Science at FRM II, Garching, Germany

[2] FZ Jülich GmbH, Institut für Festkörperforschung, Germany

The JCNS has installed the new, high-intensity reflectometer MARIA in the neutron guide hall of the FRM II reactor in Garching. This instrument uses a velocity selector for the monochromatization of the neutron beam, an elliptically focussing guide to increase the flux at the sample position and a double-reflecting supermirror polarizer to polarize the entire crosssection of the beam delivered by the neutron guide. Unique features of MARIA include (i) vertical focussing with an elliptic guide from 170 mm down to 10 mm at the sample position, (ii) reflectometer and GISANS mode, (iii) polarization analysis over a large 2d position sensitive detector as standard, (iv) adjustable wavelength spread from 10 to 1 % by a combination of velocity selector and chopper, (v) flexible sample table using a Hexapod for magnetic field and low temperature sample environment and (vi) in-situ sample preparation facilities. Together with a 400 x 400 mm^2 position sensitive detector and a time-stable ^3He polarization analyzer based on in-situ Spin-Exchange Optical Pumping (SEOP), the instrument is dedicated to investigate specular reflectivity and off-specular scattering from magnetic layered structures down to the monolayer regime. In addition the GISANS option can be used to investigate lateral correlations in the nm range. This option is integrated into the reflectometer's collimation, so it can be chosen during the measurement without any realignment. The direct measurements 120 mm behind the end of the elliptically focussing collimation section of MARIA, give for the polarized neutron flux of about $0.5*10^8$ $n/cm^2/s$ and the unpolarized neutron flux of about $1.25*10^8$ $n/cm^2/s$ at 4.5 Å with a horizontal divergence of 6 mrad. This makes MARIA one of the most powerful neutron reflectometers in the world. We will discuss specific details of MARIA and present results from first measurements.

I-20

Applications of hot Neutrons on HEiDi

M. Meven[1], V. Hutanu[1,2], G. Roth[2], G. Heger[2]

[1] Forschungs-Neutronenquelle Heinz Maier-Leibnitz (FRM II), Garching, Germany

[2] RWTH Aachen, Institut für Kristallographie, Germany

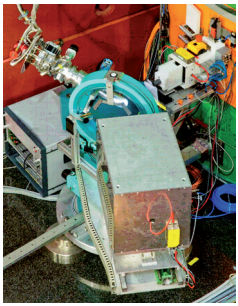

In cooperation between the TUM and the RWTH Aachen the single crystal diffractometer HEiDi was designed as a flexible tool for detailed studies on structural and magnetic properties of single crystals using fast neutrons from the hot source of the Forschungs-Neutronenquelle Heinz Maier-Leibnitz (FRM II). HEiDi offers a large flux of fast neutrons in the range between 1.1 Å and 0.4 Å and a good resolution. Thus, not only atomic positions of light elements in the neighbourhood of heavy elements and magnetic order can be determined very accurately but also anisotropic mean square displacements to discover order/disorder transitions or the specific occupancies of atomic positions with different elements with similar Z value.

Because of these key features HEiDi is most suitable for a variety of structural studies including several hot topics like

- Multiferroics and other compounds with ferro- or antiferromagnetic properties [1, 2],
- High Tc superconductors like cuprates or the recently found FeAs pnictides [3],
- Mixed compounds,which contain elements whose positions cannot be resolved with x-rays like in AsSe compounds [4],
- Ferroelectrics, to study the domain structure, e.g. under pressure and electric field in $SrTiO_3$ [5],
- H-Bonds, like in members of the KDP family [6], and
- Ionic conductors at high temperatures [7], especially in combination with
- Order/disorder phase transitions, caused by double well potentials or anharmonicities,
- Incommensurate nuclear and magnetic Phase transitions, and
- Compounds with highly absorbing elements, like Sm, Eu, Gd [3], which cannot be observed at larger wavelengths.

More details about the instrument and its application will be presented on the user meeting.

[1] M. Janoschek et al.; Single magnetic chirality in the magneto-electric $NdFe_3(^{11}BO_3)_4$; Phys. Rev. B, 81:094429 (2010).

[2] A. Sazonov et al.; Magnetic behaviour of synthetic Co_2SiO_4; Acta Cryst. B, 65(Pt 6):664 (2009).

[3] Y. Xiao et al.; Magnetic structure of $EuFe_2As_2$ determined by single crystal neutron diffraction; Phys. Rev. B, 80:174424 (2009).

[4] Rainer Niewa et al.; Crystal Structure Investigations of $ZrAs_xSe_y$ (x>y, x+y≤2) by Single Crystal Neutron Diffraction at 300 K, 25 K and 2.3 K; Journal of Solid State Chemistry, 183:1309-1313 (2010).

[5] J. Sidoruk et al.; Quantitative determination of domain distribution in $SrTiO_3$ – competing effects of applied electric field and mechanical stress; Journal of Physics, Condensed Matter, 22(23):235903-235910 (2010).

[6] In Hwan Oh et al.; Crystal Structure of LiH_2PO_4 Studied by Single-Crystal Neutron Diffraction; Journal of the Physical Society of Japan, 79(7):074606 (2010).

[7] G.D. Gatta et al.; Effects of temperature on the crystal structure of epidote: a neutron single crystal diffraction study at 293 and 1070 K; Physics and Chemistry of Minerals (2009).

I-21

Recent TOF GISANS and reflectometry experiments at REFSANS

J.-F. Moulin, M. Haese-Seiller, R. Kampmann, M. Pomm, A. Schreyer

GKSS-Forschungszentrum Geesthacht @ FRM II, Garching, Germany

Refsans is an horizontal reflectometer operated by GKSS at FRM II. This instrument is dedicated to time of flight reflectometry and diffuse scattering investigations of interfaces. Together with the TOF mode of operation, the versatility of its optics enables to investigate a great variety of samples, ranging from soft matter (polymers, biologically relevant systems) to metallic multilayers.
We will present here results obtained in these various fields and show how REFSANS can help study the structure of complex materials and bring information over a wide range of structural length scales, both in the sample plane (GISANS mode) and in the direction normal to the surface (conventional reflectometry).
In particular, application examples will be given in the field of the structure of polymer composites, of biological bilayers, of nanopatterned metals and eventually we will report of a in-situ study of the formation of sputter deposited metallic thin films.

I-22

The new neutron single crystal diffractometer BIODIFF for biological macromolecules at the FRM II

A. Ostermann[1], T. E. Schrader[2], M. Monkenbusch[3], B. Laatsch[4], P. Jüttner[1], W. Petry[1], D. Richter[3,2]

[1] Forschungs-Neutronenquelle Heinz Maier-Leibnitz (FRM II), Garching, Germany

[2] Jülich Centre for Neutron Science at FRM II, Garching, Germany

[3] FZ Jülich GmbH, Institut für Festkörperforschung, Germany

[4] FZ Jülich GmbH, Zentralabteilung Technologie, Germany

The new single crystal diffractometer BIODIFF is now in the final construction phase. The instrument is a joint project of the Forschungszentrum Jülich (FZJ/JCNS) and the Forschungs-Neutronenquelle Heinz Maier-Leibnitz (FRM II). BIODIFF is especially designed to collect data from crystals with large unit cells. The main field of application is the structure analysis of proteins, especially the determination of hydrogen atom positions. Typical questions in the field of interest are enzymatic mechanisms, ligand binding mediated by hydrogen bonds, the hydration shell of proteins and the analysis of H/D-exchange patterns.
By using a highly orientated pyrolytic graphite monochromator (PG002) the diffractometer will be able to operate in the wavelength range of 2.4 Å to about 5.6 Å. Higher order wavelength contaminations are removed by a neutron velocity selector. To cover a large solid angle and thus to minimize the data collection time the main detector of BIODIFF consists of a neutron imaging plate system in a cylindrical geometry. A Li/ZnS scintillator CCD camera is available for additional detection abilities. BIODFF is equipped with a standard Oxford Cryosystem “Cryostream 700 plus” which allows measurements in the temperature regime from 90 K up to 500 K.
The main advantage of this instrument is the possibility to adapt the wavelength to the size of the unit cell of the sample crystal while operating with a clean monochromatic beam that keeps the background level low. The construction of the monochromator housing including the monochromator unit and the shutter system is already completed. The installation and testing of the detector unit will be done within this autumn. As last step the velocity selector system will be installed in the beginning of 2011. First user operation of the instrument is anticipated to start around summer 2011.

I-23

RESI: New options and planned improvements

B. Pedersen, W. Klein

Forschungs-Neutronenquelle Heinz Maier-Leibnitz (FRM II), Garching, Germany

The single crystal diffractometer RESI is continiuosly evolving. The focussing neutron guide after the monochromator is giving better signal/noise for both large and small crystals. The focussing monochromator will be completely rebuild with new piezo drives to allow for easier change of the focus and a better alignment.

I-24

Small angle neutron instruments of JCNS at FRM II

H. Frielinghaus[1], A. Radulescu[1], V. Pipich[1], M.-S. Appavou[1], Z. Di[1], M. Heiderich[2], R. Hanslik[3], S. Staringer[1], A. Ioffe[1], D. Richter[1,2]

[1] Jülich Centre for Neutron Science at FRM II, Garching, Germany

[2] FZ Jülich GmbH, Institut für Festkörperforschung, Germany

[3] FZ Jülich GmbH, Zentralabteilung Technologie, Germany

The KWS-1 and KWS-2 classical pinhole SANS instruments with a typical Q-range from about 10^{-3} to 0.3 $Å^{-1}$ are dedicated to investigation of mesoscopic structures and structural changes due to rapid kinetic processes in soft condensed matter, chemistry, biology and solid state systems. The combination of high neutron flux supplied by the cold neutron source of FRM II, newly designed neutron guide system and new “fast” detection electronics supports the high-intensity operation mode. The neutron flux is comparable with the world leading SANS instruments. The high neutron flux allows for an optimal use of the high-resolution mode: aspherical MgF_2 lenses in combination with a high-resolution detector enable smallest Q vectors in the range of 10^{-4} $Å^{-1}$. The chromatic aberrations will be minimized by using a disc chopper that reduces the wavelength band width to 1 %. The design, operational modes and special options available for users are detailed presented.

I-25

The cold two-axis diffractometer MIRA

R. Georgii[1,2], J. Repper[1,2], G. Brandl[1,2], R. Schwikowski[1,2], P. Böni[2]

[1] Forschungs-Neutronenquelle Heinz Maier-Leibnitz (FRM II), Garching, Germany

[2] TUM, Physik Department, Garching, Germany

MIRA is a versatile instrument for cold neutrons, which is situated at the cold neutron guide NL6 in the neutron guide hall of the FRM II. MIRA provides neutrons in the wavelength range of 3.5 Å < λ < 30 Å. The movable sample-detector unit allows the use of a second beam port (MIRA2), which provides higher intensity for neutrons with a wavelength around 4 Å. Due to the long wavelength MIRA is ideally suited for samples with structures in the range from 5 nm to 50 nm. It is equipped with full polarisation analysis and thus capable for distinguishing the nuclear part from the magnetic part of the scattering function and to distinguish coherent from incoherent scattering. As the instrument set-up can be changed quickly, MIRA is ideally suited as a testing platform for realizing new instrumental set-ups and ideas. In particular, MIRA is unique in its possibilities of combining different neutron scattering methods and set-ups such as:

- Cold diffraction, especially on magnetic systems
- Polarized or non-polarized small angle scattering (SANS)
- NRSE (Neutron Resonance Spin Echo) using the MIEZE principle
- Polarized or non-polarized reflectometry
- Focusing optics for extreme conditions

MIRA is open for users since the start-up of the FRM II. Here, we present MIRA and MIRA2 in detail and show experimental results measured recently.

I-26

RESEDA (Resonance Spin Echo for Diverse Applications)

W. Häussler[1,2], J. Repper[1,2], A. Tischendorf[2], M. Wipp[1,2], P. Böni[2]

[1] Forschungs-Neutronenquelle Heinz Maier-Leibnitz (FRM II), Garching, Germany

[2] TUM, Physik Department, Garching, Germany

RESEDA is a high-resolution spin echo spectrometer installed at the cold neutron guide NL 5 in the neutron guide hall of FRM II. RESEDA supports both Neutron Spin Echo (NSE) and Neutron Resonance Spin Echo (NRSE). The wavelength is adjustable from 3.5 Å to 12 Å by a velocity selector. RESEDA provides a large time and scattering vector range for quasi-elastic measurements. Typical applications are dynamical studies in macromolecular and magnetic systems, as for example diffusion of polymers in bulk or confinement, (spin) glass dynamics, soft biological systems, magnetic fluctuations etc. RESEDA allows the measurement of two different q-values simultaneously due to two secondary spectrometer arms, which operate independently. RESEDA is now open for proposals. Here we show the instrument in detail and present first experimental results.

I-27

The reflectometer N-REX+

A. Rühm[1,3], S. V. Kozhevnikov[1,3], J. Major[1], T. Keller[2,3], B. Keimer[2]

[1] MPI für Metallforschung, Stuttgart, Germany

[2] MPI für Festkörperforschung, Stuttgart, Germany

[3] Forschungs-Neutronenquelle Heinz Maier-Leibnitz (FRM II), Garching, Germany

N-REX+ is a neutron reflectometer located in the neutron guide hall of FRM II. Typical fields of application are magnetism in layered systems (such as domain morphologies, proximity effects at superconductor interfaces, imaging with polarized neutron microbeams, etc.) as well as soft matter science on interfaces (such as polymer dewetting phenomena, manipulation of polyelectrolyte multilayers (PEM), proteins in membranes, hydrogen/deuterium depth-profiling, morphology of solid-liquid interfaces under shear, etc.).
The instrument is connected to the cold source and operates in angle-dispersive mode at a fixed wavelength in the range 2…6 Å (standard wavelength 4.26 Å), selected by a (normally) horizontally focussing HOPG monochromator with an energy resolution of 1-2%. The standard sample surface orientation is horizontal. Neutron reflectivity and off-specular scattering experiments can be performed either in polarized or unpolarized mode. For studies on magnetic systems, 4-channel polarization analysis is routinely available for reflectivity measurements, and in connection with wide-angle polarization analyzers also for off-specular experiments. Standard FRM II equipment such as cryostats and magnets (up to 7.5 T) can be used with N-REX+.
As an option, equipment for various kinds of spin-echo experiments (e.g. spin-echo resolved grazing incidence scattering (SERGIS)) can be accomodated. In addition, an add-on X-ray reflectometer is available for in-situ and/or ex-situ neutron / X-ray contrast variation.
Recent upgrades of N-REX+ include an improved detector shielding, the installation of adiabatic RF flippers, and a modified design of the focussing monochromator. Even on small samples of 1 cm^2 surface area, a dynamic range of $1{:}10^{-6}$ is now typically achieved in reflectivity experiments, both in polarized and unpolarized mode. For solid-liquid interfaces the dynamic range is limited to $1{:}10^{-5}$, due to absorption losses and intrinsic background from the samples or sample cells. For a further improvement of the neutron flux at the sample, the insertion of a horizontally focusing neutron guide between monochromator and sample is planned.
N-REX+ is running in regular user operation mode and is open for proposals.

I-28

High pressure clamp cells for neutron scattering

R. A. Sadykov

Institute Nuclear Research RAS, Moscow, & Institute for High Pressure Physics RAS, Troitsk, Russia

High pressure clamp cells up was made from TiZr zero alloy, hard Al and hard nonmagnetic HNU (NiCrAl) alloys for TOF-method on the pulse and a constant power neutron sources are presented in this report. All this is cells as for powder and single crystal as for diffraction and inelastic neutron scattering studies possible putting in the typical cryostats (on the dilution fridge insert) and high magnetic fields cryostat up to 6-10 T. Single crystal or powder NaCl (a pressure calibrant) and Fluorinert (a pressure medium) were used in all experiments on the neutron sources SINQ (Swiss), ISIS (UK), HMI (Germany) and ILL (France). We are made test a number of type Fluorinert and find that limits of solidifications distingish for different Fluorinert and max. of this limit is for FC87=23kbar. Some of these cells were used for the investigations of the magnetic spiral in $ZnCr_2S_4$, $CsCuCl_3$ and MnSi under pressure. For investigation of form-factor dependence of magnetic localized moments in $CePd(Rh)_2Si_2$ pressure up to 40kbar and H=10T by using polarized neutrons on D3 (ILL) we was made the a new non-magnetic composite piston/cylinder type cell from TiZr+HNU.

I-29

FitSuite: simultaneous evaluation various nuclear solid-state spectroscopic data

S. Sajti, L. Deák, L. Bottyán

KFKI Research Institute for Particle and Nuclear Physics, Budapest, Hungary

Experiments often provide spectroscopic data collected on the same sample by different methods, and/or using different experimental conditions, temperature, pressure, magnetic field, and the like. Part of data often depend on the same set of experimental and sample parameters therefore a *simultaneous evaluation* of all experimental data is prerequisite. However, data evaluation programs are dominantly organized around a single method therefore a simultaneous access to the data for a common simulation/fitting algorithm is not typical. Lacking suitable programs, some parameters are determined from one measurement, assumed error-free and kept constant when evaluating other experiments, an obviously incorrect approach. Besides, for different methods different programs are used, which makes it very difficult to tune parameters of such theories and their errors and correlations to each other and to extend or modify the theories to describe different experimental data. Therefore we developed FitSuite for Windows *and* Linux, a thoroughly documented program with a detailed project home page [1], which is by now suitable for evaluating data of over ten spectroscopic methods, handles the corresponding theories and sample structures consistently in a common structure. The generalized common graphics-aided and tree-structured user interface meets the needs of many potential users of nuclear solid state spectroscopies at beam lines of large facilities and in laboratories of relatively complex magnetic hyperfine spectroscopies and it is designed for possible future development to further spectroscopic methods and model schemes as well as to parallelized computing in the framework of a non-profit open-code international project. Currently FitSuite is capable of simultaneously fitting several data sets of experiments of the following kinds:

- Specular polarized neutron reflectometry (incl. *model for self diffusion* in isotopeperiodic multilayers)
- Off-specular (diffuse) polarized neutron reflectometry (domains)
- Specular x-ray reflectometry
- (Time integral, time differential and stroboscopic) Specular Synchrotron Mössbauer
- reflectometry (SMR), (incl. *model for self diffusion* in isotope-periodic multilayers)
- Off-specular (diffuse) Synchrotron Mössbauer reflectometry, DWBA
- Nuclear resonant forward scattering of synchrotron radiation
- (time differential and stroboscopic)
- Conventional Mössbauer absorption, emission and conversion electron spectroscopy

Examples of evaluated neutron reflectograms, and diffuse scatter plots, exposition of the program structure as well as principles and capabilities of FitSuite will be provided.

[1] http://www.fs.kfki.hu

I-30

The neutron imaging beam line ANTARES

M. Schulz, B. Schillinger

Forschungs-Neutronenquelle Heinz Maier-Leibnitz (FRM II), Garching, Germany

The neutron imaging facility ANTARES is located at the cold neutron beam port SR4 of the FRM II. Based on a pinhole camera principle with a variable collimator located close to the beam port, the facility provides the possibility for a flexible use in high resolution and high flux imaging. ANTARES offers two different detector positions in two separate chambers, which may be chosen according to the requirements for beam size, neutron flux and spatial resolution. A third chamber, located directly after the collimator is separately accessible for the optional installation of beam and spectrum shaping devices provided by the user. At this position ANTARES also offers built-in options such as a double crystal monochromator, interference gratings, coded apertures, and a Be-filter which are readily available for standard user operation. Furthermore, a 320 kV X-ray tube can be used for imaging in the same beam geometry as with neutrons, allowing for easy image registration and profiting of the advantages of both complementary techniques.
The ANTARES Neutron Imaging facility is designed to deliver radiographs and computed tomography of samples, similar to an X-ray machine. The achieved information is often complementary to X-ray measurements, with its most important features the high penetration of metals (Fe ~ 4 – 5 cm, Al ~20 – 30 cm, Pb ~10 – 20 cm) and the high sensitivity for hydrogen. These allow to visualize metal machine parts as well as liquids, sealants and plastics inside of metal parts. Liquid contrast agents can be employed for crack and void detection. Examples of different techniques and their typical applications will be given on the poster.

I-31

Prompt Gamma-ray 3D-imaging at the PGAA setup at FRM II

R. Schulze[1], P. Kudějová[2], L. Canella[3], S. Söllradl[4], T. Materna[5], T. Belgya[6], Z. Kis[6], L. Szentmiklosi[6], G. Festa[7], A. Türler[4], J. Jolie[1]

[1] Universität zu Köln, Institut für Kernphysik, Germany

[2] Forschungs-Neutronenquelle Heinz Maier-Leibnitz (FRM II), Garching, Germany

[3] TUM, Institut für Radiochemie, Garching, Germany

[4] Paul Scherrer Institut, Villigen, Switzerland

[5] Institut Laue-Langevin, Grenoble, France

[6] Hungarian Academy of Sciences, Institute of Isotopes, Budapest, Hungary

[7] Universita degli Studi di Roma Tor Vergata, Dipartimento di Fisica and Centro NAST, Italy

Prompt **G**amma-ray **A**ctivation **A**nalysis (PGAA) is a well-established method for the bulk, nondestructive, quantitative elemental analysis of samples from various fields of research. It is best suited for small homogeneous samples. The interest in the analysis of cultural heritage samples was driving the development of PGAA into the 3D elemental imaging method Prompt Gamma-ray Activation Imaging (PGAI) in the frame of the European Ancient Charm Project [1,2]. A 3D-PGAI setup was installed at the FRM II PGAA station [3]. After the measurements on first test objects was finished several real samples of cultural heritage interest were measured in 2D- and 3D-PGAI configuration. The combination with cold Neutron Tomography (NT) allows the creation of combined data-sets which include information about the morphological sample structure as well as the elemental distribution allover the analyzed object. The final results of the PGAI measurements performed at FRM II will be presented as well as some first steps taken to address the problems of full quantitative 3D-PGAI analysis.

The financial support of EU FP6 ANCIENT CHARM project (contract no. 15311) is gratefully acknowledged.

[1] G. Gorini. Ancient Charm: A research Project for Neutron-based Investigation of Culturalheritage Objects. Il Nuovo Cimento, 30(1):47-58, 2007.

[2] R. Schulze, L. Szentmiklosi, Z. Kis : The Ancient Charm Project: New Neutron Based Imaging Bethods for Cultural Heritage Studies, Archeologia e Calcolatori 21: 275-293, 2010 (in print).

[3] L. Canella , P. Kudějova, R. Schulze, A. Turler, J. Jolie : Characterisation and optimisation of the new Prompt Gamma-ray Activation Analysis (PGAA) facility at FRM II , Nuclear Instruments and Methods in Physics Research, Section A (in print).

I-32

Magnetic investigation at the time-of-flight spectrometer TOFTOF

G. G. Simeoni[1,2], T. Unruh[1,2], S. Busch[1,2], R. Mole[1], L. Peyker[3], R. Valicu[2], P. Böni[2], J. Neuhaus[1,2], W. Petry[1,2]

[1] Forschungs-Neutronenquelle Heinz Maier-Leibnitz (FRM II), Garching, Germany

[2] TUM, Physik Department, Garching, Germany

[3] Universität Augsburg, Institut für Physik, Germany

TOFTOF is a directgeometry multidisc chopper time-of-flight (TOF) spectrometer, installed at the Forschungs-Neutronenquelle Heinz Maier-Leibnitz (FRM II). The instrument, fed with neutrons from the undermoderated cold source operating with D_2 at 25 K, is prepared to be used with incident neutrons in the wavelength range 1.6-16 Å.
Features characterizing the TOFTOF performance are at present an extremely high signal-to-background ratio, a high intensity also at short incident neutron wavelengths, and the possibility of achieving a very high energy resolution. Thanks to that, TOFTOF turns out to be particularly suitable for investigating magnetic excitations. The covered energy range extends continuously from the traditional low energy “cold neutron” region to an higher energy region, generally reachable only by means of “thermal neutron” inelastic scattering. This and the TOF technique employed allow for a quick and general overview all over the low energy magnetic excitations, fundamental to assess the presence of spin liquid and nematic states as well as new exotic magnetic phases.
Next-future technological development of TOFTOF has been planned bearing in mind the improvement in the study of magnetic systems and the investigation of small samples, both eventually experiencing extreme conditions.
It is the case of experiments on single-crystals or employing high pressure cells as well as experiments with electromagnetic (EML) and electrostatic (ESL) levitator devices (allowing containerless measurements), for which an increased neutron flux is essential.
Within this context, McStas simulations have been recently performed for the improvement of the secondary neutron guide, in order to achieve enhanced focusing at the sample position.

I-33

DNS – A diffuse neutron scattering spectrometer with polarization analysis at FRM II

Y. Su[1], W. Schweika[2], R. Mittal[1], W. Borghols[1], A. Ioffe[1,], T. Brückel[1,2]

[1] Jülich Centre for Neutron Science at FRM II, Garching, Germany

[2] FZ Jülich GmbH, Institut für Festkörperforschung, Germany

DNS is a versatile diffuse scattering time-of-flight spectrometer with polarization analysis at FRM II. It has the capability to allow the unambiguous separation of nuclear-coherent, spin-incoherent and magnetic scattering contributions simultaneously over a large range of scattering vector Q and energy transfer E. With its compact design DNS is optimized as a high intensity instrument with medium resolution. With significantly increased flux and efficiency, DNS has been recently very attractive for the studies of complex spin correlations in highly frustrated magnets [1-2], strongly correlated electrons [3-4], magnetic nanoparticles [5] and soft condensed matters, such as the nanoscale confined polymers [6] and proteins [7]. The current status and ongoing instrument developments as well as recent scientific highlights at DNS will be presented in details.

[1] M. Krott, et al., Phys. Rev. B 80, 024117 (2009); Z. Fu, et al., New. J. Phys. (submitted).
[2] L. J. Chang, et al., Journal of Physics: Conference Series 211, 012013 (2010); arXiv:1003.4616 (2010).
[3] J. Herrero-Martin, et al., Phys. Rev. B 80, 134411 (2009); M. Tegel, et al., Europhy. Lett. 89, 37006 (2010).
[4] I. Dhiman, et al., Phys. Rev. B 81, 104423 (2010).
[5] T. Chatterji, et al., J. Magn. Magn. Mater. (in press); M. Feygenson, et al., Phys. Rev. B 81, 064423 (2010).
[6] M. Krutyeva, et al., J. Chem. Phys. 131, 174901 (2009).
[7] A. M. Gaspar, et al., Biochimica et Biophysica Acta 1804, 76 (2010).

I-34

The backscattering spectrometer SPHERES

J. Wuttke, G. J. Schneider

Jülich Centre for Neutron Science at FRM II, Garching, Germany

SPHERES (**SP**ectrometer for **H**igh **E**nergy **RES**olution) is a third-generation backscattering instrument with focussing optics and a phase-space-transform chopper. It is a versatile spectrometer for investigating atomic and molecular dynamics on a GHz scale.
The necessary filtering of neutron energies is achieved by Bragg reflection from perfect monochromator and analyzer crystals under angles close to 180°. The backscattering geometry makes it unavoidable to use a primary beam deflector and a duty-cycle chopper. In SPHERES [1], these two functions are realized jointly by a chopper that bears deflector crystals on its circumference. This leads to a particularly compact spectrometer layout so that full use can be made of the focussing neutron guide. As an additional advantage, the fast motion of the deflector crystals achieves a phase-space transform of the primary spectrum, thereby enhancing the flux at the sample.
The principal figures of merit (spectral flux, resolution, dynamic range, signal-to-noise ratio) qualify SPHERES as worldwide leading. In the near future, count rates and signal-to-noise ratio will be further improved by filling the entire instrument with argon, thereby avoiding air scattering in the secondary spectrometer. Another gain in flux will be achieved by a more effcient phase-space transform chopper, which is currently under development.
As a multi-detector instrument with relaxed angular resolution, SPHERES is particularly suited for studying tagged-particle motion by incoherent scattering. A hot topic is the dynamics of water in confined geometry. The unprecedented sensitivity of SPHERES helps us to detect the onset of quasielastic scattering deep in the supercooled state [2]. Other important applications are hyperfine splitting in magnetic materials and rotational tunneling. The high count rates allow inelastic temperature scans and real-time kinetic experiments. Our standard sample environment is a cryofurnace (4-700 K). Alternatively, we can supply a dilution cryostat (20 mK) and a furnace (so far used up to 1550 K); tests with a magnet are under preparation.
Raw histograms are accumulated on an equidistant ω grid. A script driven program, SLAW [3], is provided to normalize the raw counts, to perform optional binning, and to deliver S(q, ω) in a variety of output formats. so that users are not bound to any specific data analysis programm. In data fitting, it is critcially important to convolute theoretical models with the measured resolution function in an efficient and numerically stable way. We strive to support best practice through our FRIDA package [4].
Since commissioning began in 2007, about 70 proposals have been served. The publication record [1] has gone up from one in 2007, two in 2008 to eight in 2009, and the pipe is well filled for 2010 ...

[1] www.jcns.info/jcns_spheres
[2] W. Doster, S. Busch, A. M. Gaspar, M.-S. Appavou, J. Wuttke, H. Scheer, Phys. Rev. Lett. 104, 098101 (2010).
[3] J. Wuttke: SLAW - a neutron histogram to scattering law converter, www.messen-und-deuten.de/slaw
[4] J. Wuttke: FRIDA - fast reliable interactive data analysis, www.messen-und-deuten.de/frida

Material Science

MS-01

Analysis of antiphase domain growth in ternary FeCo alloys after different cooling rates and annealing treatments using neutron diffraction and positron annihilation

R. Gilles[1], M. Hofmann[1], F. Johnson[2], Y. Gao[2], D. Mukherji[3], C. Hugenschmidt[1], P. Pikart[1]

[1] Forschungs-Neutronenquelle Heinz Maier-Leibnitz (FRM II), Garching, Germany

[2] GE Global Research, One Research Circle, Niskayuna, USA

[3] TU Braunschweig, Institut für Werkstoffe, Germany

FeCo alloys are industrially important engineering materials which play an outstanding role in applications requiring soft magnetic materials. The challenge is to include ternary elements to improve the mechanical properties. Here noble elements as Pt or Pd were used for these experiments. With neutron diffraction and positron annihilation technique $Fe_{67}Co_{30}Pt_3$ and $Fe_{67}Co_{30}Pd_3$ (at. pct.) samples were measured to study the influence of different cooling rates on ordering and disordering. The ordering and disordering process is responsible for the mechanical properties in dependence of temperature. The correlation of ordering and defect density is described.

Neutron diffraction experiments and positron measurements of ternary FeCoPt and FeCoPd alloys allow detailed information on the mechanism of order and disorder as function of thermal history (e.g. cooling rates). The cooling rate has strong influence on the degree of order at room temperature. A more or less fully ordered or disordered state is possible by adjusting the cooling rate. Heating up to just below the T_c temperature always leads to a high degree of order of the alloy before crossing the T_c temperature whereupon complete disorder occurs. The antiphase domains created when the alloy‘s order grows with a rate directly dependent on the annealing temperature. Especially, the influence of the ternary element to the T_c temperature is clearly pointed out. Neutrons allow in-situ monitoring of the site occupation of the two main elements, Fe and Co. The positron measurement shows higher defect concentrations for the FC samples which is connected to the creation of vacancy defects at the antiphase domain boundaries, especially in the Co sublattice because of the non-stoichiometric composition.

[1] R. Gilles, M. Hofmann, Y. Gao, F. Johnson, L. Iorio, M. Larsen, F. Liang, M. Hoelzel, B. Barbier, Metallurgical and Materials Transactions A, 41A (2010) 1144-1150.

[2] R. Gilles, M. Hofmann, F. Johnson, Y. Gao, D. Mukherji, C. Hugenschmidt, P. Pikart, submitted.

MS-02

Surface strain scanning for laser hardened 42CrMo4 steel samples

V. Kostov[1], T. Filatova[1], J. Altenkirch[1], J. Gibmeier[1], J. Rebelo Kornmeier[2], M. Hofmann[2]

[1] KIT, Karlsruhe Institute of Technology, Germany

[2] Forschungs-Neutronenquelle Heinz Maier-Leibnitz (FRM II), Garching, Germany

We report on the investigation of the residual stress depth distribution in 42CrMo4 steel samples which were laser hardened to induce surface compressive residual stress for improved life time performance. The lentoid laser processing zone consists of an app. 1mm thick martensitic surface layer with a surrounding transition zone followed by the ferritic base metal. The application of neutron diffraction for determination of near surface residual stress immediately evokes the problematic nature of through surface strain scanning. As the gauge volume is only partially filled when scanning through a surface of a material showing homogeneous absorption of neutron radiation three main effects can give rise to surface related spurious strains: 1) the wavelength effect due to a horizontal gradient of the wave length across the incident beam, 2) the geometric effect as a result of differing locations of the theoretical and true centre of gravity of the gauge volume and 3) the peak clipping effect resulting from the geometrical instrument set-up. The microstructure depth gradient of the laser hardened material gives rise to an additional problem as a varying superposition of a martensite with a ferrite diffraction peak occurs with increasing depth and as such may act as an internal surface effect.

On the powder diffractometer StressSpec at FRM II through surface strain scans were performed in a) laser hardened 42CrMo4 samples, b) a stress-free annealed 42CrMo4 reference sample and c) an artificial layered two-phase (austenite and ferrite) sample with a predefined internal phase boundary. The aim of the investigation of the artificial sample is to simulate the layered structure of the surface laser hardened sample while guaranteeing a constant absorption in the two phases with diffraction peaks that can be well separated. We compare the results based on the common approaches to eliminate the outer surface effect, namely the subtraction of strain profiles obtained by scanning through the surface from opposite directions as well as the subtraction of the strain profiles obtained in a stressed and a stress-free annealed sample. The measurements in the artificial two-phase sample revealed a reduced surface effect on the inner boundary. Based on the results from these investigations we propose an approach for the determination of residual stress depth gradients in materials which have a discontinuing change of the microstructure caused by the processing.

MS-03

Influence of ion energy on damage induced in silicon carbide single crystals probed by positron lifetime and Doppler-Broadening spectroscopies

F. Linez[1], A. Gentils[1,2], L. Thome[2], W. Egger[3], P. Desgardin[1], M.-F. Barthe[1]

[1] CNRS, CEMHTI, Orléans, France

[2] CSNSM, CNRS-IN2P3-Université Paris-Sud 11, Orsay Campus, France

[3] Universität der Bundeswehr München, Institut für Angewandte Physik und Messtechnik, Germany

Silicon carbide (SiC) has low activation characteristics and excellent properties such as high breakdown strength, general chemical inertness, high thermal conductivity and low coefficient of thermal expansion [1]. Therefore, this material is very attractive for nuclear applications. It has been proposed for structural components in fusion reactors, and fuel encapsulation or cladding for gas cooled fission reactor (IVth Generation). In this application, material would be irradiated by fission products what means heavy ions at various energies. The aim of this study is to evaluate the influence of heavy ion energy on damage induced in SiC as function of fluence. Several 6H-SiC single crystals have been irradiated with 4 MeV and 20 MeV Au ions at different fluences between 10^{12} and 10^{16} cm^{-2}. The projected ion range (R_p) was calculated using SRIM program [2] and should be equal to 0.5 µm for the 4 MeV ions and 3 µm for the 20 MeV ones. According to SRIM Monte Carlo calculations, the damage corresponding to a fluence of 10^{15} cm^{-2} reaches 5.2 dpa (displacement per target atom) at the peak maximum of the damage profile for 4 MeV and 3.2 dpa for 20 MeV. Initially, each sample has been probed by Slow Positron Beam Doppler Broadening spectroscopy in CEMHTI (Orléans, France) from 0.5 and 25 keV i.e. a maximum average positron implantation depth about 2 µm. That corresponds to the cascade area for implanted 4 MeV-Au samples and to the track region for others. As expected, these measurements have shown that the low momentum annihilation fraction S increases with fluence while the high momentum fraction W decreases and becomes higher or respectively lower than the S and W values determined for the V_{Si}-V_C divacancies. It suggests an increase of the defect size.
In a second step, to better identify the nature of defects [3][4], each sample has been probed by positron lifetime spectroscopy using **P**ulsed **L**ow-**E**nergy **P**ositron-beam **S**ystem (PLEPS) of the intense positron source NEPOMUC at FRMII (Garching, Germany). The measurements have been performed from 5 keV to 14 keV (16 keV for the 20 MeV samples). For 4 MeV Au implanted samples, the measurements have shown that the average lifetime increases as function of fluence from 220 ps to nearly 290 ps for 10^{15} cm^{-2}. This lifetime evolution is in agreement with Doppler-Broadening measurements. It does not seem to be the same for the other samples (20 MeV) for which the average lifetime is almost constant up to a fluence of 10^{14} cm^{-2}. The Doppler-Broadening and lifetime results will be compared and discussed based in particular on the average lifetime as function of S and W representations.

[1] Y. Katoh et al., Journal of Nuclear Materials, 367-370 (2007) 659-671.
[2] J.F. Ziegler et al., The Stopping and Range of Ions in solids (Pergamon, New York, 1985).
[3] G. Brauer et al., Physical Review B, Vol. 54, N°5, p.3084 (1996).
[4] Thesis of Laurent Henry, Université d'Orléans (2002).

MS-04

Investigation on the stress-depth profiles in mechanically surface treated Ti-2.5Cu by using diffraction methods

E. Maawad[1], H.-G. Brokmeier[1,2], L. Wagner[1], M. Hofmann[3], C. Genzel[4], M. Klaus[4], W. Gan[3], M. Yang[1]

[1] TU Clausthal, Institut für Werkstoffkunde und Werkstofftechnik, Germany

[2] GKSS-Forschungszentrum Geesthacht, Germany

[3] Forschungs-Neutronenquelle Heinz Maier-Leibnitz (FRM II), Garching, Germany

[4] HZB für Materialien und Energie GmbH, Berlin, Germany

Residual stress evaluation is an important stage to interpret fatigue enhancements of engineering components after surface treatments. To achieve a full description of the influence of compressive and balancing residual tensile stresses on such enhancements, fatigue results on Ti-2.5Cu after shot peening and ball-burnishing were interpreted on the basis of residual stress through thickness profiles measured by combining energy-dispersive X-ray and neutron diffraction methods.

MS-05

Residual stress fields after heat treatment in cladded steel of process vessels

M. J. Marques[1,2], A. Castanhola Batista[1], J. Rebelo Kornmeier[3], M. Hofmann[3], J. P. Nobre [4], A. Loureiro[4]

[1] University of Coimbra, Department of Physics, Portugal

[2] University of Porto, Department of Physics Engineering, Portugal

[3] Forschungs-Neutronenquelle Heinz Maier-Leibnitz (FRM II), Garching, Germany

[4] University of Coimbra, Department of Mechanical Engineering, Portugal

The influence of the heat treatment on the residual stress fields of weld cladded samples is discussed in this study. The samples were elaborated from carbon steel plates, cladded in one of the faces with stainless steel filler metals by submerged arc welding. After the cladding process some of the samples were submitted to heat treatments with different parameters: one at 620° C for a holding time of 1 hour and the other at 540° C for a period of ten hours. The in-depth residual stress profiles for the three samples: as-welded sample (AW) and heat-treated samples (HT620 and HT540) were measured by neutron diffraction at FRM II, Technische Universität München, Germany. The results shown that the sample treated to 620 ºC, presented the highest residual stress relaxation. The corresponding heat treatment has the industrial benefit to be shorter than the other heat treatment.

MS-06

Reflectometric study of Fe self-diffusion in FePd alloys

D. G. Merkel[1], S. Sajti[1], F. Tanczikó[1], A. Rühm[2], R. Rüffer[3], L. Bottyán[1]

[1] KFKI Research Institute for Particle and Nuclear Physics, Budapest, Hungary

[2] MPI für Metallforschung, Stuttgart, Germany

[3] ESRF, Grenoble, France

$L1_0$ (CuAu(I)-type) ordered FePd, due to their high magnetic anisotropy, are candidate materials for future ultra-high density magnetic recording. Atomic diffusion governs the structural relaxation and associated changes in the physical and magnetic properties in these alloys. Such processes involve diffusion paths of a few angstroms. To investigate self diffusion, an isotope sensitive technique such as neutron reflectometry (NR) is needed. Another recently emerged isotope-sensitive method for studying self diffusion is **S**ynchrotron **M**össbauer **R**eflectometry (SMR). In both methods, the diffusion length was determined from the intensity decrease of the multilayer Bragg peak vs retention time *t* at temperature *T*.
Partially ordered and disordered isotope-periodic multilayer (ML) films of composition $[^{nat}Fe_{47}Pd_{53}(3\ nm)/\ ^{57}Fe_{47}Pd_{53}(2\ nm)]_{10}$ were epitaxially grown by molecular beam epitaxy (MBE). Post grown annealing was performed in an UHV chamber (~10^{-10} mbar) at varying temperatures between 370°C and 570°C. The retention time was varied from 90 to 1800 minutes. In all annealing stages, either NR on the NREX+ beam line of FRM II or SMR data on the ID22N beam line of ESRF), or both were collected. By conversion electron Mössbauer spectra recorded in each annealing stage of the samples three different microstructural FePd species were identified and related to the different hyperfine (hf) field distributions. The ordered $L1_0$, the disordered fcc FePd and the not specified iron rich (probably Fe_3Pd) local environment is identified by the hf field distribution with the low, intermediate and high average hf field distributions and their fraction is taken as the spectral contribution to the CEMS intensity. The $L1_0$ magnetization points in the crystallographic c-direction, consequently out of the plane of the epitaxial film, the intermediate field distribution correcponds to random magnetization orientation and the high hf field distribution component is magnetically coupled to the matrix it is embedded in. According to our model, the diffusion of Fe in the multilayer is, like in a random alloy, a weighed sum of the individual diffusion coefficients of the different Fe-environments. $D=x_{L10}D_{L10}+x_{fcc}D_{fcc}+x_{Fe}D_{Fe}$
Where x_{L10}, x_{fcc},x_{Fe} and D_{L10}, D_{fcc}, D_{Fe} are the ratios and the effective diffusion parameters of the ordered L10, disordered fcc and iron rich-phases, respectively. Expressing the above equation we get:

$$D(T) = x_{L1_0} D^{o}_{L1_0} e^{-\frac{Q_{L10}}{kT}} + x_{fcc} D^{o}_{fcc} e^{-\frac{Q_{fcc}}{kT}} + x_{Fe} D^{o}_{Fe} e^{-\frac{Q_{Fe}}{kT}}$$

By fitting all diffusion parameters, the activation energies (Q_i) and pre-exponential factors (D^0) for the three distinct environments of the FePd samples were determined. We obtained the highest activation energy $Q^{o}_{c,L10}$= (1.82±0.38 eV) and lowest pre-exponential factor D^{o}_{L10}=(5.76±0.35)*10^{-14} m^2/s for the ordered $L1_0$ in its crystallographic c-direction as opposed to the iron rich regions were the activation energy (1.48±0.26 eV) was found to be lowest and the pre-exponential factor the highest, (1.01±0.61)*10^{-13} m^2/s).

This work was partially supported by the Hungarian National Research Fund and the National Office for Research and Development of Hungary in project No. K62272 and NAP-VENEUS.

References had been left out by editors for reasons of space.

MS-07

Water diffusion profile measurements in casein films using neutron radiography

E. Metwalli[1], H. E. Hermes[2], U. Kulozik[3], S. U. Egelhaaf[2], P. Müller-Buschbaum[1]

[1] TUM, Physik Department, Garching, Germany

[2] Universität Düsseldorf, Institut für Experimentelle Physik der kondensierten Materie, Germany

[3] TUM, Lehrstuhl für Lebensmittelverfahrenstechnik und Molkereitechnologie, Freising-Weihenstephan, Germany

A major milk protein is casein that forms micelles with radius of about 100-300 nm. Casein-protein based films are widely used as an adhesive for labeling glass bottles and other containers because of their superior mechanical stabilities in different humidities at temperatures between 2 and 40°. This study demonstrates the use of neutron radiography as a viable method for the determination of the diffusion profile of water in casein films. A gel film of casein micelles in D_2O was prepared and packed in an aluminum cell followed by heating at different temperatures for different times to form 0.3 mm thick dry casein films. The dry casein film is submerged in water (H_2O) and neutron radiographs were collected as function of total time. Profiles of the water concentration were successfully probed. By imaging water concentration in the casein film, two diffusion processes are observed: a) fast diffusion within the voids and holes between the micelles and their aggregates, b) slow diffusion due to water exchange with the hydration water bounded to the casein proteins. Time evolution of the later diffusion process is compared with our recent GISANS investigation [1] hydration behavior of casein thin films in water vapor.

[1] E. Metwalli, J.-F. Moulin, R. Gebhardt, R. Cubitt, A. Tolkach, U. Kulozik, P. Müller-Buschbaum, Langmuir 25, 4124, 2010.

MS-08

Neutron scattering measurements a useful tool for the development of new CoRe-based alloys for high temperature gas turbine applications

D. Mukherji[1], P. Strunz[2], R. Gilles3, M. Hofmann[3], M. Hoelzel[4], J. Rösler[1]

[1] TU Braunschweig, Institut für Werkstoffe, Germany

[2] Nuclear Physics Institute ASCR, Řež near Prague, Czech Republic

[3] Forschungs-Neutronenquelle Heinz Maier-Leibnitz (FRM II), Garching, Germany

[4] TU Darmstadt, FB für Material- und Geowissenschaften, Germany

Development of high temperature material is mainly driven by gas turbine needs. Today, Ni-based superalloys are the dominant material class in the hot section of gas turbines, but they operate very close to their melting temperature. Therefore, new alloys with higher melting point are needed for the future. Co-Re-based alloys are being developed at the Technische Universität Braunschweig, with this aim. The goal is to develop alloys for applications at +100°C metal temperature above present day single crystal Ni-base superalloys. The refractory metal Re has very high melting point (T_M - 3182°C) and dissolves readily in Co. Therefore, very high melting alloys can be achieved in Co-Re system. Alloying further with Cr, Si, Ta, C etc. is however required to achieve good strength and oxidation resistance in Co-Re-based alloys. The Co-Re system has not been explored so far and this alloy development concept is rather new. Also information on this system is scanty in the literature and therefore basic structural characterization and phase stability information are lacking. Neutron scattering is extensively used in our development work to supplement microstructural investigations. Useful information is obtained through high temperature insitu neutron diffraction measurements, which is invaluable for the alloy development. Some selected results will be presented here. Fig. 1 shows results from in-situ diffraction measurements at FRM II on 2 Co-Re based alloys CoRe-1 (Co-17Re-23Cr-2.6C) and CoRe-2 (Co-17re-23Cr-1.2Ta-2.6C). A heating / cooling cycle between 1100° and 1300°C showed for the first time that a hysteresis exists in the hcp ⇆ fcc phase transformation of the Co matrix [1, 2]. It may be noted that pure cobalt exists in two allotropic forms: low temperature ε (hcp) and high temperature γ (fcc) phases and undergoes fcc ⇆ hcp allotropic transformation around ~ 420°C - by a diffusionless martensitic mechanism.

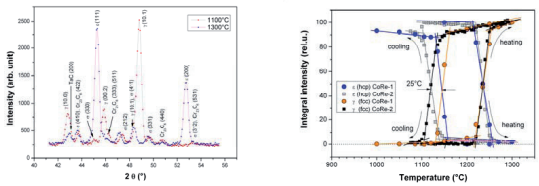

Fig. 1. a) Diffractograms measured on CoRe-2 sample (limited 2θ range) during in-situ heating at Stress-Spec. b) The transformation: hcp → fcc on heating occur at the same temperatures in CoRe-1 and CoRe-2, but on cooling the reverse transformation: fcc → hcp in CoRe-2 lags behind (occurs at lower temperature) by 25°C. CoRe-2 data points measured at Stress-Spec and CoRe-1 ones at SPODI.

1. D. Mukherji, P. Strunz, R. Gilles, M. Hofmann, F. Schmitz and J. Rösler: Mater. Lettrs. (2010), DOI: 10.1016/j.matlet.2010.08.066.
2. D. Mukherji, P. Strunz, S. Piegert, R. Gilles, M. Hofmann, M. Hölzel and J. Rösler: Mater. Trans. A (2010) submitted.

MS-09

Infiltration and backfilling of the network structure of nanoporous titania films for applications in photovoltaics

M. Rawolle[1], K. Sarkar[1], M. Niedermeier[1], P. Lellig[2], J. S. Gutmann[2], P. Busch[3], J.-F. Moulin[4], M. Haese-Seiller[4], P. Müller-Buschbaum[1]

[1] TUM, Physik Department, Garching, Germany

[2] MPI für Polymerforschung, Mainz, Germany

[3] Jülich Centre for Neutron Science at FRM II, Garching, Germany

[4] GKSS-Forschungszentrum Geesthacht, Germany

One possible approach to photovoltaic energy conversion systems is the so-called solid-state dye-sensitized solar cell (ssDSSC), which is a combination of a dye-sensitized solar cell (DSSC) also known as Grätzel cell and a polymer solar cell. This type of solar cell consists of a thin nanostructured titania layer which is dye-sensitized and backfilled with a holeconducting polymer between two electrodes [1-3]. The titania structure that appears most promising is a sponge structure with mesopores of a few tens of nanometers combined with macropores with a larger diameter. The mesopores provide a large surface important for the charge generation whereas the macropores facilitate the backfilling of the porous titania. Block copolymers can be used in a 'good-poor' solvent pair induced phase separation process coupled with sol-gel chemistry to create structured titania films in a reproducible way. In this study, the diblock copolymer PDMS-MA(PEO) was used in combination with titanium tetraisopropoxide (TTIP) as the source of titania.

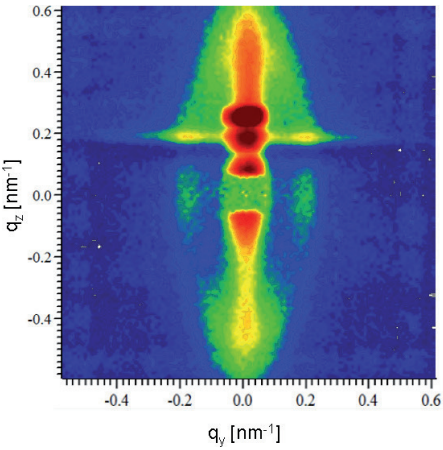

Fig. 1. 2d scattering image of nanoporous titania, measured at KWS-1. The upper half of the 2d pattern contains the reflected signal (GISANS) with the Yoneda peak and the specular peak in $q_z$direction and peaks originating from a lateral structure in $q_y$direction, the lower half contains the transmitted signal where a beamstop at the axes origin blocks the direct beam signal.

With grazing incidence small angle neutron scattering (GISANS) measurements at REFSANS and KWS-1 the porosity of the pure titania film [4], the infiltration of a small molecule like the dye, mimicked with D_2O, as well as the degree of backfilling with the hole-conducting polymer were probed.

[1] J. Perlich al., ChemPhysChem , 799-805 (2009).
[2] M. Memesa al., Energy Environ. Sci. , 783-790 (2009).
[3] G. Kaune al., ACS Appl. Mater. Interfaces , 2862-2869 (2009).
[4] G. Kaune et al., J. Polym. Sci. Part B: Polym. Phys. , 1628-1635 (2010).

MS-10

Effect of macroscopic relaxation on residual stress analysis by diffraction methods

J. Repper[1], M. Hofmann[1], C. Krempaszky[2], B. Regener[2], W. Petry[1], E. Werner[3]

[1] Forschungs-Neutronenquelle Heinz Maier-Leibnitz (FRM II), Garching, Germany

[2] TUM, Christian-Doppler-Labor für Werkstoffmechanik von Hochleistungslegierungen, Garching, Germany

[3] TUM, Lehrstuhl für Werkstoffkunde und Werkstoffmechanik, Garching, Germany

One of the basis assumptions of macroscopic residual stress determination by diffraction methods is the identity of the microscopic stress state in the component of interest and the used reference sample. The latter one is often cut from the strained component. In this contribution the effect of macroscopic relaxation on the microscopic stress state was studied by stepwise machining of a hot-forged and water quenched disc of the Nickel-base superalloy IN718. Neutron diffraction allows the observation of the evolution of the stress state along the center axis of the disc and its comparison with stress distributions predicted by FEM. It is demonstrated that the development of micro-stresses during the unloading has to be taken into account in a reliable macroscopic residual stress analysis by neutron diffraction.

MS-11

Micro-stress investigations by neutron diffraction

J. Repper[1], M. Hofmann[1], P. Link[1], A. Senyshyn[1], C. Krempaszky[2], W. Petry[1], E. Werner[3]

[1] Forschungs-Neutronenquelle Heinz Maier-Leibnitz (FRM II), Garching, Germany

[2] TUM, Christian-Doppler-Labor für Werkstoffmechanik von Hochleistungslegierungen, Garching, Germany

[3] TUM, Lehrstuhl für Werkstoffkunde und Werkstoffmechanik, Garching, Germany

It is well known that in macroscopic residual stress analysis by diffraction experiments type II residual stresses (micro-stresses) may affect the results. Whereas, the formation of macroscopic residual stresses is well understood, the accumulation of microscopic residual stresses is more complex and known to a lesser extend. In-situ mechanical loading tests show the evolution of micro-stresses during plastic deformation.
In this contribution we present the results of micro-stress evolution studies on 5 sets of IN 718 samples, which differ in microstructure. By the combination of thermal and cold neutron diffraction both intergranular and interphase micro-stresses become accessible.

MS-12

Phase transition studies of $LaAlO_3$ by neutron Larmor diffraction

J. Repper[1], T. Keller[2], W. Schmahl[3]

[1] Forschungs-Neutronenquelle Heinz Maier-Leibnitz (FRM II), Garching, Germany

[2] MPI für Festkörperforschung, Stuttgart, Germany

[3] LMU, Sektion Kristallographie, München, Germany

Neutron Larmor diffraction (LD) is a high-resolution diffraction technique based on the Larmor precession of polarized neutrons. LD does not depend on the accurate measure ent of Bragg angles. Thus, in contrast to conventional diffraction, the resolution is independent of the beam collimation and monochromaticity. At present, a relative resolution for the determination of the crystal lattice spacing d of $\Delta d/d = 10^{-6}$ is achieved. This is at least one order of magnitude superior to conventional neutron techniques. $LaAlO_3$ shows a phase transition from a rhombohedral ($T<T_t$) to a cubic crystal structure ($T>T_t$) at approx. $T_t = 813$ K. This phase transition is accompanied by a small lattice strain. In this contribution we present in-situ studies of the phase transition in $LaAlO_3$ by LD measurements carried out at TRISP. The evolution of lattice straining dependent on thermal load for the {220}, the {200} and the {020} lattice planes is shown. In addition, the change of crystal lattice parameters during the phase transition was observable by high-resolution LD.

MS-13

Neutron and x-ray study formation of nanoparticles in the alloy structure 40HNYU-one of the hard nonmagnetic material for high pressure cells

R. A. Sadykov[1], M.-S. Appavou[4] , V. S. Litvin[1], A. V. Gulyutin[2], V. P. Glazkov[3], S. N. Aksenov[1], A. Ioffe[4]

[1] Institute Nuclear Research RAS, Moscow, Russia

[2] Institute for High Pressure Physics RAS, Troitsk, Russia

[3] RRC Kurchatov Institute, Moscow, Russia

[4] Jülich Centre for Neutron Science at FRM II, Garching, Germany

Diffraction and small angle neutron scattering (SANS) has been investigated nanostructure of a number of samples alloy 40HNYU (Ni 58%, Cr 39%, Al 3%) with different hardness. Preliminary samples were tested by X-ray method. Non-magnetic alloy 40HNYU of great practical interest, because of the hardness of it does not yield hardened steel (up to 60HRc) and at the same time, there remain non-magnetic (magnetic susceptibility of less than 0,003 SGSM / g) at temperatures above 0.1 K. In In addition, this alloy has an unusual behavior during quenching and annealing: hardening at 1200°C leads to a decrease in hardness and annealing to increase it. Maximum hardness is reached at an annealing temperature of 650°C. The measurements were carried out on small-angle neutron installation KWS-2 research reactor FRM II in Garching, Germany. When the hardness of above 24 HRc, a substantial change in the structure at the nanoscale. In the unannealed state of the alloy has a quasiperiodic structure with a period of 70 nm. Annealing causes the appearance of nanoparticles with a diameter of 20-30 nm, presumably, Ni3Al. The nature of the curve indicates the relative concentration of nanoparticles of a few percent. Was also studied the evolution nanostructure of the alloy during annealing of the quenched state. In the unannealed state of the alloy has a quasiperiodic structure with a period of 35 nm. Annealing temperature above 450 ° C the formation of nanoparticles with a relative density of the order of several percent.

MS-14

FeCr model alloys treated by Helium implantation and studied by positron annihilation lifetime technique

V. Slugen, S. Sojak, J. Veterniková, M. Petriska, M. Stacho

Slovak University of Technology, Faculty of Electrical Engineering and Information Technology, Bratislava, Slovakia

Reduced Activation Ferritic/Martensitic (RAFM) steels with high chromium content (up to 12 wt%) were studied. This paper is focused on the chromium influence on the microstructural changes of iron based alloys under radiation treatment. Our experimental method – the positron annihilation lifetime spectroscopy (PALS) enables an observation of size and density changes of the vacancy type defects in the material microstructure. Defects have been created by implantation of charged particles (He^{2+}).

For the low Cr alloys there is clearly defined maximum for the implantation dose about $1{,}87.10^{18}$. The highest positron lifetime (the largest clusters of vacancies) was measured for 2,5% of Cr alloy and its value 235ps should correspondent to a cluster of 3 – 4 empty vacancies or slightly larger clusters containing helium. Higher Cr content alloys, containing 9 or 11% of Cr, respectively, are more resistant to creating of vacancy clusters which can be seen via lower positron lifetime τ_2. Maximum value of 192ps should be assigned to mono- and di-vacancy, respectively. This lifetime shows that Fe8.39%Cr material has the optimal chemical composition, from the studied materials, from the radiation damage resistance point of view.

The performed measurements showed that chromium plays an important role in the formation of the microstructure under radiation treatment. In particular, chromiu content in FeCr alloys has an influence on the vacancy cluster forming. In the low chromium alloys the small vacancy clusters have been observed up to the size of 4 vacancies agglomeration. However, such clusters of the vacancies have not been observed in high chromium materials. It means, that Cr concentration on the level 9 wt% was confirmed as optimal having in mind the resistance to the radiation induced defects agglomerations. Mono- and/or di-vacancies are more acceptable than their agglomerations from the radiation embrittlement resistance point of view.

MS-15

Influence of thermal annealing on ions implanted Fe-Cr model alloys investigated by PLEPS technique

S. Sojak[1], V. Slugen[1], V. Kršjak[1], W. Egger[2], L. Ravelli[2], M. Petriska[1], S. Stanč[1], K. Vítázek[1], M. Stacho[1], J. Veterníková[1]

[1] Slovak University of Technology, Department of Nuclear Physics and Technology, Bratislava, Slovakia

[2] Universität der Bundeswehr München, Institut für Angewandte Physik und Messtechnik, Germany

Reduced activation ferritic/martensitic (RAFM) steels are considered as structural materials for application in future nuclear facilities. Their resistance against a high irradiation doses, thermal and mechanical treatment is essential. In our laboratory conditions, the alfa radiation damage was experimentally simulated by high energy helium ions implanted into selected specimens using cascade accelerator.

The **P**ulsed **L**ow **E**nergy **P**ositron **S**ystem (PLEPS) at the high intensity positron source NEPOMUC at the research reactor FRM II in Garching was used to study the depth profiling of annealed Fe-Cr model alloys. Binary Fe-11.62%Cr model alloys were investigated in as-received state as well as after helium ions implantation in two steps at different energies (100 keV, 250 keV) with doses up to 3.12×10^{18} cm^{-2}. In order to study changes in dependence on the temperature, thermal annealing was performed. Up to now, the annealing at 400, 475 and 525 °C in argon atmosphere at pressure 100 kPa was performed and specimens were measured by PLEPS. Anneal out of defects at chosen temperatures was not significant as was expected and some uncertainties are present. Decrease of the defects size was, from specific depth, very well recognizes in as-received specimen but specimens implanted by ions did not show so definite results and one could say that the defects size even increased. Slight damage decrease in ions implanted specimens was observed in higher depths starting from ~ 350 nm.

Particle Physics

PP-01

On the origin of ROT-effect in prompt fission gamma rays

G. V. Danilyan[1], J. Klenke[2], V. A. Krakhotin[1], V. V. Novitsky[1], V. S. Pavlov[1], P. B. Shatalov[1]

[1] Alikhanov Institute for Technical and Experimental Physics, Moscow, Russia

[2] Forschungs-Neutronenquelle Heinz Maier-Leibnitz (FRM II), Garching, Germany

We have measured the angular distribution and ROT-effect of prompt fission gammarays emitted by fragments at ^{235}U fission induced by cold polarized neutrons. The experiment has been carried out on MEPHISTO polarized cold neutron beam. The dependence of the anisotropy on the gamma-rays energy occurs to be approximately the same as the dependence of the the ROT-effect. It means that the main part to the observed ROT-effect in gamma-rays accompanied the fission of ^{235}U induced by cold polarized neutrons is contributed by prompt fission gamma-rays emitted by excited fission fragments. Such conclusion based on the Strutinsky hypothesis that spins of the fission fragments are oriented orthogonal to direction of the fissile nucleus deformation axis.

PP-02

Discovery of the neutron radiative decay during the first FRM II experiment and its subsequent research

R. U. Khafizov[1], I. A. Kolesnikov[1], M. V. Nikolenko[1], S. A. Tolokonnikov[1], V. D. Torokhov[1], V. A. Solovei[2], M. R. Kolhidashvili[2], I. A. Konorov[3]

[1] RRC Kurchatov Institute, Moscow, Russia

[2] Petersburg Nuclear Physics Institute, Gatchina, Russia

[3] TUM, Physik Department,Garching, Germany

This report is dedicated to the very first experiment we conducted at FRM II in 2004-2005 and the subsequent study of neutron decay discovered during that experiment. One of the important results of the first experiment was the measurement of the main characteristic of the rare radiative branch of neutron decay, its branching ratio BR=$(3.2\pm1.6)\times10^{-3}$ (with C.L.=99.7% and gamma quanta energy over 35 keV) [1]. Besides, we demonstrated that our results correspond to the results of the emiT group experiment on regular neutron decay [2]. However, we cannot say the same about the experiment conducted by the group from NIST, which studied not radiative neutron decay but rather the well-known phenomenon of the artificial radioactivity [3]. Here it is important to note that the BR value obtained in our experiment exceeds the theoretical value, calculated within the framework of the electroweak interaction theory, by 1.5 times. However, due to a significant experimental error we cannot claim that we see a deviation from the standard model, so all of our actions from 2005 were dedicated to preparing a new experiment on BR measurements. As a result of this work, we created a new, more precise system for collecting and analyzing data, which would allow us to measure BR with precision of 1% [3]..

[1] R.U. Khafizov et al. JETP Letters, v. 83(1), 2006, p. 5.

[2] L.J. Lising, et al., Phys. Rev. C. v.6, 2000, p. 055501.

[3] Khafizov R.U., Kolesnikov I.A., Tolokonnikov S.V., Torokhov V.D., Solovei V.A., Kolhidashvili M.R., Konorov I.A. New experiment on the neutron radiative decay. ISINN-17, XVII International Seminar on Interaction of Neutrons with Nuclei; Neutron Spectroscopy, Nuclear Structure, Related Topics, Dubna, May 27-29, 2009, Reports, p. 368.

PP-03

Neutron reactions on Ge-background in neutrinoless double beta decay experiments

G. Meierhofer[1], L. Canella[2], P. Grabmayr[1], J. Jochum[1], P. Kudějová[3]

[1] Universität Tübingen, Physikalisches Institut, Kepler Center for Astro and Particle Physics, Germany

[2] TUM, Institut für Radiochemie, Garching, Germany

[3] Forschungs-Neutronenquelle Heinz Maier-Leibnitz (FRM II), Garching, Germany

The possible observation of the neutrinoless double beta decay ($0\nu\beta\beta$) is a proof of the Majorana nature of the neutrino. If theory provides precise matrix elements the effective neutrino mass can be derived from the measured half life time. A promising approach to observe the $0\nu\beta\beta$ decay uses germanium crystals, isotopically enriched in ^{76}Ge($Q_{\beta\beta}$=2039keV), which serve as source and HPGe detector at the same time. The upcoming GERDA and MAJORANA experiments will be based on this method.

Fast neutrons produced by cosmic muons are source of background due to various reactions with the Ge nuclei in the detectors. The most severe contribution is the β-decay of ^{77}Ge after neutron capture on ^{76}Ge. High energetic β-particles emitted by this decay may cause signals in the detectors identical to $0\nu\beta\beta$ events. Furthermore the (n,p)-reaction and neutron scattering have to be considered in the background analysis in the region of interest at 2039 keV. Experiments performed at the FRM II to quantify these contributions and their results will be presented.

This work was supported by the German DFG (GRK683) and BMBF (05A08VT1).

PP-04

Investigation of different converter materials for the production of ultra-cold neutrons

F. Böhle[1], R. Bozhanova[1], A. Frei[1], E. Gutsmiedl[1], T. Huber[1], S. Paul[1], S. Wlokka[1], J. Klenke[2]

[1] TUM, Physik Department, Garching, Germany

[2] Forschungs-Neutronenquelle Heinz Maier-Leibnitz (FRM II), Garching, Germany

We have investigated solid ortho-deuterium (o-D_2), solid α-oxygen (α-O_2) and solid III-tetradeuteromethane (III-CD4) concerning their properties as superthermal converters for the production of ultra-cold neutrons (UCN). In a first series of experiments the crystal preparation was examined. Optically transparent or semi-transparent crystals of these three materials have been prepared at T = 8 K. In a second series of experiments these crystals have been exposed to the cold neutron flux of the MEPHISTO beam line of the FRM II. Ultra-cold neutrons produced inside the crystals have been extracted and the count rates have been measured at different converter temperatures. The results of these measurements give a clear signal of the superthermal production mechanism for all three materials. Especially for α-O_2 superthermal UCN-production due to antiferromagnetic lattice excitations has been observed for the first time experimentally.
This presentation will give an overview of the experimental setup and of the measured results. The three materials will be compared concerning their properties for superthermal UCN-production and extraction. Possible applications will be discussed.

Soft Matter

SO-01

Structure and dynamics of thermoresponsive poly(styrene-*block*-**N-isopropyl acrylamide**-*block*-styrene) hydrogels

J. Adelsberger[1], A. Meier-Koll[1], W. Wang[1], A. M. Bivigou-Koumba[2], A. Laschewsky[2], T. Hellweg[3], O. Holderer[4], V. Pipich[4], P. Busch[4], P. Müller-Buschbaum[1], C. M. Papadakis[1]

[1] TUM, Physik Department, Garching, Germany

[2] Universität Potsdam, Institut für Chemie, Golm, Germany

[3] Universität Bayreuth, Physikalische Chemie I, Germany

[4] Jülich Centre for Neutron Science at FRM II, Garching, Germany

As thermoresponsive polymer gels display strong changes in volume when heated above the lower critical solution temperature (LCST), they are interesting candidates for applications in ultrafiltration or as drug delivery systems. Our research is focused on triblock copolymers having two hydrophobic polystyrene (PS) end blocks and a thermoresponsive poly(N-isopropyl acrylamide) (PNIPAM) middle block. In aqueous solution they form core-shell micelles or micellar networks. Contrast matching with fully deuterated PS end blocks in combination with D_2O as solvent allows to selectively investigate the micellar shell. The structure of the micelles and their correlation are determined using small-angle neutron scattering (SANS) at KWS-2 at FRM II [1,2]. Concentrations of 50, 200 and 300 mg/ml were investigated. For all concentrations studied, the micellar radius shows a sudden decrease at the LCST, i.e. the hydrophilic shell shrinks and becomes hydrophobic. Above the LCST, the collapsed micelles form large clusters, and water is released. For concentrations of 300 mg/ml, one observes a lower LCST than for 50 and 200 mg/ml.

In addition to SANS, neutron spin-echo spectroscopy (NSE) measurements were carried out at J-NSE at FRM II in order to study the segmental dynamics of the hydrophilic block. The intermediate scattering function displays the fast PNIPAM segmental motion and the slow micellar diffusion [1]. Below the LCST, the diffusion coefficient of the fast internal PNIPAM dynamics is temperature-independent and decreases with increasing polymer concentration. Above the LCST, the diffusion coefficient of segmental dynamics is independent of concentration, which we attribute to the collapse to a PNIPAM melt. SANS and NSE thus allow a detailed characterization of self-organized thermoresponsive networks.

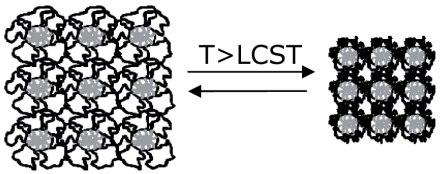

Fig. 1: Schematics of network formation by self-assembly of the triblock copolymers and the network collapse.

[1] Adelsberger, J.; Kulkarni, A.; Jain, A.; Wang, W.; Bivigou-Koumba, A. M.; Busch, P.; Pipich, V.; Holderer, O.; Hellweg, T.; Laschewsky, A.; Müller-Buschbaum, P.; Papadakis, C. M.; Macromolecules 2010, 43, 2490.

[2] Jain, A.; Kulkarni, A.; Bivigou Koumba, A. M.; Wang, W.; Busch, P.; Laschewsky, A.; Müller-Buschbaum, P.; Papadakis, C. M.; Macromol. Symp. 2010, 291-292; 221.

SO-02

Magnetic field and particle concentration competitive effects on ferrofluid based silicone elastomer microstructure

M. Balasoiu[1,2], I. Bica[3], Y. L. Raikher4, V. T.Lebedev[5], L. Almasy[6], E. B. Dokukin[2], A. I. Kuklin[2]

[1] National Institute of Physics and Nuclear Engineering, Bucharest, Romania

[2] JINR, Dubna, Russia

[3] West University of Timisoara, Department of Electricity and Magnetism, Romania

[4] Institute of Continuum Media Mechanics, Ural Branch of RAS, Perm, Russia

[5] Petersburg Nuclear Physics Institute, Gatchina, Russia

[6] PSI, Villigen, Switzerland

Combination of magnetic and elastic properties of magnetic elastomers leads to various phenomena which these composites display under an applied magnetic field. Various structures could be formed inside the material or the already existing structures would be changed due to the magnetic field.

In the present paper, results on small angle neutron scattering investigations on the static microstructure of ferrofluid based silicone-rubber elastomer samples are presented. The investigated samples from the present work consist of the following components: RTV-2 silicones, catalyst 60R, 10% mass concentration of ferrofluid (transformer oil based; particle content 12,8 vol.%). Polymerization of the magnetic nanoparticles – oligomer mixtures was carried out under several values of a constant magnetic field and 3 values of particle volume concentration. Small angle neutron scattering (SANS) experiments on the elastomer samples doped with magnetite nanoparticles was performed on the SINQ time-of-flight spectrometer SANS II (PSI, Villigen) and on the Membrana facility in function at VVR reactor (PNPI, Gatchina). By means of small angle neutron scattering, variation of the structure factor with particle concentration and the induction of the magnetic field applied during polymerization are found. In fig. 1 the interparticle correlation distance obtained by means of small angle neutron scattering measurements is plotted versus the particle volume concentration. The results show that at the particle concentrations greater than 3 vol. % has a stronger effect on the interparticle correlation distance than that of the magnetic field up to 56 mT imposed during the polymerization process. Contrary to this fact, for small particle volume concentrations (of the order of 1 vol. %), the magnetic field applied during the polymerization process affects the interparticle correlation distance to a considerable extent.

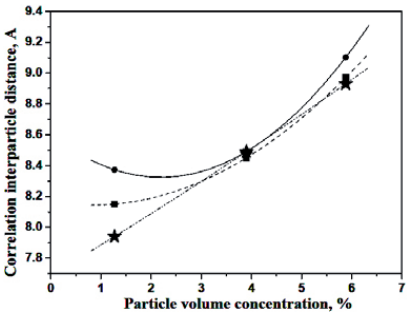

Fig. 1. Variation of the interparticle correlation distance with the particle volume concentration for different values of the polymerization magnetic field: B = 0 (solid circles), 28mT (solid stars) and 56 mT (solid squares).

SO-03

Dynamics of confined surfactant membranes in microemulsions near planar surfaces

H. Frielinghaus[1] M. Kerscher[2], O. Holderer[1]

[1] Jülich Centre for Neutron Science at FRM II, Garching, Germany

[2] FZ Jülich GmbH, Institut für Festkörperforschung, Germany

Microemulsions near planar hydrophilic surfaces are ordered lamellar, while the bulk structure is bicontinuous. The static structure has been characterized by grazing incidence small angle neutron scattering measurements (GISANS) and neutron reflectometry. The depth resolution of the GISANS measurements was achieved by tuning the penetration depth of the evanescent wave by varying the incident angle and the overall contrast of the liquid against the solid. The lamellar region is 400 Å thick, and thus embraces 2 double layers of oil and water domains. Static structures and their scattering results were simulated by a computer model, and an agreement could be achieved to some extent. Latest dynamic measurements were successfully achieved by combining the grazing incidence method with neutron spin echo spectroscopy. Again, depths between 300 and 800 Å were resolved. The characteristic time of the membrane undulations was the same for the bulk of the transmission measurement and at large penetration depths, and comparable for the lamellar region near the surface. At a depth of ca. 600 Å, the characteristic time shows a clear dip to half the value. In this depth we expect an intermediate structure, the perforated lamellar structure. This intermediate state shows a faster relaxation since it is out of equilibrium. The high sharpness of the dip of the characteristic time arises from non-linear effects which opposes to an underlying simple Laplace transformation.

SO-04

Density and solvent content at the polymer-solid interface

E. T. Hoppe[1], B. Wang[1], M. Haese-Seiller[2], J.-F. Moulin[2], M. Port[3], B. Menges[3], C. M. Papadakis[1]

[1] TUM, Physik Department, Garching, Germany

[2] GKSS-Forschungszentrum Geesthacht @ FRM II, Garching, Germany

[3] MPI für Polymerforschung, Mainz, Germany

Close to the interface between a polymer film and a solid, the polymer properties have been found to deviate from the bulk and to form an interphase. This change in physical behaviour is of importance for the adhesion of polymer coatings to solids, e.g. in medical implants and in nanocomposites.

The aim of the project is the investigation of the influence of the polymer-solid interaction on the physical properties of the polymers near the interface. We focus on the correlation between the changes of density, viscosity and chain orientation of the polymer melt near the interface. Remaining solvent from the sample preparation is an important issue which may falsify the results.

Polybutadiene melts from toluene solutions on oxidized silicon are studied as a model system. To tune the interface interactions between substrate and polymer melt, the substrate surface is modified chemically and by silanization.

The density profile near the solid interface is investigated systematically by **t**ime-**o**f-**f**light **n**eutron **r**eflectometry (TOF-NR) at REFSANS. 100 nm thin films of deuterated polybutadiene with a molar mass of 55 kg/mol are investigated on dry thermal oxidized silicon substrates. The properties of the substrate are altered by silanization with polybutadiene-modified silane. TOF-NR curves have been measured at several incident angles between 0.2° and 2.0° corresponding to a scattering vectors Q_z to 0.14 $Å^{-1}$.

The optical properties of polybutadiene are investigated in the bulk using optical waveguide spectroscopy, whereas the interphase is characterized by monitoring the surface plasmon. Gold-coated heavy flint glass is used as substrate for thick films of polybutadiene with various degrees of polymerization. We have found that low molar mass PB has a higher capacity for solvent storage. The refractive index in the interphase close to the gold-coated glass is lower compared to the bulk if the sample is not dried by means of vacuum.

Combining TOF-NR with optical waveguide and surface plasmon spectroscopy gives thus valuable insight into the density profile and the solvent content in polymers near a solid interface.

SO-05

Switching behavior of thermoresponsive poly(2-oxazoline) copolymers

S. Jaksch[1], J. Adelsberger[1], S. Salzinger[2], S. Huber[2], R. Jordan[2], Z. Di[3], C. M. Papadakis[1]

[1] TUM, Physik Department, Garching, Germany

[2] TUM, Department Chemie, Garching, Germany

[3] Jülich Centre for Neutron Science at FRM II, Garching, Germany

Amphiphilic copolymers in aqueous solution exhibit a wide range of morphologies ranging from micellar and other colloidal structures to hydrogels at high concentrations. Poly(2-oxazoline)s represent a very attractive class of materials as their properties can be tuned from hydrophilic via thermoresponsive to hydrophobic by changing the side group R (Fig. 1a) from methyl over propyl to nonyl. Moreover, the fraction of thermoresponsive and hydrophobic blocks in the copolymers can be changed, and the architecture of the polymer can be varied from homopolymers to block and gradient copolymers [1]. We present here a temperature-dependent investigation of two gradient copolymers from thermoresponsive isopropyl-2-oxazoline (iPrOx) and hydrophobic *n*-nonyl-2-oxazoline (NOx) gradient copolymers. The aim of the study is to investigate the influence of the fraction of hydrophobic monomers on the thermoresponsive behavior.

Temperature-dependent SANS experiments were carried out at KWS 2 around the lower critical solution temperature (LCST) for P(*i*PrOx$_{48}$-g-NOx$_2$) and P(*i*PrOx$_{46}$-g-NOx$_4$) in dilute solution in D_2O (20 mg/ml). P(*i*PrOx$_{48}$-g-NOx$_2$) behaves like the thermoresponsive homopolymer PiPrOx$_{50}$ with molecularly dissolved chains that collapse at the LCST of PiPrOx and form large aggregates (above 500 nm) above (fig. 1b). The behavior of the radius of gyration is described by a power law (fig. 1b). P(*i*PrOx$_{46}$-g-NOx$_4$) has a more compact chain conformation even below the LCST which we attribute to the presence of two additional hydrophobic monomers.

Apart from that, it shows very similar switching behavior to P(*i*PrOx$_{48}$-g-NOx$_2$).

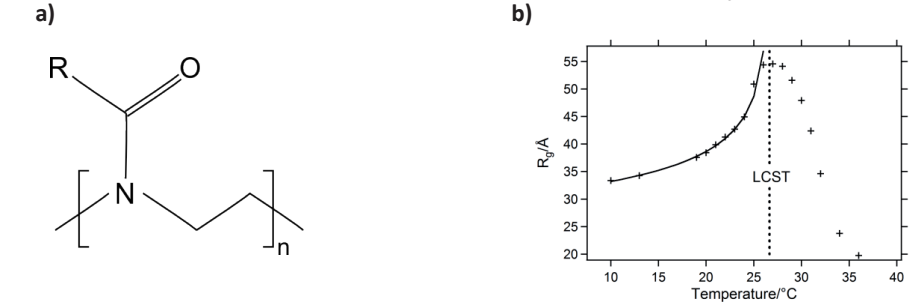

Fig. 1. (a) Structure of the poly(2-oxazoline) monomer. (b) Radius of gyration versus temperature. The LCST is marked by a dashed line. The fit shows a behavior described by a power law.

[1] T.B. Bonné, K. Lüdtke, R. Jordan, C.M. Papadakis, Macromol. Chem. Phys. 208, 1402 (2007).

SO-06

Supported polyelectrolyte multilayer under mechanical stress: sequential change of the internal structure

J. Früh[1], A. Rühm[2], H. Möhwald[1], R. Krastev[3], R. Köhler[1,4]

[1] MPI für Kolloid- und Grenzflächenforschung, Potsdam, Germany

[2] MPI für Metallforschung, Stuttgart, Germany

[3] NMI an der Universität Tübingen, Reutlingen, Germany

[4] HZB für Materialien und Energie GmbH, Berlin, Germany

Polyelectrolyte (PE) Multilayer (PEM) are composite materials build-up of alternating layers of organic polyions of opposite charge. Due to the good adjustability of the physico-chemical parameters of the PEM (e.g. thickness, surface roughness, or particle incorporation) [1], they become promising materials for technical applications (e.g. coatings, and function-alization). Hereby the mechanical properties of PEM such as stiffness, resistance, and fatigue are crucial. This makes the studies on the properties of PEM under mechanical stress an important topic. Several studies on the mechanics of free-standing PEM build as micro-capsules [2] and supported PEM films [3] mainly address the macroscopic properties of the layers such as elastic module and its change under different ambient conditions (e.g. humidity). Our study aims to correlate the changes of the internal structure of mechanically loaded PEM on molecular level.

The PEM were build with two strong polyelectrolytes on solid support. The polyanion was polystyrene sulphonate (PSS). Poly-diallyldimethylammonium chloride (PDADMAC) was used as the polycation. For studying small elongations ($\varepsilon \leq 0.2\%$) glass slides coated with PEM were deformed. The change in the film thickness and density of the PEM upon elongation was measured using neutron and X-ray reflectivity and ellipsometry. For studying larger deformations (up to $\varepsilon = 10\%$) Pyrene labelled PEM coated onto poly-dimethylsiloxane sheets were elongated and investigated. Pyrene molecules in close distance to each other (≈ 5Å) form eximers which show a characteristic peak in the fluorescence spectra. Changes of these spectra indicate excimer formation or decomposition.

The molecular rearrangement of PEMs under mechanical stress can be studied using Pyrene labelled PSS enabling the detection of molecular arrangement and local polarity. An irreversible decrease in the excimer to monomer fluorescence intensity ratio and an increase in the polarity of the PEM were observed upon stretching which causes an irreversible molecular decoiling. Drying of PEMs changes the molecular orientation of PEMs and leads to a molecular decoiling caused by internal shear forces. When the limit of plastic deformation is exceeded, i.e. the molecules are almost fully decoiled, macroscopic cracks are observed indicating the destruction limit of the PEM. The molecular decoiling also yields to an increase in the polarity of the PEM, which was found to be irreversible after 10% elongation. The scattering experiments show decrease in the film thickness although the PEM density stays constant. This might be a result of formation of “molecular cavities” in the films upon stretching. The detailed study on the response of the PEM on external mechanical stress opens one new possibility to finely tune the properties of the PEM on molecular level.

[1] G. Decher; J.D. Hong; J. Schmitt, Thin Solid Films 1992, 210/211, 831-835; M. Schönhoff, J.Physics: Condensed Matter 2003, 15, 1781-1808; Klitzing, R. v. PCCP 2006, 8, 5012-5033; G. Decher; J.B. Schlenoff; J.M. Lehn, Multilayer Thin Films: Sequential Assembly of Nanocomposite Materials.Wiley-VCH 2003.

[2] G. Changyou; S. Leporratti; S. Moya; E. Donath; H. Möhwald, Langmuir 2001, 17, 3491-349.

[3] A. J. Nolte; N. D. Treat; R. E. Cohen; M. F. Rubner, Macromolecules 2008, 41, 5793-5798.

SO-07

Residual solvent study in homopolymer films utilizing neutron reflectivity measurements

R. Meier[1], M. Schindler[1], A. Nathan[1], A. Diethert[1], R. Georgii[2], P. Müller-Buschbaum[1]

[1] TUM, Physik Department, Garching, Germany

[2] Forschungs-Neutronenquelle Heinz Maier-Leibnitz (FRM II), Garching, Germany

In the last years polymers have proven to have great application possibilities not only for the standard plastic industry but also for different niche products such as advanced optical coatings or organic thin film electronics. One of their main advantages is the solution processability, which allows the fabrication of homogeneous ultrathin films by multiple methods. Besides spray coating and solution casting spin coating is the method of choice for polymeric films with a film thickness in the nanometer region.
For all these methods the polymers are dissolved in suitable solvents first. It is known from gas chromatography measurements that thin polystyrene (PS) films have a residual solvent content of 5%, if they are spin coated from toluene solution [1]. In addition Perlich et. al. have revealed a solvent distribution showing an enrichment layer of the residual solvent at the substrate interface in such films by using neutron reflectivity measurements [2]. In this work we show the influence of the polymer on the amount of solvent in the thin films by changing to polymethymethacrylate (PMMA), which is often used as an alternative to glass. This also allows a generalization of the storage mechanism of the residual solvent molecules in a surrounding polymer matrix. In addition also the dependence of the solvent uptake on the molecular weight and the substrate treatment is investigated.
The study is complemented with X-ray reflectivity measurements and optical microscopy images.

[1] J. García-Turiel et. al., Colloid&Polymer Science, 2007, 285, 14.
[2] Perlich et al., Macromolecules, 2009, 42 (1), 337-344.

SO-08

Short time dynamics of medium length molecules

H. Morhenn[1], S. Busch[1], D. Richter[2], T. Unruh[1]

[1] Forschungs-Neutronenquelle Heinz Maier-Leibnitz (FRM II), Garching, Germany

[2] FZ Jülich GmbH, Institut für Festkörperforschung, Germany

The description of transport mechanisms in molecular liquids is a challenging task. Especially the mechanism of molecular self-diffusion in liquids of organic medium-chain molecules is not fully understood yet.

With time-of-flight quasielastic neutron scattering (TOF-QENS) it is possible to get an experimental access to the motions on a molecular length scale in the pico- to nanosecond time regime [1]. In this regime one has to assume a superposition of several (intra)molecular motions (e. g. long-range diffusion, methyl group rotation). It could be shown previously that the diffusion coefficients of short- and medium-chain *n*-alkanes measured by TOF-QENS deviate increasingly from the long-time long-range values determined by PFG-NMR with increasing chain length of the molecules and decreasing temperature [2].

In this context the dynamics of molecular chains could be supposed to depend on the dimensions of the considered chain. A critical value in this context is the so-called entanglement molecular weight. Theoretical models as the reptation model of de Gennes and the bead-spring model of Rouse were developed to describe large scale chain motion above and below the entanglement length, respectively.

TOF-QENS experiments were performed on a polyethylene melt (*n*-$C_{100}H_{202}$ [3,4]), and a polydimethylsiloxane melt (PDMS [5], molecular weight approx. 17,250). Both chains are long enough to show gaussian chain statistics in their confirmations, but are still in the unentangled regime so that it was possible to check the validity of the Rouse model on this time and length scale. It could be shown that the simple Rouse model cannot describe the TOF-QENS data satisfactorily and an additional fast motion is observed. The data can be described better by also considering the atoms as brownian particles in a harmonic potential (see fig. 1). The separation of the independent motions makes it possible to compare the long-range motion. This shows that the longer PDMS molecules seem to relax faster than the C_{100}.

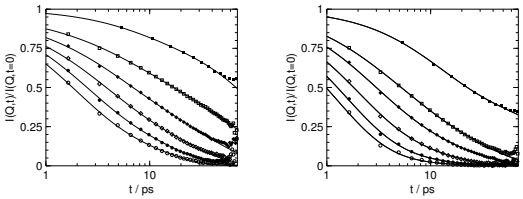

Fig. 1: Evaluation of I(Q,t) of C(left) and PDMS (right) at 373 K. The fit functions consider long-range diffusion and intramolecular motions. Q-values from top to bottom: 0.4, 0.6, 0.8, 1.0,1.2 and 1.4 $Å^{-1}$.

[1] T. Unruh, C. Smuda, S. Busch, J. Neuhaus and W. Petry. J. Chem. Phys. , 121106 (2008).

[2] C. Smuda, S. Busch, G. Gemmeker and T. Unruh. J. Chem. Phys. , 014513 (2008).

[3] W. Paul, G. D. Smith, D. Y. Yoon, B. Farago, S. Rathgeber, A. Zirkel, L. Willner and D. Richter. Phys. Rev. Lett. 80, 2346 (1998).

[4] G. D. Smith, W. Paul, D. Y. Yoon, A. Zirkel, J. Hendricks, D. Richter and H. Schober. J. Chem. Phys. 107, 4751 (1997).

[5] D. Richter, B. Ewen, B. Farago and T. Wagner, Phys. Rev. Lett. 62, 2140 (1989).

[6] V. Arrighi, F. Ganazzoli, C. Zhang and S. Gagliardi. Phys. Rev. Lett. , 58301 (2003.)

SO-09

Self-assembling in solution of crystalline-amorphous olefin block copolymers studied by wide-*Q* small angle neutron scattering

A. Radulescu[1], G. Goerigk[1], L. J. Fetters[2], D. Richter[1,3]

[1] Jülich Centre for Neutron Science at FRM II, Garching, Germany

[2] Cornell University, School of Chemical and Biomolecular Engineering, Ithaca, USA

[3] FZ Jülich GmbH, Institut für Festkörperforschung, Germany

The self-assembling behaviour in solution of crystalline-amorphous olefin block copolymers (OBC-Infuse) obtained by chain shuttling technology [1] was studied over a wide temperature range (between the single coil regime at 120°C and the aggregation regime down to 0°C) by small-angle neutron scattering (SANS). The commercial OBCs consist of crystallizable ethylene-octene blocks (hard) with very low co-monomer content and high melting temperature, alternating with amorphous ethylene-octene blocks (soft), with high co-monomer content and low glass transition temperature. Complex morphologies revealing multiple structural levels hierarchically organized over a length scale between 1nm and several microns form and evolve in decreasing temperature. These morphologies were characterized by combining classical pinhole SANS and mirror focusing SANS techniques at the KWS-2 and KWS-3 SANS diffractometers [2,3] of JCNS at FRM II reactor (fig.1). The crystallization of the hard blocks at 105°C leads to formation of correlated lamellar structures that alternate with soft blocks containing amorphous regions. The elongated lamellae associate and grow laterally in spheriform clusters several microns in size and resembling spherulitic morphologies as revealed by crossed-polarizers microscopy.

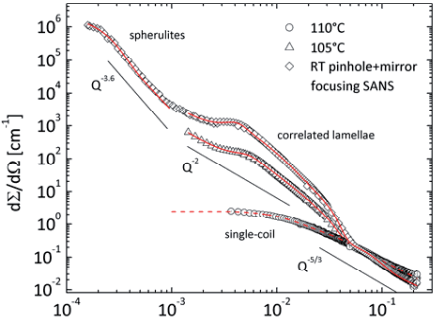

Fig.1: Typical scattering patterns from OBC copolymers in d-dodecane solution; single coil (110°C), correlated core-brush lamellae (105°C) and large scale spherulitic (25°C) morphologies were identified and characterized; the lines represent fitting results of the experimental data according to different structural models.

[1] D.J.Arriola et al., Science 312 714 (2006).
[2] A.Radulescu and A.Ioffe, Nuclear Instruments and Methods A 586 55 (2008).
[3] T.Vad, W.F.C.Sager, J.Zhang, J.Buitenhuis, A.Radulescu, J.Appl.Cryst. 43 686 (2010).

SO-10

Neutron reflectivity study on solvent residuals in thin conducting polymer films

M. Schindler[1], R. Meier[1], H.-Y. Chiang[1], A. Nathan[1], A. Diethert[1], R. Georgii[2], P. Müller-Buschbaum[1]

[1] TUM, Physik Department, Garching, Germany

[2] Forschungs-Neutronenquelle Heinz Maier-Leibnitz (FRM II), Garching, Germany

Conducting polymers show a wide range of possible applications such as organic solar cells or organic light emitting diodes. Neutrons provide means to investigate thin films made of these polymers without causing damage to their chemical structure. Presently, there is contradictory evidence on remaining solvent in thin polymer films after their fabrication. Perlich et al. [1] report that a significant amount of solvent remains in thin films of coiled homopolymers prepared via spin-coating. Such a remaining amount of solvent in thin conducting polymer films would have a major impact on the film morphology and aging properties. On the other hand, Zhang et al. state that there are no significant solvent residuals detectable in similar systems [2]. The electrical performance of diverse polymer based organic thin-film applications would be affected by solvent residuals. With a high resolution reflectivity setup the remaining solvent inside thin conducting polymer films is investigated. We probe novel and widely used polymers such as M3EH-PPV, MDMO-PPV, P3HT and F8BT. Moreover, the neutron scattering length densities for these conducting polymers are determined and the influence of different protonated and deuterated solvents is tested.

[1] Perlich et al., Macromolecules, 2009, 42 (1), 337-344.
[2] Zhang et al., Macromolecules, 2010, 43, 1117-1123.

SO-11

The influence of different solvents on the LCST behavior of P(S-b-MDEGA-b-S) hydrogel films

Q. Zhong[1], J. Adelsberger[1], M. Niedermeier[1], A. Golosova[1], A. M. Bivigou-Koumba[2], A. Laschewsky[2], C. M. Papadakis[1], P. Busch[3], S. Botta[4], S. S. Funari[4], P. Müller-Buschbaum[1]

[1] TUM, Physik Department, Garching, Germany

[2] Universität Potsdam, Institut für Chemie, Germany

[3] Jülich Centre for Neutron Science at FRM II, Garching, Germany

[4] HASYLAB @ DESY, Hamburg, Germany

Thermo-responsive hydrogels exhibit interesting properties which attract more and more attention due to a large variety of applications. As the novel thermo-responsive homopolymer poly(monomethoxy diethyleneglycol acrylate) (PMDEGA) exhibits a higher lower critical solution temperature (LCST) when compared to the frequently investigated thermoresponsive polymer poly(N-isopropylacrylamide) (PNIPAM), it can be an interesting alternative to the use of PNIPAM. In order to create an internal ordering in the hydrogel film, polystyrene end-blocks are introduced to PMDEGA resulting in the triblock copolymer, P(S-b MDEGA-b-S). Because the triblock copolymer consists of hydrophobic parts (PS) and hydrophilic parts (PMDEGA), by choosing PS selective or PMDEGA selective solvents, the micelle structure in the solutions can be changed. In addition, the LCST can be influenced. The P(S-b-MDEGA-b-S) films were prepared by solution casting of tri-block copolymer solution with different solvents onto Kapton foil. For the swelling experiments, each film was placed in a small cell, and D_2O was injected into the cell. During the measurements, the temperature of cell was increased from 30°C to 50°C in steps of 2°C. The structural changes caused by passing the LCST was investigated by small-angle neutron scattering (SANS) at the KWS2 instrument. A sample-to-detector distance of 1.67 m and 7.67 m was applied, while the wavelength was 6.996 Å. For comparison, the tri-block polymer films with the same preparation and measurement protocol were probed with small-angle X-ray scattering (SAXS) at instrument A2 at HASYLAB. The observed dependencies of the polymer structure on solvent and temperature are discussed.

Structure

ST-01

Phase behaviour of $CoCl_2$-$MnCl_2$ mixed crystals

J. Davaasambuu[1], F. Güthoff[1], M. Hoelzel[2], A. Senyshyn[2], G. Eckold[1]

[1] Universität Göttingen, Institut für Physikalische Chemie, Germany

[2] TU Darmstadt, FB für Material- und Geowissenschaften, Germany

Demixing reactions in solids can be used for the preparation of self-organised nanoscaled structures if the phase separation is dominated by spinodal decomposition[1]. Controlling its kinetics by suitable ageing conditions allows one to predict the characteristic length scales. A necessary condition for this type demixing is a miscibility gap with a suitable lattice parameter mismatch of the constituents.

The system $CoCl_2$-$MnCl_2$ could principally provide a suitable magnetic model system since a broad miscibility gap with an upper critical temperature of about 109°C has been predicted on the basis thermodynamic calculations [2].

Thermal properties of $CoCl_2$, $MnCl_2$ and their mixed crystals are investigated by means of temperature dependent neutron powder diffraction and time-resolved small angle neutron scattering. Temperature dependent powder diffraction experiments were carried out at the high-resolution powder diffractometer SPODI at the FRM II from 50K to 475K for pure $CoCl_2$ and $MnCl_2$ as well as for the solid solution $Co_{0.5}Mn_{0.5}Cl_2$.

After quenching a mixed crystal from 250°C to room temperature, time-resolved small angle neutron scattering measurements were performed at the KWS-2 instrument at FRM II. The scattered intensity does not change with time at all. The intensity profile can well be described by the Porod-law.

Neutron powder diffraction as well as neutron small angle scattering show that $CoCl_2$ and $MnCl_2$ form a homogeneous solid solution between 50K and the liquid phase. There is no experimental evidence for the pronounced miscibility gap as predicted by Robelin et al.[2]. Hence, it must be concluded that the simple Bragg-Williams model applied by these authors is not adequate to describe the interactions within this system.

[1] A.Ringe, P.Elter, H.Gibhardt, G.Eckold, Solid State Ionics 177, (2006), 2473.

[2] C.Robelin, P.Chartrand, A.D.Pelton, J.Chem.Thermodynamics 36, (2004), 793.

ST-02

$Al_{14}Ba_8La_{26.4}Ru_{18}Sr_{53.6}O_{167}$: a variant from the cubic perovskite with isolated RuO_6

F. J. Zúñiga[1], F. J. García-García[2], M. Hoelzel[3], A. Reller[4]

[1] Universidad del País Vasco, Facultad de Ciencia y Tecnología, Bilbao, Spain

[2] Universität Augsburg, Institut für Physik, Germany

[3] TU Darmstadt, FB für Material- und Geowissenschaften, Germany

[4] Universität Augsburg, Institut für Physik, Germany

The crystal structure of the title compound has been solved and refined using neutron powder diffraction to establish the parameters of the oxygen sub-lattice and then single-crystal x-ray diffraction data for the final refinement. The structure is a cubic modification of the perovskite structure type, ABO_3.
The refined composition is $Ba_{0.167}La_{0.54}Sr_{1.118}Ru_{0.375}Al_{0.291}O_{3.483}$, and with respect to the basic perovskite structure type it might be written as $(Ba_8Sr_{32.784}La_{15.216})(Ru_{17.904}Al_{14.096}Sr_{20.48}La_{11.52})O_{192-\chi}$, where $\chi \approx 24.08$. In the A sites there are Ba, La Sr atoms. The Ba atoms are located in regular cuboctahedral environment whereas La and Sr atoms share the same positions with an irregular coordination of O atoms. Type B-type sites are divided between two different Wyckoff positions, occupied by Ru/Al and La/Sr respectively. Only Al and Ru atoms occupy positions close to the ideal ones in a perovskite while La and Sr move away from these positions toward the (111) planes with high Al content. The structure contains isolated RuO_6 form tetrahedral substructural units.

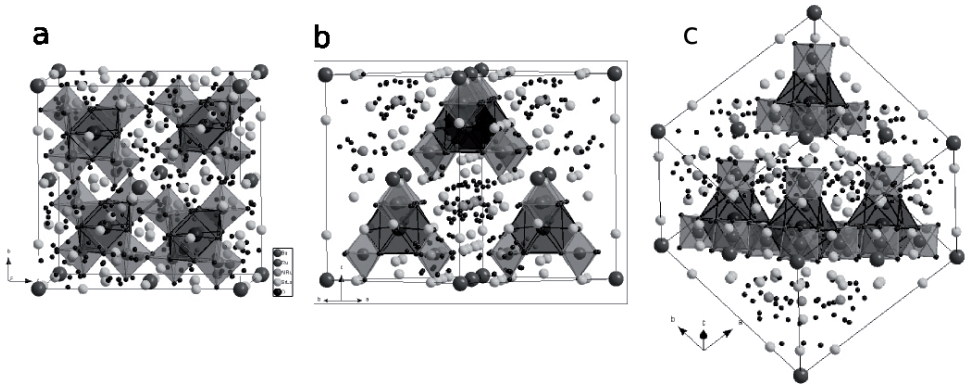

Fig. 1: Projections of the structure down [100] in (a), [110] in (b) and [111] in (c).

ST-03

Magnetic properties at the interface between $YBa_2Cu_3O_7$ and $La_{2/3}Ca_{1/3}MnO_3$ multilayer

J. Kim, V. Hinkov, L. Mustafa, S. Soltan, B. Keimer

MPI für Festkörperforschung, Stuttgart, Germany

Using polarized neutron reflectometry, we have studied the magnetic properties of the interface between a ferromagnetic metal $La_{2/3}Ca_{1/3}MnO_3$ (LCMO) and an unconventional superconductor $YBa_2Cu_3O_7$ (YBCO) heterostructure grown on [110]- oriented $SrTiO_3$ (STO) substrates as a function of temperature and magnetic field. From comparison our data taken at N-REX$^+$ with simulated reflectivity curves, we identified possible magnetic induction depth profiles. The structure properties of STO substrate of the superlattice will also be discussed.

ST-04

Structural-, magnetic transitions and electronic structure of $La_{2-x}Sr_xCoIrO_6$ ($0 \leq x \leq 2$) and $La_{2-x}Ca_xCoIrO_6$ ($0 \leq x \leq 0.75$)

N. Narayanan[1,2], D. Mikhailova[1,2], D. Trots[3], A. Senyshyn[1], R. Laskowski[4], P. Blaha[4], K. H. Schwarz[4], H. Fuess[1], H. Ehrenberg[2]

[1] TU Darmstadt, FB für Material- und Geowissenschaften, Germany

[2] Leibniz-Institut für Festkörper- und Werkstoffforschung Dresden, Institut für komplexe Materialien, Germany

[3] Bayerisches Geoinstitut, Universität Bayreuth, Germany

[4] TU Wien, Institut für Materialchemie, Austria

In recent years double perovskites (DP) $A_2BB'O_6$ with 3d transition metals at B-site and 4d or 5d transition metals at B′-site have been extensively studied due to their interesting physical properties such as structural phase transitions or interesting magnetic ordering, that could be tuned by changing the electronic structure. In DP this can be done by manipulating the size, band filling (B-site), oxygen deficiency or site disorder degree of freedom. In this sense Ir based DPs are less investigated compared to Re or W based ones. But the combination of a large spin-orbit coupling and electron correlation should result in interesting physical properties. Cobalt on the other hand is interesting due to the fact that within a certain oxidation state, it may exhibit different spin states. In this work only the A-site substitution is investigated. The $La_{2-x}Sr_xCoIrO_6$ system (LaSr) has therefore both the size and band filling degrees of freedom, whereas the $La_{2-x}Ca_xCoIrO_6$ system (LaCa) has only the band filling degree of freedom. The synthesis of LaSr is a solid state reaction of La_2O_3, $SrCO_3$, CoO and IrO_2 at 1200°C, whereas LaCa is synthesized at 1340°C using $CaCO_3$ instead of $SrCO_3$. Laboratory x-ray, synchrotron and neutron powder diffraction (NPD) techniques were combined to investigate the temperature and composition dependence of the crystal structure for five different compositions x=0, 0.5, 1, 1.5 of LaSr and two different compositions x=0.5 and 0.75 of LaCa. The magnetic structure was determined using NPD whereas the magnetic properties and resistivity (band gap determination) were determined using a SQUID magnetometer and a PPMS respectively. DFT (density functional theory) calculations were performed with WIEN2K.

As the average size of the A-site cation increases, depending on the temperature, the following sequence of phases exists in the LaSr system: $P2_1/n \rightarrow P2_1/n+ I2/m \rightarrow I2/m \rightarrow I4/m \rightarrow Fm\text{-}3m$. The LaCa undergoes no structural phase transitions. Both LaSr and LaCa exhibit non-collinear magnetism, evident from the existence of both hysteresis loops and negative paramagnetic Curie temperatures . However as the average size of the A-site cation increases, the anti-ferromagnetic (AFM) interaction becomes dominant thus resulting in a reduction of the non-collinearity. Concerning the magnetic structures, depending on the composition both systems exhibit a magnetic phase transition from an AFM k=(0,0,0) structure, where the NN (nearest neighbour) interactions between Co ions dominate on a frustrated edge shared tetrahedron geometry to an AFM k=(1/2,0,1/2) structure with dominating NNN (next NN) interactions of Co. The refined AFM moment |μ| varies from 1.7 μ_B for x = 0 to a value around 2.7 μ_B for x=2 at Co sites for LaSr and to 1.6 μ_B for x=0.75 at Co sites for LaCa. Symmetry analysis reveals that the ferromagnetic component of 0.7 μ_B/ f. u. was along the b axis for x = 0. The Curie-temperature is around 90 K up to x=1.5 and drops to 70 K for x=2 of LaSr and drops to 61 K for x=0.75 of LaCa. Furthermore the substitution has influence on other properties such as the band gap, that changes from 0.26 eV for x=0 to 0.05 for x=1.5 within the LaSr, consistent with DFT calculations and the spin state of Co, that is calculated by DFT using the refined structural parameters. The band gap does not change upon Ca substitution.

References had been left out by editors for reasons of space.

ST-05

New synthetic cyclosilicates as potential Li/Na-ionic conductors

S.-H. Park[1], C. J. Pietsch[1], I. F. Akter[1], J. Labbe[1], L. B. Garcia[1], A. Senyshyn[2], M. Hoelzel[2]

[1] LMU, Sektion Kristallographie, München, Germany

[2] TU Darmstadt, FB für Material- und Geowissenschaften, Germany

For realizing all-solid-state electrochemical cells, we have explored solid-solution materials providing anisotropic charge transfer, such as sugilite-sogdianite and willemite solid-solutions. Their frameworks are built commonly with 6-membered rings (6MRs) with regular SiO_4-tetrahedra, exhibiting high thermal stability up to 1250 K. As a result from the investigation, various new synthetic sugilite-type compounds and Na/Li-willemite are synthesized (Table 1). Rietveld calculations with neutron powder diffraction data (SPODI) and chemical analysis confirm new structures.

Large changes in anisotropic atomic parameters for Li and Na are visible in all sugilite-type materials, in particular within the double-ring layers (i.e. $\perp$c-axis), which is enhanced above 650K. These anisotropic thermal motions are consistent with thermal expansion dominant in [100] above 650K. A D.C. conductivity value of ~$1x10^{-3}$ [S cm^{-1}] was estimated from impedance spectra of sugilite materials at T = 1093 K, requiring activation energy of 1,08(3) eV. Difference Fourier maps evaluated from variable temperature neutron powder diffraction data of Na/Li-willemite show positive, diffuse densities of neutron scattering lengths (nsl) at (0,0,0), i.e. the center of 6MR-channel and negative, diffuse nsl at (1/3, 2/3, 0,187). The former is assigned to the missing Na position, while the latter to Li. Dramatic changes in those diffuse nsl-densities at elevated temperatures point to fast dynamic motions of both Na and Li within 6MR-channels of Na/Li-willemite. This is the first case for the presence of conducting Li/Na cations within 6MR-channels of the willemite-topology.

Table 1: Results from Rietveld refinements. The changes of cell parameters of these synthetic sugilites reflect the presence of different multivalent cations at octahedral A sites.

Compound	a [Å]	c [Å]	Volume [$Å^3$]	Ionic radii [Å]	Occupation at A
Fe-sugilite	10,0708(2)	14,1013(4)	1238.57(7)	Fe3+: 0,645	100% Fe
Ga-sugilite	10.0119(2)	13.9960(4)	1214.97(4)	Ga3+: 0,62	100%Ga
Ti-Fe-sugilite	10,0545(4)	14,0824(8)	1232.9(1)	Ti4+: 0.605	90%Fe;10%Ti
Ge-Fe-sugilite	9,960(2)	14,096(3)	1211.1(4)	Ge4+: 0,53	86%Fe;14%Ge

A figure had been left out by editors due to lack of space.

ST-06

Pyroxene from martian meteorite NWA856: Structural investigations by X-ray and neutron diffraction

F. Frey[1], E. Weidner[1], B. Pedersen[2], H. Boysen[1], M. Burghammer[3], M. Hoelzel[4]

[1] LMU, Sektion Kristallographie, München, Germany

[2] Forschungs-Neutronenquelle Heinz Maier-Leibnitz (FRM II), Garching, Germany

[3] ESRF, Grenoble, France

[4] TU Darmstadt, FB für Material- und Geowissenschaften, Germany

Despite high mosaicity and complex micro structures in pyroxenes from Mars average occupancies and average atomic positions of pigeonite were determined from X-ray single crystal and neutron and X-ray powder diffraction data. The chemical composition of selected single crystals varied between $En_{39}Fs_{55}Wo_6$ and $En_{60}Fs_{34}Wo_6$. The average composition of the whole sample was determined from powder diffraction to be about $En_{43}Fs_{51}Wo_6$. The ordering of the cations on the M1 and M2 positions, expressed by a partitioning or distribution coefficient KD, in the pigeonite structure was determined and a closure temperature of about 540 °C was estimated for crystals stemming from the core of our specimen. General trends of the crystal chemistry with KD are compared with literature data. From in-situ high temperature neutron powder data, however, it is deduced that a simple intra-phase-ordering process is not adequate, since diffusion processes between intimately intergrown augite and pigeonite phases at temperatures above 600°C also take place. This makes the usual interpretation of structural data towards the prior history of the martian sample material doubtful.

ST-07

Larmor diffraction studies on the ferromagnetic superconductor UGe_2

R. Ritz[1], D. Sokolov[2], T. Keller[3], A. D. Huxley[2], C. Pfleiderer[1]

[1] TUM, Physik Department, Garching, Germany

[2] University of Edinburgh, School of Physics and Astronomy and Centre for Science at Extreme Conditions, United Kingdom

[3] MPI für Festkörperforschung, Stuttgart, Germany

We present high resolution measurements of the lattice constants of UGe_2 under pressure by means of Larmor diffraction, a novel technique based on the Larmor precession of polarized neutrons that surpasses the resolution of conventional scattering methods by two orders of magnitude [1,2,3]. For decreasing temperature UGe_2 enters a ferromagnetic state (FM1) at a characteristic temperature T_C, which is followed by a second transition at T_X to a ferromagnetic state (FM2) with a larger magnetic moment. The transitions at T_X and T_C are suppressed for pressures exceeding p_X=12 kbar and p_C=16 kbar, respectively. Superconductivity is observed deep in the ferromagnetic state for pressures in the range 10 kbar<p<16 kbar with a maximum in the superconducting transition temperature at p_X [4,5].
We have measured the relative change of lattice constants $\Delta d/d$ at ambient pressure and under pressures of 10, 11 and 12 kbar. With increasing pressures dis- tinct features in $\Delta d/d$ seen at T_C shifted to lower temperatures and become discontinuous at 10 kbar, characteristic of a first order transition. The phase diagram we observe is consistent with literature. However, we observe the largest lattice expansion at 10 kbar, suggesting the strongest magnetoelastic coupling for pressures in the range where the superconductivity emerges. Thus magnetoelastic coupling may be an important ingredient for the coexistence of ferromagnetism with superconductivity in UGe_2.

[1] M.T. Rekveldt et al., EPL 54, 342 (2001).
[2] T. Keller et al., Appl. Phys. A 74 , S332 (2002).
[3] C. Pfleiderer et al., Science 316, 1871 (2007).
[4] S. S. Saxena, et al., Nature 406, 587 (2000).
[5] A. Huxley et al., Phys. Rev. B 63, 144519 (2001).

ST-08

Domain distribution in $SrTiO_3$: effect of applied electric field and mechanical stress

J. Sidoruk[1], J. Leist[1], H. Gibhardt[1], M. Meven[2,3], K. Hradil[3], G. Eckold[1]

[1] Universität Göttingen, Institut für Physikalische Chemie, Germany

[2] RWTH Aachen, Institut für Kristallographie, Germany

[3] Forschungs-Neutronenquelle Heinz Maier-Leibnitz (FRM II), Garching, Germany

Strontium titanate ($SrTiO_3$) has a cubic perowskite structure with space group Pm3m at ambient temperature. Below its ordering temperature at 105 K the antiphase rotation of adjacent TiO_6-octahedra leads to an antiferrodistortive transition into a tetragonal phase with three different kinds of domains. The phase transition is associated with the condensation of a zone-boundary mode at the R-point. The competing polar Γpoint softmode shows an incomplete softening, even at low temperatures. A long range ferroelectric order is suppressed by quantum fluctuations but can be stabilized under the influence of an electric field [1]. Without an external perturbation none of the three tetragonal domains is expected to be favoured. The domain distribution can be changed by mechanical stress [2]. Since the tetragonal distortion corresponds to a c/a-ratio slightly larger than unity, stress along the [110]-direction leads to a preference of domains with the tetragonal axis along [001] (z-domains). It was also observed that the domain distribution is influenced by the application of an electric field [3]. The main goal of the present study is to determine the quantitative domain distribution of strontium titanate under external loads as a function of temperature. Therefore, elastic neutron scattering experiments have been performed at the hot neutron diffractometer HEIDI and the thermal three axes spectrometer PUMA at the FRM II neutron source in Garching. The intensities of a good number of superlattice reflections were measured and fitted to a structure factor model. The determination shows that even the reference sample has a non-uniform domain distribution with a favoured z-domain volume. This preference might be due to residual strains from growth process or sample preparation [4]. Applying mechanical stress of 15 MPa along [110]-direction leads to an increase of z-domains and an almost monodomain sample. The effect of external stress is temperatureindependent and irreversible, even after heating to 120 K (memory-effect). Application of an electric field of 9.2 kV/cm along [001]-direction at 20 K leads to an opposite temperature-dependent effect: Almost all z-domains are suppressed. The effect is irreversible at 20 K if the sample is unstrained. Simultaneous application of stress and field are competing effects. The application of electric field overcompensates the effect of mechanical stress. Therefore, it is impossible to obtain monodomain samples.

[1] J. Hemberger et al., J. Phys. Condens. Matter 8, 4673 (1996).

[2] K. A. Müller, W. Berlinger, M. Capizzi, H. Gränicher, Solid State Commun. 8, 549 (1970).

[3] J. Leist, J. Sidoruk, H. Gibhardt, K. Hradil, M. Meven, G. Eckold, accepted in diffusion fundamentals.

[4] J. Sidoruk, J. Leist, H. Gibhardt, M. Meven, K. Hradil and G Eckold, J. Phys. Condens. Matter 22, 235903 (2010).

ST-09

Magnetoelastic coupling in $CaMn_7O_{12}$

W. Sławiński[1], R. Przeniosło[1], I. Sosnowska[1], M. Bieringer[2]

[1] University of Warsaw, Institute of Experimental Physics, Poland

[2] University of Manitoba, Department of Chemistry, Winnipeg, Canada

The mixed manganese oxide $CaMn_7O_{12}$ is a multiferroic material [1] with a distorted perovskite structure [2]. The crystal structure [3] and the magnetic ordering [4] of $CaMn_7O_{12}$ have been studied by using high resolution SR diffraction and high resolution neutron diffraction. These diffraction studies show a modulation of the atomic positions in $CaMn_7O_{12}$ at temperatures below 250K and magnetic structure modulation below T_N = 90K [5,6].
The modulation of atomic positions has been described by using a quantitative model with a propagation vector $(0,0,q_p)$ [5] which gives good agreement with the results of both SR and neutron diffraction studies [6]. The neutron diffraction studies of $CaMn_7O_{12}$ show a modulated magnetic ordering below the Néel temperature T_N = 90K. The modulation of the magnetic structure is described with a propagation vector $(0,0,q_m)$. Both magnetic and positional modulations are coupled together. The modulation length of the atomic positions (L_p) and of the magnetic moment modulation length (L_m) fulfill the relation $L_m = 2\ L_p$ at temperatures between 50K and the Néel temperature T_N. The temperature dependence of the modulation vectors q_p and q_m is shown in fig. 1. The relation between modulation lengths Lp and Lm as well as minimum and maximum of the lattice constant c clearly show the magnetoelastic coupling in $CaMn_7O_{12}$ [1,6]. Below 50K there is a magnetic phase transition which is associated with important changes of the magnetic modulation length (see Fig.1) and also with the increase of magnetoelectric coupling [1].

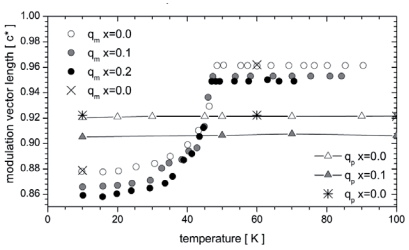

Fig. 1 Temperature dependence of the magnetic modulation vector length q_m for $CaCu_xMn_{7-x}O_{12}$ (x = 0.0 (open circles), 0.1 (gray circles) and 0.23 (black circles)) measured on neutron diffractometer D20 (ILL). Two additional points show q_m values obtained on neutron diffractometer D2B for $CaMn_7O_{12}$ (crosses). The temperature dependence of atomic position modulation vector q_p for $CaCu_xMn_{7-x}O_{12}$ (x = 0.0 (open triangles) and 0.1 (gray triangles)) measured by synchrotron radiation diffractometer ID31 (ESRF) and for x = 0.0 (asterisk) measured with neutron diffractometer D2B.

[1] M. Sánchez-Andújar, S. Yáñez-Vilar, N. Biskup, S. Castro-García, J. Mira, J. Rivas, M. Señarís-Rodríguez, J. Magn. Magn. Mater. 321 (2009) 1739-1742.

[2] B. Bochu, J. L. Buevoz, Solid State Communications 36(2) (1980) 133–138.

[3] W. Sławinski, R. Przeniosło, I. Sosnowska, M. Bieringer, I. Margiolaki, A. N. Fitch, E. Suard, Journal of Solid State Chemistry 179(8) (2006) 2443–2451.

[4] R. Przeniosło, I. Sosnowska, D. Hohlwein, T. Hauß, I. O. Troyanchuk, Solid State Communications 111(12) (1999) 687–692.

[5] W. Sławiński, R. Przeniosło, I. Sosnowska, M. Bieringer, I. Margiolaki, E. Suard, Acta Crystallogr. B65 (2009) 535-542.

[6] W. Sławiński, R. Przeniosło, I. Sosnowska, M. Bieringer, J. Phys.: Condens. Matter 22 (2010) 186001-6.

ST-10

Proximity effect in complex oxide superlattices of $YBa_2Cu_3O_7/La_{2/3}Ca_{1/3}MnO_3$

M. A. Uribe–Laverde[1], D. K. Satapathy[1], J. Kim[2], I. Marozau[1], V. K. Malik[1], S. Das[1], M. Rössle[1], C. Marcelot[1], V. Hinkov[2], A. Rühm[3], T. Keller[2], J. Stahn[4], B. Keimer[2], C. Bernhard[1]

[1] University of Fribourg, Department of Physics and Fribourg Center for Nanomaterials, Switzerland

[2] MPI für Festkörperforschung, Stuttgart, Germany

[3] MPI für Metallforschung, Stuttgart, Germany

[4] ETH Zürich, Laboratory for Neutron Scattering @ PSI, Villigen, Switzerland

In order to study the interaction between ferromagnetic and superconducting order parameters, the evolution of the magnetic induction depth profile as a function of temperature, applied magnetic field and doping of the superconducting layer in superlattices consisting of the superconducting $YBa_2Cu_3O_{7-\delta}$ and the ferromagnetic $La_{2/3}Ca_{1/3}MnO_3$ has been studied by means of specular and off-specular polarized neutron reflectometry. The difference in the measured reflectivity for different incident spin polarization states reveals the presence of magnetism inside the layers, moreover, in the specular case the presence of the structurally forbidden second Bragg peak is clear evidence that the magnetic field inside the layers and near to the interface is not homogeneous, suggesting the occurrence of a proximity induced effect. The off-specular measurements show Bragg sheets and magnetic Yoneda wings, whose magnetic field and temperature dependence enable the extraction of information about the magnetic correlations along the direction parallel to the sample surface. More details about the evolution of proximity effects in these complex oxide materials will be presented.

ST-11

Neutron diffraction studies on hydrogen adsorption in hexacyanometallates

H. Yee-Madeira[1], E. Reguera[2], G. Ramos[3], J. Jiménez-Gallegos[2], M. Hoelzel[4], G. Eckold[5]

[1] Instituto Politécnico Nacional, Escuela Superior de Física y Matemáticas, México, Mexico

[2] Instituto Politécnico Nacional, CICATA-Legaria, México, Mexico

[3] Instituto Politécnico Nacional, CICATA-Querétaro, Querétaro, México

[4] Forschungs-Neutronenquelle Heinz Maier-Leibnitz (FRM II), Garching, Germany

[5] Universität Göttingen, Institut für Physikalische Chemie, Germany

Physical absorption of hydrogen in zeolites-like hexacyanometallates offer high reversibility at low temperatures and are promising candidates for hydrogen storage. Their storage capacity is thought to be favored by the electric field gradients within the porous framework. Because of the small weight fraction adsorbed in the samples, neutron diffraction studies allows the study of modifications of the crystallographic structure due to introduction of hydrogen (deuterium). In the present work the structure modifications of the Hexacyanometallates $Zn_3K_2[Fe(CN)_6]_2{*}xH_2O$ and $Cu_3[Co(CN)_6]_2{*}xH_2O$ with the introduction of deuterium at 80 K is reported. XRD and Neutron powder diffraction show the structure change of $Zn_3K_2[Fe(CN)_6]_2$ from R-3C to monoclinic upon dehydration, while $Cu_3[Co(CN)_6]_2$ does not change its structure. The resulting structures were refined using the Rietveld method.

Index and List of Participants

Index

F

G

H

I

J

K

L

M

N

O

P

R

S

T

U

V

W

Y

Z

List of Participants

Adams, Tim	tim.adams@frm2.tum.de
Adelsberger, Joseph	joseph.adelsberger@ph.tum.de
Alhamdany, Nowfal	composite83@yahoo.com
Altenkirch, Jens	jens.altenkirch@kit.edu
Appavou, Marie-Sousai	m.s.appavou@fz-juelich.de
Balasoiu, Maria	balasoiumaria@yahoo.com
Beyer, Katrin	katrin.beyer@bam.de
Birke, Michael	michael.birke@desy.de
Blanchard, Didier	didier.blanchard@risoe.dk
Böni, Peter	pboeni@frm2.tum.de
Boysen, Hans	boysen@lmu.de
Brückel, Thomas	t.brueckel@fz-juelich.de
Calzada, Elbio	elbio.calzada@frm2.tum.de
Canella, Lea	lea.canella@frm2.tum.de
Ceeh, Hubert	hceeh@frm2.tum.de
Chang, Lieh-Jeng	liehjeng.chang@jaea.go.jp
Chillal, Shravani	shravani.chillal@ph.tum.de
Danilyan, Gevorg	danilyan@itep.ru
Däubler, Miriam	mdaeuble@frm2.tum.de
Davaasambuu, Jav	jdavaas@gwdg.de
Deeg, Andreas	andreas.deeg@physik.uni-muenchen.de
Demoulin, Thibault	thibault.demoulin@frm2.tum.de
do Carmo Freitas, Maria	cfreitas@itn.pt
Eckold, Götz	geckold@gwdg.de
Egger, Werner	werner.egger@unibw.de
Ener, Semih	semih.ener@ph.tum.de
Erhan, Raul Victor	raul.erhan@gmail.com
Faulhaber, Enrico	enrico.faulhaber@frm2.tum.de
Frielinghaus, Henrich	h.frielinghaus@fz-juelich.de
Gan, Weimin	weimin.gan@gkss.de
Garcia Garcia, Francisco Javier	javier.garcia@physik.uni-augsburg.de
Gebhardt, Ronald	ronald.gebhardt@wzw.tum.de
Georgalis, Yannis	yannis.georgalis@tum.de
Georgii, Robert	robert.georgii@frm2.tum.de
Gibmeier, Jens	jens.gibmeier@iwk1.uni-karlsruhe.de
Gilles, Ralph	ralph.gilles@frm2.tum.de
Goerigk, Guenter	g.goerigk@fz-juelich.de
Granja, Carlos	carlos.granja@utef.cvut.cz
Griesche, Axel	axel.griesche@bam.de
Gutberlet, Thomas	t.gutberlet@fz-juelich.de
Gutberlet, Tobias	gutberlet@cbm.bv.tum.de
Gutsmiedl, Erwin	erwin.gutsmiedl@frm2.tum.de
Hannemann, Andreas	andreas.hannemann@bam.de

Häußler, Wolfgang	wolfgang.haeussler@frm2.tum.de
Hertrich, Samira	samira.hertrich@physik.lmu.de
Hilbig, Harald	hilbig@cbm.bv.tum.de
Ho Dung, Manh	m.hodzung@itn.pt
Hofmann, Michael	michael.hofmann@frm2.tum.de
Holderer, Olaf	o.holderer@fz-juelich.de
Hölzel, Markus	markus.hoelzel@frm2.tum.de
Hoppe, Tilo	tilo.hoppe@ph.tum.de
Hradil, Klaudia	klaudia.hradil@frm2.tum.de
Hugenschmidt, Christoph	hugen@frm2.tum.de
Inosov, Dmytro	d.inosov@fkf.mpg.de
Jaksch, Sebastian	sebastian.jaksch@ph.tum.de
Keller, Thomas	t.keller@fkf.mpg.de
Khafizov, Rashid	rash@pretty.mbslab.kiae.ru
Khaydukov, Yury	khaiduk@nf.jinr.ru
Kim, Junghwa	jh.kim@fkf.mpg.de
Klauser, Christine	christine.klauser@frm2.tum.de
Klein, Wilhelm	wilhelm.klein@frm2.tum.de
Klenke, Jens	jens.klenke@frm2.tum.de
Köhler, Ralf	ralf.koehler@helmholtz-berlin.de
Köster, Ulli	koester@ill.fr
Kostov, Vladimir	vladimir.kostov@kit.edu
Kozhevnikov, Sergey	sergey.kozhevnikov@frm2.tum.de
Kreuzpaintner, Wolfgang	wolfgang.kreuzpaintner@frm2.tum.de
Kühnholz, Olaf	olaf.kuehnholz@desy.de
Kunej, Vojko	kunej@idbscb.de
Kutova, Polina	polina.kutova@gmail.com
Lazaropoulou, Polyxeni	polylaza@pme.duth.gr
Leao, Juscelino	juscelino.leao@nist.gov
Lefmann, Kim	lefmann@fys.ku.dk
Li, Weijun	jessie@xtal.rwth-aachen.de
Linez, Florence	florence.linez@cnrs-orleans.fr
Link, Peter	peter.link@frm2.tum.de
Longeville, Stéphane	slongeville@cea.fr
Löwe, Benjamin	bloewe@ph.tum.de
Loewenhaupt, Michael	loewenhaupt@physik.tu-dresden.de
Maawad, Emad	eksm@tu-clausthal.de
Mangiapia, Gaetano	mangiapia.gaetano@alice.it
Märkisch, Bastian	maerkisch@uni-heidelberg.de
Masalovich, Sergey	sergey.masalovich@frm2.tum.de
Mattauch, Stefan	s.mattauch@fz-juelich.de
Meier, Robert	rmeier@ph.tum.de
Meierhofer, Georg	meierhofer@pit.physik.uni-tuebingen.de
Merkel, Daniel	merkel@rmki.kfki.hu
Metwalli, Ezzeldin	ezzmet@ph.tum.de
Meven, Martin	martin.meven@frm2.tum.de

Mole, Richard	richard.mole@frm2.tum.de
Morhenn, Humphrey	hmorhenn@frm2.tum.de
Moulin, Jean-François	jean-francois.moulin@gkss.de
Mukherji, Debashis	d.mukherji@tu-bs.de
Mühlbauer, Martin	martin.muehlbauer@ph.tum.de
Müller-Buschbaum, Peter	muellerb@ph.tum.de
Munnikes, Nathalie	nathalie.munnikes@frm2.tum.de
Nafradi, Balint	nafradi@yahoo.com
Nagy, Béla	nagyb@rmki.kfki.hu
Narayanan, Narendirakumar	n.narayanan@ifw-dresden.de
Neuhaus, Jürgen	juergen.neuhaus@frm2.tum.de
Nickel, Bert	nickel@lmu.de
Oberdorfer, Bernd	oberdorfer@tugraz.at
Ostermann, Andreas	andreas.ostermann@frm2.tum.de
Paduano, Luigi	luigi.paduano@unina.it
Papadakis, Christine M.	papadakis@tum.de
Park, So-Hyun	sohyun.park@lmu.de
Pedersen, Bjørn	bjoern.pedersen@frm2.tum.de
Petry, Winfried	w.petry@frm2.tum.de
Pigozzi, Giancarlo	giancarlo.pigozzi@empa.ch
Pikart, Philip	philip.pikart@frm2.tum.de
Posselt, Dorthe	dorthe@ruc.dk
Radulescu, Aurel	a.radulescu@fz-juelich.de
Ravelli, Luca	luca.ravelli@unibw.de
Rawolle, Monika	monika.rawolle@ph.tum.de
Rebelo Kornmeier, Joana	joana.kornmeier@frm2.tum.de
Reinecke, Uwe	uwe.reinecke@frm2.tum.de
Reiner, Markus	markus.reiner@frm2.tum.de
Repper, Julia	julia.repper@frm2.tum.de
Ritz, Robert	robert.ritz@frm2.tum.de
Rühm, Adrian	ruehm@mf.mpg.de
Sadykov, Ravil	rsadykov@inr.ru
Sajti, Szilárd	szilard@rmki.kfki.hu
Sarvas, Jürgen	juergen.sarvas@frm2.tum.de
Schillinger, Burkhard	burkhard.schillinger@frm2.tum.de
Schindler, Markus	markus.schindler@ph.tum.de
Schmakat, Philipp	philipp.schmakat@frm2.tum.de
Schmidt, Julia	julia.schmidt@physik.uni-muenchen.de
Schneidewind, Astrid	astrid.schneidewind@frm2.tum.de
Schreckenbach, Klaus	klaus.schreckenbach@frm2.tum.de
Schulte, Alfons	afs@physics.ucf.edu
Schulz, Michael	michael.schulz@frm2.tum.de
Schulze, Ralf	r.schulze@ikp.uni-koeln.de
Schwahn, Dietmar	d.schwahn@fz-juelich.de
Schweinichen, Petrico von	petrico.von.schweinichen@iehk.rwth-aachen.de
Senyshyn, Anatoliy	anatoliy.senyshyn@frm2.tum.de

Sidoruk, Jakob	jsidoru@gwdg.de
Simeoni, Giovanna	giovanna.simeoni@frm2.tum.de
Siouris, Ioannis	jsiou@pme.duth.gr
Slawinski, Wojciech	wojciech@fuw.edu.pl
Slugen, Vladimir	vladimir.slugen@stuba.sk
Sojak, Stanislav	stanislav.sojak@stuba.sk
Solbrig, Konrad	konrad.solbrig@hs-owl.de
Söllradl, Stefan	stefan.soellradl@frm2.tum.de
Sosnowska, Izabela	izabela@fuw.edu.pl
Sperr, Peter	
Sprengel, Wolfgang	w.sprengel@tugraz.at
Su, Yixi	y.su@fz-juelich.de
Sveinbjörnsson, Dadi	dasv@exchange.risoe.dk
Teichert, Anke	anke.teichert@frm2.tum.de
Unruh, Tobias	tobias.unruh@frm2.tum.de
Uribe Laverde, Miguel Angel	miguelangel.uribelaverde@unifr.ch
Visser, Dirk	d.visser@tudelft.nl
Wlokka, Stephan	swlokka@e18.physik.tu-muenchen.de
Wuttke, Joachim	j.wuttke@fz-juelich.de
Yee, Hernani	hernaniyee@hotmail.com
Zamponi, Michaela	m.zamponi@fz-juelich.de
Zeitelhack, Karl	karl.zeitelhack@frm2.tum.de
Zhang, Fajun	fajun.zhang@uni-tuebingen.de
Zhong, Qi	qi.zhong@ph.tum.de

Please note:

We would be very grateful for receiving your abstracts for the FRM II Annual Report 2010 before November 14th, 2010.

Please contact

jahresbericht@frm2.tum.de